A ROLE FOR AMYLOID PRECURSOR PROTEINS IN REGULATING NEURONAL MOTILITY THROUGH G_o-DEPENDENT SIGNALING

by

Jenna Marie Ramaker

A DISSERTATION

Presented to the Neuroscience Graduate Program

and the Oregon Health & Science University

School of Medicine

in partial fulfillment of

the requirements for the degree of

Doctor of Philosophy

October 28, 2013

School of Medicine
Oregon Health & Science University

CERTIFICATE OF APPROVAL

This is to certify that the Ph.D. dissertation of
JENNA RAMAKER
has been approved on October 28, 2013

Advisor, Philip Copenhaver, Ph.D.

Member and Chair, David Morton, Ph.D.

Member, Doris Kretzschmar, Ph.D.

Member, Marcel Wehrli, Ph.D.

Member, Joseph Quinn, M.D.

TABLE OF CONTENTS

ACKNOWLEDGEMENTS

I am extremely grateful for all the help and support I have received throughout my graduate training. First, I would like to thank my advisor, Dr. Philip Copenhaver, for his outstanding mentorship throughout my time in his laboratory. His scientific expertise and insight were instrumental to the progression of this project, and his willingness to guide me through reading, writing, and presenting have greatly facilitated my development as a researcher. I would also like to thank all members of the Copenhaver laboratory, past and present. In particular, I am grateful to Ms. Tracy Swanson, who trained me in the laboratory and whose technical expertise was critical to the completion of this work. Additionally, Mr. Jonathon Zweig and Ms. Amy Nicolaysen provided outstanding support that contributed towards the completion of these studies.

I would like to thank the members of my Thesis Examination Committee: Drs. David Morton (chair), Philip Copenhaver, Doris Kretzschmar, and Marcel Wehrli. I would also like to thank Dr. Lawrence Sherman, who served on my Thesis Advisory Committee, and Dr. Joseph Quinn, who served as the outside member for my Thesis Examination. My thanks to all of them for their critical input, their willingness to review manuscripts and grant applications, and for their support throughout my training.

I would like to thank all of the great colleagues and friends I have met at OHSU. In particular, I would like to thank my classmates, Drs. Rachel Clemens Grisham and Molly Harding, for their critical feedback on numerous documents and presentations.

Additionally, I owe a huge thank you to my twin sister and colleague, Dr. Marcia Ramaker, whose continued support both personally and professionally has been

essential to my success in graduate school. Her willingness to spend countless hours providing feedback on my presentations, editing documents, and discussing our research has greatly benefited me throughout this process. Finally, I am extremely grateful to my significant other, Cedric Walker, and to my mother, whose support I could not have done this without.

This work was supported by funds from National Institute on Aging (T32 TG AG023477), Oregon Partners for Alzheimer's Research, Vertex Pharmaceuticals, and a Tartar Trust fellowship to JMR as well as grants NIH RO1 AG025525 and R21 NS080036 to PFC.

ABSTRACT

During formation of the nervous system in many organisms, neurons must migrate over long distances to reach their appropriate locations and establish proper connections with their synaptic targets. To facilitate their guidance in the developing embryo, neurons express a variety of receptors that can both sense extracellular cues and elicit intracellular signaling cascades that mediate stage-specific types of motile behavior, including cellular migration, axonal outgrowth, and synaptic formation. Amyloid precursor protein (APP) has been shown to regulate numerous aspects of neuronal motility *in vitro*, supporting its role as a guidance receptor in the developing nervous system. However, elucidating the function of APP *in vivo* has been complicated by the expression of two closely related genes (APLP1 and APLP2) in mammals that share partially overlapping functions with APP, and the discovery that different APP isoforms are expressed by multiple cell types besides neurons in vertebrate model systems.

As an alternative strategy, I have utilized the developing enteric nervous system (ENS) of the hawkmoth, *Manduca sexta*. During formation of the ENS, a population of approximately 300 neurons (EP cells) reaches their correct target locations on the gut musculature by migrating along an identified set of muscle band pathways that are permissive to their growth. Previous studies in the Copenhaver laboratory demonstrated that APPL (APP-like), the sole ortholog of APP in insects, is expressed by the EP cells during active phases of migration and outgrowth, co-incident with their expression of the heterotrimeric G protein Goα. Although activation of Goα has been shown to induce stalling responses in migrating EP cells and their axons, the upstream receptor in this pathway has remained unidentified.

Work from several groups has suggested that APP functions as an unconventional G protein-coupled receptor, capable of regulating a variety of cellular

responses via the heterotrimeric G protein, Goα. However, most of these investigations employed artificial liposome preparations and transfected cell lines, leaving the validity of this model in doubt. To test whether insect APPL might also function by regulating Goα-dependent aspects of neuronal migration and outgrowth, I discovered that blocking APPL signaling in the EP cells induced a pattern of ectopic, inappropriate growth and migration in the *Manduca* ENS, identical to the effects of inhibiting Goα activity. Using a combination of biochemical, pharmacological, and bimolecular fluorescence complementation assays, I showed that APPL directly interacts with Goα in the developing nervous system, in cell culture, and at synaptic terminals within the fly brain, and that this interaction is regulated by Goα activity. Corresponding assays using both murine and human brain tissue samples revealed that Goα (but not other G proteins) also interacts with endogenously expressed APP, and that this interaction is specific to the full-length (transmembrane) protein. These results support the model that APP family proteins function as Goα-coupled receptors that prevent neuronal migration and outgrowth from occurring in nonpermissive regions.

To date, authentic ligands for APP family proteins are not known. As an alternative approach for activating APPL, I used established methods for antibody crosslinking to induce APP signaling in murine neuronal cultures. These studies revealed a role for APP in promoting Go-dependent growth cone collapse and retraction. To test whether similar responses could be elicited *in vivo*, I treated cultured *Manduca* embryos with Fc fusion constructs of one of its candidate ligands, Mscontactin. Treating premigratory EP cells with Mscontactin-Fc resulted in a stalling response, consistent with the expected effect of activating APPL in this system. Whether APPL-Goα signaling lies downstream of Mscontactin in mediating this effect is still to be determined.

Lastly, using a combination of biochemical and immunohistochemical methods, I identified APP phosphorylation at one specific residue within its cytoplasmic domain (Thr_{668}) as a potential regulator of APP-Goα interactions. Unexpectedly, I discovered that Goα preferentially interacts with the nonphosphorylated form of Thr_{668}, suggesting that kinase-dependent phosphorylation of APP at this site may provide another mechanism for regulating APP-Goα signaling. In combination, this work identifies a role for the evolutionarily conserved APP family in regulating key aspects of neuronal motility and outgrowth by functioning as Goα-coupled receptors. Future studies will be needed to determine how APP-Goα signaling is regulated in the developing nervous system, and how perturbations in this signaling pathway may contribute to the progression of neurodegenerative diseases in the adult brain (including Alzheimer's disease).

CHAPTER 1

Thesis Introduction

Alzheimer's disease (AD) is a fatal neurodegenerative disease afflicting over 5 million Americans, for which no effective treatment exists (Mangialasche et al., 2010, Wimo et al., 2010). It is characterized by the accumulation of extracellular β-amyloid (Aβ) peptides, which are produced by sequential β and γ cleavage of amyloid precursor protein (APP). In familial AD, the cause of 5-10% of AD cases, mutations in either APP itself or the gamma secretase complex lead to increased Aβ 42:40 ratios, amyloid plaques, hyperphosphorylated tau, synaptic loss, and neuronal death (O'Brien and Wong, 2011). Additionally, in sporadic cases of AD, increased levels of oligomeric Aβ are associated with AD (Blennow et al., 2006). These associations have resulted in the "amyloid hypothesis," which postulates that the generation of neurotoxic Aβ peptides by secretase processing of APP is a primary cause of AD (Loo et al., 1993, Hardy and Selkoe, 2002). However, therapies targeting Aβ have not resulted in clinical improvement, suggesting that other APP-related activities may contribute to AD (Mangialasche et al., 2010). Given that APP has been postulated to regulate a variety of physiological processes such as neuronal outgrowth, synaptic formation and maintenance, and LTP (Cullen et al., 1997, Nalbantoglu et al., 1997, Galvan et al., 2006), an alternative hypothesis is that disruption of the normal functions of APP in the brain may contribute to the neurodegeneration seen in AD. The overall goal of this thesis was to better understand the physiological role of APP in the developing nervous system.

An overview of neuronal migration

Proper migration of developing neurons is critical for these cells to reach their target locations, acquire appropriate cell identities, and establish connectivity. In order for neurons to develop properly, they must send out axons and migrate over long distances during precise periods of development. The ability of neurons to follow a particular path is due in part to their specialized growth cone, which contains a dynamic cytoskeleton that can rapidly alter its movements in response to local cues (Sotelo, 2002). Actin bundles in the peripheral domain of growth cones form filopodial protrusions that can extend and retract in response to environmental cues. When input from local cues causes actin polymerization on one side of the growth cone and concurrent depolymerization on the other, it generates a traction force that turns the growth cone (Mitchison and Kirschner, 1988). The actin-rich growth cone can rapidly change direction, retract, and branch in response to an array of factors, but it is only upon microtubule invasion of the central growth cone that the axon stabilizes, elongates, and establishes directionality (Buck and Zheng, 2002, Yuan et al., 2003).

In order to incorporate directional information from the environment, growth cones express a multitude of guidance receptors capable of detecting extracellular cues and transducing intracellular responses. The cues recognized by receptors exist in a variety of forms, including membrane-bound ligands that require cell-cell contact, secreted ligands that form directional gradients, or adhesion molecules that provide traction along a substrate. Guidance molecules can induce either attractive or repulsive responses within migrating cells via the regulation of specific signal transduction pathways, and multiple signaling pathways can act either in concert or in opposition to one another to ultimately guide a neuron to its target location (Tessier-Lavigne and Goodman, 1996). For these reasons, predicting how migrating neurons will respond to a

complex array of guidance cues and distinguishing the contribution of individual pathways has been experimentally challenging.

Defects in neuronal guidance are the cause of numerous neurodevelopmental disorders, and notably, many of the events that underlie neuronal positioning in the developing nervous system may also underlie reshaping and maintenance of neuronal connections in the adult brain. Therefore, understanding the complex integration of signals that regulate proper neuronal guidance will provide insight into how disruptions in these signaling pathways may also contribute to neurological disorders at later stages of life. However, many questions about how a neuron integrates signals to make decisions about cell movements remain: (1) How do different regions of the neuron, such as the cell body and growing axon, distinctly respond to specific cues? (2) How do changes at the growth cone influence the movement of the cell body? (3) How do signals that terminate axon growth subsequently permit axon branching and target innervation? And finally, (4) how are these events re-employed in adult neurons to ensure maintenance of existing connections? To fully understand these events will require further deciphering of the mechanisms by which guidance receptors activate intracellular cascades that regulate cytoskeletal dynamics. A particularly effective means of addressing this issue *in vivo* is through the use of simple model systems, such as *Drosophila* and *Manduca.*

The role of APP in neurons

APP is a single-pass transmembrane glycoprotein that structurally resembles a cell surface receptor (Kang et al., 1987). Mammalian APP is expressed in all neurons, in addition to its almost ubiquitous expression in other cell types, suggesting that it may serve critical roles in cellular function (Forloni et al., 1992). In the developing nervous system, the spatial and temporal expression pattern of APP may provide insight into its role in neuronal differentiation. APP expression commences during embryogenesis,

coincident with periods of axon outgrowth (Salbaum and Ruddle, 1994) and synaptogenesis (Clarris et al., 1995). It is highly expressed at the cell surface of growth cones (Ferreira et al., 1993, Yamazaki et al., 1997, Sabo et al., 2003), both at presynaptic and postsynaptic regions (Hoe et al., 2009a, Wang et al., 2009), as well as within intracellular compartments throughout the cell body, axon, and neurites, demonstrating that it undergoes dynamic trafficking that may modulate its function in neurons (Muresan and Muresan, 2005, Muresan et al., 2009). Notably, *in vitro* studies have supported potential roles for APP in regulating numerous aspects of neuronal development, such as cell adhesion (Breen et al., 1991, Soba et al., 2005), neurite outgrowth (Perez et al., 1997, Small et al., 1999), and synaptogenesis (Priller et al., 2006, Wang et al., 2009). However, the authentic functions of APP *in vivo* have remained elusive.

Consistent with a role for APP in regulating key aspects of neuronal development, both the extracellular and intracellular domains of APP interact with a number of molecules that may regulate neuron motility. The extracellular domain of APP, which has been crystalized (Rossjohn et al., 1999), contains multiple protein-folding domains that give it a complex secondary structure. Within the large ectodomain are subdomains, E1 and E2, that have been shown to be critical for interactions between APP and integrins (Yamazaki et al., 1997), laminin (Narindrasorasak et al., 1992), and collagen (Beher et al., 1996), supporting a role in cell adhesion. APP also binds a variety of other proteins like Reelin (Hoe et al., 2009b), F-spondin (Ho and Sudhof, 2004), LDL-R (Andersen et al., 2005, Fuentealba et al., 2007, Brodeur et al., 2012), and contactin family members (Osterfield et al., 2008), all of which are thought to regulate aspects of neuronal positioning or axon guidance (Nadarajah and Parnavelas, 2002). Additionally, APP cleavage products can bind the extracellular domain of transmembrane APP (Gralle et al., 2009, Sola Vigo et al., 2009), potentially acting as a ligand for the full-length receptor.

APP may also regulate important aspects of neuronal development through interactions mediated by its cytoplasmic domain, which contains a Go-binding domain adjacent to the transmembrane domain, as well as a tyrosine-based protein sorting domain adjacent to its cytoplasmic tail, called the internalization domain. The internalization domain has been postulated to regulate growth cone dynamics and synaptic remodeling by interacting with Fe65 (Sabo et al., 1999, Sabo et al., 2003), induce axon arborization by interacting with Abl tyrosine kinase (Leyssen et al., 2005), facilitate synapse formation by interacting with X11/MINT (Ashley et al., 2005), and regulate neuronal positioning through its interaction with Dab 1 (Young-Pearse et al., 2007). Notably, Torroja et al., has demonstrated that insect APP is necessary for proper synaptic bouton formation in *Drosophila*, and both the internalization domain and the Go-binding domain can mediate distinct aspects of synaptic formation (Torroja et al., 1999b). However, while these interactions suggest that APP may play a key role in regulating multiple aspects of neuronal development, the mechanisms by which it may do so remain unknown.

Neuronal migration in the developing cortex: a role for APP

The developing mammalian cortex is one of the best-studied models of neuronal migration. Seminal work on this system demonstrated that in order for neurons to establish the highly structured layers of the cortex, they undergo a well-organized pattern of migration (Berry and Rogers, 1965, Rakic, 1974). The newly generated neurons, which arise in the ventricular zone, migrate through the intermediate zone to the cortical plate, stopping at their target location before they reach the pial layer of the marginal zone. Each wave of newly-born neurons migrates past the previous cortical layer, producing an inside-out laminar structure (Rakic, 1974). While formation of this structure is very stereotyped, not all neurons arrive at their target location using the

same mechanisms. In early phases of migration, neurons primarily utilize glial-independent somal translocation, in which migrating cells extend their leading process over short distances and then translocate their cell bodies towards their target location by shortening their process (Nadarajah et al., 2001). However, as new cortical layers form and each wave of new neurons must traverse a progressively wider cortex (with a more complex assortment of cues), neurons rely on glial-guided locomotion. In this form of migration, the length of the neuron's leading process stays relatively constant, while the migrating cell body moves along pre-established radial glia, interspersed with a phase in which the neuron detaches from the glia and switches to a multipolar, exploratory state (Nadarajah et al., 2001). During periods of exploration, the neuron extends and retracts multiple processes and can then either re-associate with its original radial glial pathway or switch to somal translocation to reach its final destination (Tabata and Nakajima, 2003, Noctor et al., 2004).

These distinct phases of migration and the precisely regulated targeting of neurons to their proper cortical layer highlight the complexity of cues that neurons must integrate to respond to their environment. One potentially important molecule for guiding neurons to their target location in the developing cortex is APP. However, elucidating the function of APP in vertebrates has been complicated by a number of factors, including the redundant expression of APP with two closely related gene products, APLP1 and APLP2 (amyloid precursor like proteins 1 and 2).

Although the role of APP in neuronal migration is still unclear, gain- and loss-of-function studies have suggested that APP plays a role in regulating neuronal migration. Triple knockout of APP, APLP1, and APLP2 revealed that in the absence of all three APP family members, cortical neurons migrated past their target locations in the cortical plate, forming ectopic lissencephalies. These results suggest that APP family proteins may function as an inhibitory signal, directing neurons to stop migrating once they reach

their target location (Herms et al., 2004). To experimentally prevent compensation by APLP1 and 2, Young-Pearse and colleagues transiently knocked down APP expression in neural progenitors by electroporating E13 (embryonic day) mouse embryos with APP shRNA. This manipulation prevented neuronal precursors from migrating into the cortical plate and the cells remained trapped in the intermediate zone (Young-Pearse et al., 2007). In contrast to the aforementioned studies by Herms et al., these results suggest that APP promotes neuronal migration, and consistent with these conclusions, overexpressing APP increased the number of neurons that reached the cortical plate by E16 (Young-Pearse et al., 2007). In part, this disparity may be explained by a more recent study demonstrating that knocking down APLP2 in neuronal progenitors prevented their proper differentiation and subsequent migration, while knocking down APLP2 in post-mitotic neurons had no effect (Shariati et al., 2013). Since APLP2 and APP are coexpressed by neuronal progenitors of the ventricular zone (Visel et al., 2004, Lopez-Sanchez et al., 2005, Diez-Roux et al., 2011), transiently knocking down APP may have similarly caused defects in cell fate determination, thereby complicating an analysis of migration *per se* via the methods used by Young-Pearse et. al. Thus, while these results demonstrate that APP is important for proper neuron migration, the actual role of APP in neuronal development is still not clear.

Complications in understanding the role of APP in the mammalian brain

Although the developing mouse cortex has served as a useful model for revealing key features underlying neuronal migration, analyzing the role of APP in this process has been complicated by the complexity of this system. On the other hand, simpler model systems, such as *Manduca* and *Drosophila*, provide many advantages for studying the role of APP *in vivo*. Four key challenges in elucidating the role of APP in

neuronal migration using mammalian model systems, as well as the corresponding advantages of using invertebrate model systems, will be discussed below.

In contrast to the robust role for APP *in vitr*o, APP KO mice are viable, fertile, and do not have significant reductions in neuron number, synaptic boutons number, nor altered dendrite morphology in the hippocampus (Phinney et al., 1999, Senechal et al., 2008). In contrast, triple knockout of APP, APLP1, and APLP2 results in postnatal lethality (Herms et al., 2004). These results suggest that APP family proteins are able to functionally compensate for each other. However, APP and APLP2 expression overlaps in neuronal progenitors within the subventricular and ventricular zones, whereas APP and APLP1 coexpression is restricted to differentiated neurons in the cortical plate (Visel et al., 2004, Lopez-Sanchez et al., 2005, Diez-Roux et al., 2011). These unique expression patterns support both distinct and redundant functions for each of these gene products. Therefore, understanding the role of APP in neuronal migration in the mammalian brain also requires considering the unique role of each APLP, a factor which has thus far complicated an analysis of the function of APP in developing neurons. In contrast, *Manduca* and *Drosophila* express only one APP ortholog (APPL), simplifying an analysis of the role of this protein in neuronal migration.

As already noted, mammalian APP is highly expressed in neurons but is also expressed in most other cell types. Therefore, when Herms et. al. and Young-Pearse et. al. disrupted APP expression in the developing cortex, they did so in both neurons and glia. Since cortical neurons rely on both somal translocation and glial-guided locomotion to reach their target location, the potential roles of APP in glial guidance versus neuronal motility in this system are difficult to distinguish. In contrast, *Manduca* and *Drosophila* possess only one APP isoform, which is expressed exclusively in neurons. Therefore, these model systems permit an *in vivo* analysis of APP proteins exclusively in neurons.

Another complication of using the mammalian cortex to understand the role of APP in neuronal development is that during embryonic development, as differentiated neurons establish themselves in appropriate layers within the cortical plate, mitotically active neuroblasts that will generate future cortical layers still reside in the ventricular zone. Manipulating APP during embryogenesis may therefore perturb the normal positioning of cortical neurons by disrupting differentiation rather than migration itself (Shariati et al., 2013). An ideal model system would enable analysis specifically in post-mitotic neurons that can be individually manipulated. As described below, *Manduca* provides such a model system.

Finally, although several of the mechanisms controlling axon guidance are unique from cell body migration, other aspects of their motility utilize overlapping pathways. At any given time in the developing mammalian cortex, subsets of neurons are undergoing somal translocation and rapidly extending their axons, while other later-born neurons are concurrently utilizing glial-guided locomotion to move their cell body. Therefore, to distinguish whether signaling molecules play a role in axon guidance or cell migration, an ideal model system would be one in which cell migration and axon outgrowth occur during distinct phases of development, as is the case in EP cells of *Manduca*.

Drosophila*: a model system for studying the function of APP *in vivo

APP family proteins are highly conserved across species, permitting a model systems approach for studying their roles *in vivo*. Insects contain just one APP isoform, APP-like (APPL) (Rosen et al., 1989), which is expressed exclusively in neurons (Martin-Morris and White, 1990). In contrast to the critical (but non-neural) function of the APP ortholog APL-1 in C. elegans (Daigle and Li, 1993, Hornsten et al., 2007), loss of APPL in *Drosophila* is not lethal. Similar to the non-lethal effects of deleting APP in mammals,

APPL null flies are viable and fertile, and show only minor locomotor defects. Notably, the deficits in phototaxis observed in APPL null flies could be rescued by human APP (Luo et al., 1992), demonstrating that these proteins are both functionally and structurally conserved; these results further support the use of insect model systems for understanding the role of APP *in vivo*. Notably *Drosophila* APPL loss- and gain-of-function studies (described below) have been informative for identifying a role for APPL in regulating synaptic formation, neuronal excitability, neurite outgrowth, and cytoskeletal dynamics. However, a role in neuronal migration remains to be identified.

Genetic studies in *Drosophila* have demonstrated a role for APPL in certain aspects of bouton formation: APPL null larvae have fewer synaptic boutons per neuromuscular junction (nmj) than wild type larvae (Torroja et al., 1999b), while overexpression of APPL increases bouton number (Ashley et al., 2005). Notably, the Go-binding domain of APPL is necessary for promoting parent bouton formation, while the internalization domain mediates satellite bouton formation (Torroja et al., 1999b). APPL null flies have also been shown to exhibit altered synaptic function. When motor neurons from third instar larvae were stimulated electrophysiologically, recordings made from their corresponding muscle targets revealed that APPL null flies had reduced excitatory junction potential (EJP) amplitudes compared to wild type controls. APPL null flies had higher mini EJP (mEJP) frequency and increased mEJP amplitude, but reduced quantal content, indicating alterations in presynaptic function (Ashley et al., 2005). Another study using cultured embryonic *Drosophila* neurons showed that APPL null neurons had lower potassium (K+) channel activation and enhanced A-type K+ currents compared to wild type neurons (Li et al., 2004), suggesting that APPL plays a role in altering the activation properties of neurons. Together these studies support a role for APPL in regulating synaptic formation and function.

Drosophila APPL has also been shown to alter neurite extension and branching in developing neurons, although the mechanisms by which it does so remain unresolved. In cultured neurons lacking APPL, neurite branching was enhanced, whereas APPL overexpression diminished branching. Paradoxically, both the overexpression and deletion of APPL reduced neurite length (Li et al., 2004). This is in contrast to another study in the adult *Drosophila* brain that showed that APPL overexpression in a subset of neurons enhanced axon arborization (Leyssen et al., 2005). Interestingly, these authors showed that APPL was upregulated following neuronal injury (similar to the upregulation of APP at sites of injury in the human brain) (Van Den Heuvel et al., 2000, Iwata et al., 2002), while flies lacking APPL had higher mortality rates following injury. These studies support a role for APPL in regulating neurite outgrowth both during development and in response to injury, but they do not clarify the mechanisms by which APPL regulates these responses.

APPL has also been postulated to regulate cytoskeletal dynamics. Li et al. showed that overexpressing mutated APPL resulted in tangled microtubules and mislocalization of actin filaments from growth cones to the neurite shaft (Li et al., 2004). Because this phenotype resulted from overexpression of a non-cleavable form of APPL, these observations do not distinguish between a possible gain- or loss-of-function effect. However, they do demonstrate a potential role for APPL in regulating cytoskeletal dynamics (Li et al., 2004), which in turn may provide a mechanism by which APPL signaling can ultimately regulate key aspects of neuronal development and motility. However, a robust assay for investigating the role of APPL in neuronal migration during development has until recently been lacking.

Manduca*: a model system for studying neuronal migration *in vivo

The developing *Manduca* Enteric Nervous System (ENS) provides an advantageous model system to study neuronal migration *in vivo* (Copenhaver, 2007). The insect gut is comprised of a foregut (FG), midgut (MG), and hindgut (HG) and like the vertebrate ENS, formation of the ENS in *Manduca* requires enteric neurons to undergo directed migration over a substantial distance to form a pair of small ganglia and an enteric plexus that innervates the gut (Copenhaver and Taghert, 1989a, b, Copenhaver et al., 1996). Unlike the neurons that form the vertebrate ENS, the enteric plexus cells (EP cells) of *Manduca* migrate along superficially-positioned longitudinal muscles (Copenhaver et al., 1996), permitting experimental manipulations and imaging throughout development (Copenhaver, 2007). Since embryonic development in *Manduca* is temperature-dependent, embryos can be precisely staged such that at 25^{o}C, each hour post-fertilization corresponds with 1% of development. The Copenhaver laboratory has developed a culture protocol for manipulating migrating EP cells while leaving the nervous system of the embryo completely intact. This experimental approach permits an *in vivo* analysis of candidate signaling molecules in migration. In addition, since the migratory sequence of EP cells is both stereotyped and well characterized, the effects of experimental manipulations in one group of animals can be precisely matched to identically staged controls (Copenhaver and Taghert, 1989a, b).

Previous studies described the developmental sequence of EP cell migration within the developing ENS in detail (schematically represented, Fig. 1.1A-D). At 35% of embryonic development, a population of about 300 EP cells delaminates from the neurogenic placode within the foregut epithelium, and the neurons become post-mitotic before beginning their first phase of migration (Copenhaver and Taghert, 1989b, a, 1990). From 40-55% of development, the EP cells spread bilaterally around the foregut, and then extend exploratory processes posteriorly onto one of eight preformed muscle

band pathways. The band pathway selected by each neuron is probabilistic and depends on their proximity to a particular pathway as well as on dispersal cues from neighboring cells (Copenhaver and Taghert, 1989b, a). Over the next 5-7 hours (55-62% of development), individual EP cells migrate along their selected muscle band pathway (b). Throughout this period of migration, the EP cells actively extend and retract their filopodia, exploring their environment, but ultimately stay aligned with their selected muscle band pathways while avoiding the adjacent interband regions (ib). After migration of the EP cells is complete (by 65% of embryogenesis), the neurons transition to a period of axon outgrowth, extending their axons posteriorly along the muscle band pathways. Meanwhile, a population of mitotically active glia, which over the past 10 hours have begun spreading out along the FG/MG boundary, migrates along the pathways established by the neurons (Copenhaver, 1993). By 75% of development (after cell migration and axon outgrowth is complete) the neurons undergo terminal differentiation and acquire position- and lineage-specific phenotypes (Copenhaver and Taghert, 1989a, 1990, Copenhaver et al., 1996). By the time of hatching at 100%, the neurons' cell bodies are fully ensheathed by glia, and the neurons have extended lateral branches to innervate the gut musculature (Copenhaver, 1993).

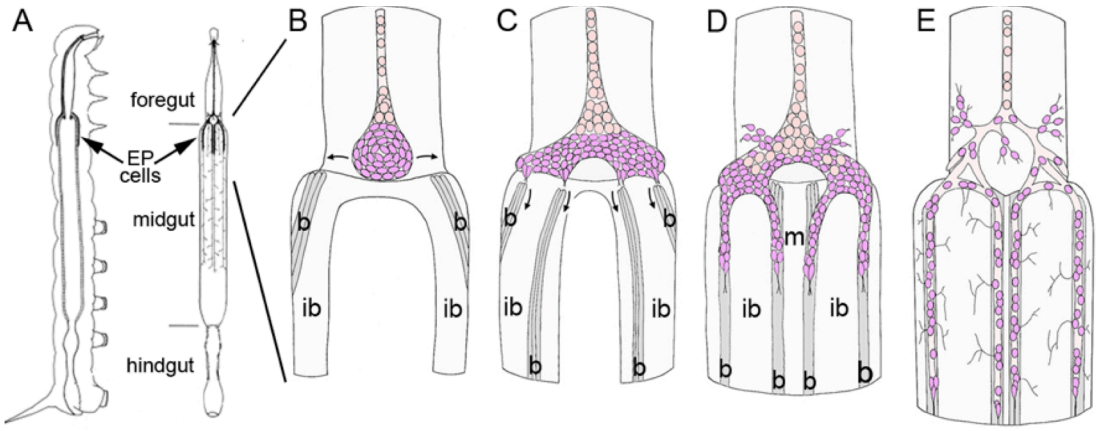

Figure 1.1. *Schematic representation of EP cell migration and development in the Manduca ENS.* **A)** Dorsal view of the *Manduca* ENS, demonstrating the positions of the foregut (FG), midgut (MG), and hindgut (HG) relative to the whole embryo. Arrows point to the migratory population of enteric plexus (EP) cells that innervate the musculature of the MG. **B-D)** Enlarged view of the FG/MG boundary, showing the pattern of EP cell migration during key periods of embryogenesis. **B)** At 40% of embryogenesis, EP cells (magenta) arise from invagination of the foregut epithelium, while proliferating glia (pink) emerge from neurogenic zones of foregut. **C)** By 55% of development, longitudinal muscle cells have formed eight band pathways "b" (four of the dorsal pathways are shown). EP cells have spread bilaterally around the FG/MG boundary and align their filopodia with the band pathways. **D)** From 55-62% of development, EP cells migrate along the muscle bands, while avoiding the interband region "ib" that is inhibitory to their growth. Meanwhile, a population of proliferating glia spread around the gut. **E)** By 80% of development, both cell migration and axon outgrowth are complete. EP cells differentiate and innervate the gut musculature. Glial cells, whose migration followed the path of the EP cells, ensheath the EP cell bodies. Figure adapted from Copenhaver and Taghert 1989a and Copenhaver 2007.

Using EP cell migration as an assay to study the role of APP in neuronal migration has many advantages over vertebrate systems. Like *Drosophila*, *Manduca* express just one APP isoform, APP-like (APPL), whose expression is restricted to neurons (Swanson et al., 2005). This cell type-specific expression pattern of *Manduca* APPL facilitates an analysis of its function in developing neurons without potential complications of additional APP isoforms in multiple cell types (as occurs in vertebrates). Additionally, since EP cells do not commence migration until after their terminal mitosis, the role of APPL in neuronal migration can be separated from its potential role in cell cycle determination. As noted above, since EP cell migration occurs prior to glial migration, experimental manipulations can also be focused on a period of development in which neuronal migration occurs independent of glial guidance. Finally, since the

migratory sequence of EP cells is both well characterized and precisely regulated, the role of APPL in filopodial extension, cell migration, and axon outgrowth can be experimentally separated.

To determine the role of a candidate signaling molecule in neuronal migration within the developing ENS, precisely staged *Manduca* embryos can be opened in culture with a small incision to expose the premigratory EP cells while leaving the nervous system completely intact. The neurons can then be treated with pharmacological reagents, bioactive peptides and antibodies, antisense constructs, and synthetic RNAs to alter gene expression and function in the entire population of neurons or in individual neurons (Horgan et al., 1995, Coate et al., 2007, Coate et al., 2008). Because the neurons remain accessible to experimental manipulation and imaging throughout development, these experimental strategies can be used to analyze the role of candidate guidance cues during distinct phases of neuronal differentiation. After the embryos have completed development, the preparations can be fixed as whole-mount preparations, immunostained, and analyzed with quantitative confocal methods and camera lucida analyses to assess multiple aspects of neuronal migration, axon outgrowth, and synaptic targeting (Wright et al., 1998, Wright et al., 1999, Copenhaver et al., 2011).

Previous studies in the Copenhaver laboratory have identified a number of guidance factors that direct EP cells to their target locations. Both the muscle band pathways and the EP cells express the Ig-CAM Fasciclin II (Fas II), and during phases of active migration, homophilic interactions mediated by Fas II on the neurons and their pathways direct the EP cells posteriorly along the gut musculature (Wright et al., 1999, Wright and Copenhaver, 2000). Guidance signals expressed along the band cells are required to guide EP cells into the developing ENS: when an individual band was ablated, neurons that could align with adjacent bands re-adjusted their course to an alternative pathway but never migrated onto the interband regions. This manipulation

demonstrated that attractive cues along the muscle band pathways are essential for EP cell migration and suggested that inhibitory cues in the interbands prevented neurons from migrating into those regions (Copenhaver et al., 1996). Consistent with this hypothesis, the Copenhaver laboratory identified the expression of *Manduca* Eph receptors in a population of inhibitory cells within the midline interband regions of the gut, which are normally repulsive to the EP cells. Conversely, the corresponding *Manduca* Ephrin ligand (MsEphrin) is expressed only by the motile EP cells, and activation of MsEphrin reverse signaling by midline MsEph receptors triggers EP cell retraction and prevents ectopic midline crossovers (Coate et al., 2007, Coate et al., 2008, Coate et al., 2009). In contrast, the receptors and ligands that prevent the EP cells from migrating onto the lateral interband regions have until recently remained unknown.

G protein signaling

Heterotrimeric G proteins consist of α, β, and γ subunits that transduce signals from a diversity of transmembrane G protein-coupled receptors (GPCRs). Ligand-induced activation of the GPCR causes GDP-to-GTP exchange on the α subunit that results in its dissociation from the $\beta\gamma$ dimer and from the receptor, and both the activated α-subunit and liberated $\beta\gamma$ dimer can then interact with a variety of downstream effectors, such as adenylyl cyclase, phospholipase C, or ion channels, among many others (Hille, 2001). Hydrolysis of GTP-to-GDP returns Gα to its inactive form and allows it to re-associate with the $\beta\gamma$ dimer, permitting the cycle of G protein signaling to continue.

In most instances, the α subunits are thought to confer specificity to the G protein that associates with a particular GPCR and have been characterized according to their classic downstream functions. For example Gsα was originally named for its ability to "stimulate" adenylyl cyclase, while Giα was found to "inhibit" adenylyl cyclase, although

most Gα subunits are now known to regulate multiple effector pathways in different contexts. Goα, on the other hand, was named for a largely unknown "other" function, and its role in neuronal development is still poorly understood.

Conventionally, GPCRs are 7-transmembrane spanning receptors that undergo ligand-dependent conformational changes to activate their associated G proteins. However, several single-pass transmembrane receptors have been identified that also regulate G protein activity, such as the Gi-activating insulin-like growth factor receptor (Nishimoto et al., 1987, Nishimoto, 1993). Although the mechanism by which these single-transmembrane GPCRs activate G proteins remains unclear, a common feature of single-pass GPCRs is a conserved BBXXB domain (Okamoto et al., 1990; Wu et al., 1995; Timossi et al., 2004). Based on sequence conservation of this domain and its ability to bind Go *in vitro*, APP was identified as a potential GPCR (Nishimoto et al., 1993).

APP can function as a Goα-associated receptor *in vitro*

Initial studies investigating whether APP could function as a G protein-associated receptor demonstrated that incubating synthetic human APP with heterotrimeric Go in phospholipid vesicles led to Goα activation (Nishimoto et al., 1993, Okamoto et al., 1995). In particular, a 20 amino acid region of the APP cytoplasmic domain encompassing the BBXXB domain (His 657-Lys 676) was shown to be both necessary and sufficient to induce Goα activation, identifying this region of APP as the putative Go-binding domain (Nishimoto et al., 1993). Full-length APP, in the absence of secretases or APP fragments, were also shown to activate Goα, consistent with the model that APP can function as a single-pass transmembrane GPCR. When APP was transfected into cultured cells, it coimmunoprecipitated Goα, whereas activating G proteins with GTPγS

reduced this association. These results support the hypothesis that APP functions as a Go-associated receptor that binds inactive Goα, whereas activation of the subunit causes it to dissociate from the receptor.

Although an endogenous ligand for activating APP in neurons remains unidentified (Zheng and Koo, 2011), antibodies targeting the extracellular domain of APP have been able to induce Goα activation *in vitro*. When APP and heterotrimeric Go complexes were expressed in phospholipid vesicles, application of 22C11, a monoclonal antibody targeting the extracellular domain of APP (APP_{66-81}), enhanced the generation of Goα-GTP (Okamoto et al., 1995). Notably, full-length APP was expressed in the absence of other signaling molecules in these assays, suggesting that APP can function as a receptor that promotes ligand-induced Goα activation. In contrast, when APP antibodies were applied to extracted membrane fractions derived from rat neurons, APP antibodies reduced Goα activation rather than enhancing it (Brouillet et al., 1999). However, since all of these studies were conducted in highly artificial systems, their contradictory results highlight the importance of validating APP-Go interactions *in vivo*.

The role of Goα in developing neurons

Goα is the most abundant protein in growth cones, and accordingly has been postulated to regulate multiple aspects of synaptogenesis and axogenesis (Edmonds et al., 1990). Consistent with this potential function, Goα expression is both temporally and spatially regulated in the nervous system; in both rat and *Drosophila* neurons, Goα expression commences just prior to axogenesis (Chang et al., 1988, Wolfgang et al., 1991, Fremion et al., 1999). In flies with Goα mutations, longitudinal motor axons were either misrouted or missing, suggesting that Goα plays a role in axon guidance (Fremion et al., 1999). In *Manduca*, Goα is the only heterotrimeric G protein detected in the motile

EP cells during their initial migration, and can be detected in both their cell bodies and leading processes (Copenhaver et al., 1995). Consistent with a developmental role for Goα in neurons, its expression commences just prior to migration onset and increases during periods of migration and axon outgrowth (Horgan et al., 1994).

To determine whether Go signaling regulates axon outgrowth, previous studies in the Copenhaver laboratory utilized mastoparan, a wasp venom capable of activating Goα and Giα. When individual EP cells were injected with mastoparan, neuronal migration was stalled, an effect that could be prevented with pretreatment of pertussis toxin (PTX) (Horgan et al., 1995). PTX inhibits Goα and Giα in most species by ADP-ribosylating a cysteine residue near their carboxyl terminal (West et al., 1985). However, since insect Giα lacks the cysteine residue targeted by PTX (Thambi et al., 1989) and Goα is the only detectable heterotrimeric G protein in the EP cells during migration (Copenhaver et al., 1995), these results indicate that Goα activation inhibits cell migration. Notably, injecting individual EP cells with preactivated Goα recapitulated the stalling phenotype, but injection of the $\beta\gamma$ dimer alone had no effect (Horgan and Copenhaver, 1998). These results suggest that Goα activation restricts the extent of EP cell migration, presumably in response to local environmental cues that interact with Goα-coupled receptors expressed by the EP cell filopodia.

Horgan and colleagues delineated this pathway further when they discovered that stimulating Goα in the EP cells induced the activation of large calcium (Ca^{+2}) transients through voltage-independent channels, whereas preventing Ca^{+2} influx or buffering Ca^{+2} elevation in the neurons precluded the inhibitory effects of Goα activation (Horgan and Copenhaver, 1998). This work supports a model whereby Goα activation leads to Ca^{+2}-dependent inhibition of neuron migration. However, the receptor responsible for activating Go in this pathway had not been identified.

In more recent work, the Copenhaver laboratory discovered that EP cells commence expression of APPL just prior to migration onset, and that APPL colocalizes with Goα in migrating neurons (Swanson et al., 2005). Based on the model that APP might function as a Go-coupled receptor (as described above), these findings support the hypothesis that APPL might also function as the Goα-coupled receptor in the EP cells, whereby APPL responds to inhibitory cues encountered in the interband regions and mediates Go-dependent repulsive responses in the EP cells and their leading processes. In addition, APPL undergoes a dynamic sequence of trafficking, processing, and post-translational modifications in developing neurons, but it is not understood how these dynamic events are associated with the potential role of APPL signaling in neuronal migration (Swanson et al., 2005).

APP-Go signaling in disease

In vitro evidence supporting a role for APP as a Go-coupled receptor also suggests a link for this pathway to AD pathology. As noted above, studies using artificial liposomes and extracted membrane preparations showed that APP can regulate Goα activity (Nishimoto et al., 1993), while cells transfected with familial AD-associated mutations in APP caused constitutive Goα activation (Okamoto et al., 1996) and accelerated cell death (Yamatsuji et al., 1996a, Yamatsuji et al., 1996b, Giambarella et al., 1997). Notably, these effects were prevented by treatment with the Goα inhibitor pertussis toxin (PTX) or when using FAD isoforms of APP lacking their Goα-binding domain (Yamatsuji et al., 1996a). In human brain samples from AD patients, disease progression correlated with elevated G protein activity and reduced APP-Goα interactions, suggesting a pattern of enhanced Goα activation and release (Reis et al., 2007, Shaked et al., 2009). This elevated G-protein activity is consistent with *in vitro*

studies showing that hyperactivation of Goα by APP can trigger a pathway that is neurotoxic (Galvan et al., 2006, Sola Vigo et al., 2009). These results suggest that aberrant APP-Go signaling may also be linked to AD pathology, although the mechanisms underlying this response are poorly understood. Determining whether APP-Go signaling plays a role in regulating aspects of neuron guidance, axon outgrowth, or synaptic formation under physiological conditions may therefore provide insight into how dysregulation of this pathway may contribute to neurodegenerative disease.

Thesis overview

The goal of this thesis was to (a) determine whether APPL may function as a Goα-associated receptor to regulate neuronal motility (Chapter 2); (b) determine the role of APPL signaling in neuronal migration and whether it is Go-dependent (Chapter 3); and (c) characterize the key changes in APPL trafficking and modifications that may regulate its role as a Go-associated guidance receptor (Chapter 4).

CHAPTER 2

Amyloid precursor proteins interact with the heterotrimeric G protein Go in the control of neuronal migration

Published in:

The Journal of Neuroscience. June 12, 2013. 33(24): 10165-10181

Abbreviated title: APP-Goα signaling in neuronal migration

Authors: Jenna M. Ramaker [1, 2], Tracy L. Swanson[1], and Philip F. Copenhaver[1, 2].

[1]Department of Cell and Developmental Biology and [2] Neuroscience Graduate Program, Oregon Health & Science University, Portland, OR, 97239. USA.

ACKNOWLEDGEMENTS

We thank Drs. Doris Kretzschmar, David Morton, and Larry S. Sherman for critical input on the manuscript. We also thank Drs. Vivian Budnik, Michael Gorczyca, and Kalpana White for generously sharing their APPL antibodies, fly lines, and helpful suggestions. Primary cultures of embryonic rat hippocampal neurons were provided by Dr. Gary Banker and Ms. Barbara Smoody, Jungers Center, OHSU. Mouse brain samples were kindly provided by Dr. Joseph Quinn and Christopher Harris (Department of Neurology, Portland Veterans Administration Medical Center, and Layton Center for Aging and Alzheimer's Disease Research, OHSU). Frozen samples of human brain tissue were made available by the Oregon Brain Bank (following established protocols), with the generous assistance of Dr. Randall L. Woltjer (Department of Pathology, OHSU). We thank Dr. Stephen Michnick (University of Montreal) for providing plasmids containing the coding domains for complementary portions of Venus Fluorescent Protein (Vn1 and Vn2). We are grateful to Dr. Stefanie Kaech and Ms. Aurelie Snyder for assistance with the confocal imaging analysis that was performed in the Advanced Light Microscopy Core, Jungers Center, OHSU. Support for this work was provided by NIH RO1 AG025525 and R21 NS080036 (to PFC), and by a grant from the Oregon Partners for Alzheimer's Research to JMR, who is a Vertex Scholar. The Oregon Brain Bank is supported by the Layton Aging and Alzheimer's Disease Center, NIH P30 AG8017. Confocal imaging was supported by NIH P30 NS061800. The authors declare no competing financial interests.

ABSTRACT

Amyloid precursor protein (APP) belongs to a family of evolutionarily conserved transmembrane glycoproteins that has been proposed to regulate multiple aspects of cell motility in the nervous system. Although APP is best known as the source of β-amyloid fragments (Aβ) that accumulate in Alzheimer's disease (AD), perturbations affecting normal APP signaling events may also contribute to disease progression. Previous *in vitro* studies showed that interactions between APP and the heterotrimeric G protein Goα regulated Goα activity and Go-dependent apoptotic responses, independent of Aβ. However, evidence for authentic APP-Goα interactions within the healthy nervous system has been lacking. To address this issue, we have used a combination of *in vitro* and *in vivo* strategies to show that endogenously expressed APP family proteins colocalize with Goα in both insect and mammalian nervous systems, including human brain. Using biochemical, pharmacological, and bimolecular fluorescence complementation assays, we have shown that insect APP (APPL) directly interacts with Goα in cell culture and at synaptic terminals within the insect brain, and that this interaction is regulated by Goα activity. We have also adapted a well-characterized assay of neuronal migration in the hawkmoth *Manduca* to show that perturbations affecting APPL and Goα signaling induce the same unique pattern of ectopic, inappropriate growth and migration, analogous to defective migration patterns seen in mice lacking all APP family proteins. These results support the model that APP and its orthologs regulate conserved aspects of neuronal migration and outgrowth in the nervous system by functioning as unconventional Goα-coupled receptors.

INTRODUCTION

Amyloid precursor protein (APP) is best known as the source of β-amyloid (Aβ) peptides that have been postulated to cause Alzheimer's disease (AD) (Hardy and Selkoe, 2002). However, therapeutic strategies targeting Aβ have been unsuccessful (Karran et al., 2011), suggesting that other APP-related processes may contribute to the disease (Mangialasche et al., 2010). APP is a member of an evolutionarily ancient family of type 1 glycoproteins that possess highly conserved extracellular and intracellular domains, indicating that they can participate in transmembrane signaling events (Turner et al., 2003, Gralle and Ferreira, 2007). Both full-length APP and its cleavage products have been ascribed multiple roles in neuronal motility (Perez et al., 1997, Sabo et al., 2003, Young-Pearse et al., 2008), including the control of neuronal migration in the developing brain (Herms et al., 2004, Rice et al., 2012). However, attempts to validate these functions *in vivo* have produced conflicting results, in part due to molecular redundancy with two closely related proteins (APLP1 and APLP2) and compensatory interactions by other guidance cues (Heber et al., 2000, Bergmans et al., 2010). Although APP may interact with a plethora of adapter and signaling proteins (Reinhard et al., 2005), the mechanisms by which APP and its orthologs regulate neuronal motility in the nervous system have remained elusive.

Intriguing studies have shown that APP interacts with the heterotrimeric G protein Goα, at least under some conditions. In artificial liposomes and extracted membranes, APP can regulate Goα activity (Nishimoto et al., 1993, Okamoto et al., 1995), while cells transfected with APP isoforms associated with familial AD (Hornsten et al.) exhibit constitutive Goα activation and accelerated apoptosis (Okamoto et al., 1996, Yamatsuji et al., 1996a, Yamatsuji et al., 1996b). Notably, these effects were prevented by the Gi/o inhibitor pertussis toxin or by expressing APP isoforms lacking their putative Go-binding

domain (Yamatsuji et al., 1996a, Yamatsuji et al., 1996b). Elevated G protein activity and decreased APP-Goα interactions have also been detected in brain samples from AD patients (Reis et al., 2007, Shaked et al., 2009), while cell culture studies suggest that Aβ peptides induce neurotoxic effects via the dysregulation of APP-Goα signaling (Sola Vigo et al., 2009). These results support the model that APP might function as an atypical Go-coupled receptor whose normal functions are disrupted in AD. However, a viable assay for investigating endogenous APP-Goα interactions in neurons has been lacking.

To address this issue, we have established the embryonic nervous system of *Manduca sexta* (hawkmoth) as a novel preparation for testing how APP family proteins control neuronal migration. As in other invertebrate models, *Manduca* express only one APP ortholog (APP-like; APPL), and previous studies have shown that both APPL and Goα are robustly expressed by migratory neurons in this system (Horgan et al., 1995, Swanson et al., 2005). We have now used a combination of *in vitro* and *in vivo* assays to determine whether endogenously expressed APP family proteins interact with Goα in neurons from multiple species; whether this interaction is direct; and whether APPL-Goα signaling regulates neuronal migration within the developing nervous system.

MATERIALS AND METHODS

Whole-mount immunostaining of staged embryos

Synchronous groups of embryos of either sex were collected from an in-house colony of *Manduca sexta* and staged according to a panel of external and internal developmental markers (Copenhaver and Taghert, 1989a, b). When reared at 25°C, embryogenesis is complete in 100 hr, whereby 1% of development is equivalent to 1 hour post fertilization (hpf). Embryos were collected at 55, 58, and 65 hpf (before, during, and after EP cell migration) and dissected in defined saline (140mM NaCl, 5mM KCl, 28mM glucose, 40mM CaCl2, and 5mM HEPES, pH 7.4) to expose the Enteric Nervous System (ENS), as described previously (Coate et al., 2007). For immunohistochemical analysis, embryos were filleted dorsally to expose the developing ENS and subsequently fixed in 4% paraformaldehyde (PFA; Sigma/Aldrich) in phosphate-buffered saline (PBS) for 1 hr at room temperature. After extensive rinsing in PBS plus 0.1% Triton X-100 (PBST), embryos were pre-incubated for 1 hr in blocking solution (10% normal horse serum plus 0.1% sodium azide in PBST). Embryos were then incubated in antibodies diluted in blocking solution with constant agitation for either 1 hr at room temperature or overnight at 4°C.

For immunostaining, antibodies were used at the following concentrations: mouse anti-Fasciclin II (Fas II; C3 monoclonal), 1:20,000 (Wright et al., 1999); affinity-purified anti-Goα, 1:100 (generated against AA 343-355 of *Manduca* Goα; Horgan et al., 1995); anti-cAPPL, 1:2500 (previously referred to as anti-msAPPL-cyt), generated against the sequence YENPTYKYFEVKE within the cytoplasmic domain of *Manduca* APPL (Swanson et al., 2005). We also generated an additional polyclonal antiserum (anti-nAPPL, #21506; 1:5000) against a fusion protein derived from the E1 ectodomain region of *Manduca* APPL (AA 1-197). The specificity of this antiserum for APPL was

validated in western blots of *Manduca* and *Drosophila* lysates; by coimmunohistochemical staining with our other APPL antibodies; by pre-adsorption against the fusion protein (versus control fusion proteins); and by cross-immunoprecipitation with other anti-APPL antibodies (data not shown). Primary antibodies against Fas II and APPL were detected with fluorochrome-conjugated secondary antibodies diluted in blocking solution. Antibodies conjugated to Alexa Fluor 488, 568 or 647 (Molecular Probes/Life Technologies) were used at a final concentration of 1:1000; antibodies conjugated to Cy3 and DyLight 549 (Jackson ImmunoResearch) were used at 1:400. Anti-Goα was detected with anti-guinea pig secondary antibodies coupled to horseradish peroxidase (HRP) and visualized using the tyramide signal amplification system (TSA Plus Fluorescence Kit, PerkinElmer), following the manufacturer's instructions. Whole-mount immunostained preparations were stored in Elvanol (Banker G, 1998) and imaged with an Olympus FluoView 300 laser scanning confocal head mounted on an Olympus BX51 microscope (located in the Live Cell Imaging Facility, Center for Research on Occupational and Environmental Toxicology), or with an inverted Zeiss LSM710 confocal microscope (located in the Advanced Imaging Center of the Jungers Institute, OHSU). Maximum intensity projections of flattened Z-stack confocal images were generated using MetaMorph software. To illustrate the relationships between the EP cells and their muscle band pathways (shown in Figure 2.1), Fas II immunostaining in each panel was cropped at either the FG/MG boundary (55 hpf) or at positions adjacent to the most posterior neurons on each pathway (58-65 hpf). The cropped Fas II images were then montaged with the flattened Z-stack images of APPL immunostaining in the same preparations.

To examine the colocalization of mammalian APP with Goα, primary cultures of embryonic rat hippocampal neurons (grown on coverslips) were provided by Dr. Gary

Banker (Dotti et al., 1988). Neurons were fixed with 4% PFA in PBS for 15 min at room temperature, permeabilized for 10 min with 0.1% PBST, and blocked for 15 min with 5% fish skin gelatin in PBST. The following primary antibodies were applied for 60 min at room temperature: anti-22C11 targeting AA 66-81 of human APP (Millipore #MAB348, 1:100); anti-pAPP, specific to p(Thr_{668}) within AA 666-670 of human APP (Sigma-Aldrich #SAB4300153; 1:200); and affinity-purified anti-Goα, 1:300 (Horgan et al., 1995). Secondary antibodies conjugated to Alexa Fluor 488, 568 or 647 (Molecular Probes/Life Technologies) were used at a final dilution of 1:1000. Coverslips were mounted in Elvanol and imaged as described above.

Coimmunoprecipitation and immunoblotting

Staged *Manduca* embryos (20 per reaction; dissected at 65 hpf) and adult *Drosophila* heads (20 per reaction) were collected on dry ice and homogenized in 1% Triton lysis buffer (1% Triton X-100, 150 mM NaCl, 50 mM Tris, pH 8) or 1% NP40 lysis buffer (150 mM NaCl, 50 mM Tris, pH 8). Aliquots of each lysate were centrifuged at 16,000 rpm for 10 min, and the supernatants were pre-cleared with Protein A/G beads (Santa Cruz Biotechnology). The supernatants were then incubated with primary antibodies (described below) for 1-3 hr at room temperature or overnight at 4°C and incubated with prewashed beads for 1 hr. The bead-bound antibody complexes were then pelleted by centrifugation. After washing in chilled lysis buffer, immunoprecipitated protein complexes were eluted by boiling the beads in SDS sample buffer for 1 min (Swanson et al., 2005). The samples were then separated on 10% or 4-12% Criterion polyacrylamide gels (Bio-Rad), transferred to nitrocellulose, and immunoblotted with antibodies diluted in Tris-buffered saline plus 0.1% Tween-20 (Polysorbate) and 5% Carnation dry milk.

For coimmunoprecipitations using mouse brain, frozen tissue samples were provided by Dr. Joseph Quinn and Christopher Harris (Department of Neurology, Portland Veterans Administration Medical Center, and Layton Center for Aging and Alzheimer's Disease Research, OHSU). Brains were divided in half under liquid nitrogen, extracted in NP40 lysis buffer, and immunoprecipitated by the methods described above. Alternatively, membranes were prepared from lysed mouse brain samples following the protocol described in (Hortsch, 1994). Briefly, tissue was homogenized in hypotonic saline (100 mM Tris-HCl, pH 8.0; 1mM EDTA) and centrifuged at 100,000 g for 1hr at 4^{o}C. The pellets were then re-suspended in NP40 lysis buffer, incubated with primary antibodies for 3 hr at room temperature or overnight at 4^{o}C, and immunoprecipitated as described above. For coimmunoprecipitations using human brain tissue, frozen samples were made available from the Oregon Brain Bank (collected and distributed following established protocols), with the assistance of Dr. Randall L. Woltjer (Department of Pathology, OHSU). Approximately 90 mg tissue per reaction was homogenized with a Dounce homogenizer in 1 mM EDTA, 100 mM NaCl, 50 mM Tris-HCl (pH 8), plus 1% Triton X100 (Strickler et al.) and 0.5% sodium cholate (Sigma-Aldrich). Undigested protein was then pelleted in a Beckman L7-55 ultracentrifuge for 1 hr at 100,000 g at 4^{o}C, and the supernatants used for subsequent immunoprecipitation reactions (as described in Shaked et al., 2009). Samples were incubated with antibodies overnight at 4^{o}C with continuous rocking and then immunoprecipitated, as described above.

The following antibodies were used to immunoprecipitate APP-associated proteins: for *Manduca* lysates, we used anti-cAPPL and anti-nAPPL-EX, previously referred to as anti-msAPPL-ect (generated against the sequence EDDDYTDADDSAWPRPES within the extracellular domain of *Manduca* APPL; Swanson et al., 2005). For *Drosophila* lysates, we used anti-cAPPL. For mouse lysates, we used anti-nAPP (Sigma-Aldrich #8967, targeting amino acids 46-60 of human

APP_{695}) and anti-APP_{668} (Sigma-Aldrich #SAB4300464, targeting AA 666-670 of human APP_{695}); and for human brain lysates, we used anti-nAPP (Sigma-Aldrich #8967). For each experiment, replicate lysates were immunoprecipitated with matched control immunoglobulins: purified IgY (7.5 μg, Aves #N-1010) was used in experiments employing chicken-derived antibodies; purified IgG (10-12 μg, Jackson Laboratories #1-000-003) or normal rabbit serum (1-3 μl) was used in experiments employing rabbit-derived antibodies. The following antibodies were used to detect G proteins that were coimmunoprecipitated with APP or APPL: anti-Goα (1:100-1:250; Horgan et al., 1995); anti-Gsα (1:1K) against a conserved sequence shared by *Drosophila* and mammalian Gsα (Santa Cruz Biotechnology #sc-383); anti-Giα (1:1000), targeting the conserved C-terminal sequence 327–355 (gift from Dr. Michael Forte; as described in Copenhaver et al., 1995); and anti-Gβγ (1:75, BD Transduction Laboratories). Secondary antibodies coupled to Horseradish Peroxidase (HRP) were purchased from Jackson ImmunoResearch and used at 1:10K, and detected using standard chemiluminescent protocols (with either West Pico or West Femto substrates from Thermo-Fisher).

For coimmuniprecipitation experiments to test whether the Go-binding domain in APPL was required for APPL-Goα interactions in *Drosophila*, we used the following transgenic lines (provided by Dr. Vivian Budnik and Michael Gorczyca): $Appl^{d}$, a null mutation of the *Appl* gene (Luo et al., 1992); *UAS-*$Appl^{sd}$, encoding an in-frame mutation that lacks AA 758-791 (and has the point mutations $Arg_{795}Arg_{796}$-$Leu_{795}Ser_{796}$), which is insensitive to secretase cleavage (secretase-deficient APPL; Luo et al., 1992); and *UAS-*$Appl^{sd\Delta Cg}$, secretase-deficient APPL that lacks AA 845-855 within its Go domain ($APPL^{sd}\Delta Cg$; Torroja et al., 1999b). The UAS transgenes were crossed into $Appl^{d}$ flies to test the interactions of each APPL variant in the absence of wild type protein; $Appl^{d}$ flies (lacking all APPL) served as a negative control. Expression of the transgenes was

accomplished with the GAL4/UAS system (Brand and Perrimon, 1993), using the eye-specific GMR-GAL4 driver line (Bloomington Stock Center). For these assays, *Drosophila* lysates were immunoprecipitated with anti-Goα (EMD/Calbiochem #371726) and immunoblotted with either anti-cAPPL (1:2500) or anti-G$\beta\gamma$ (1:75), as described above.

Analysis of direct Goα-APPL interactions by BiFC

Plasmids containing the coding domains for complementary portions of Venus Fluorescent Protein (Vn1 and Vn2) were provided by Dr. Stephen Michnick (University of Montreal) and used for a modified version of the Protein-fragment Complementation Assay (Remy et al., 2004). The APPL-Vn1 plasmid construct was generated in pcDNA3 (Invitrogen) by ligating the full-length coding domain of APPL in-frame with Vn1, consisting of AA 1-158 of Venus Fluorescent Protein plus a 10 amino acid glycine-rich linker domain (Benton et al., 2006, Mervine et al., 2006). The APPLΔGo-Vn1 construct was generated using PCR primers designed to omit the full Go-binding domain of *Manduca* APPL (AA 762-791; HAQGEVQVEQTGVVAPTPEERHVANMQING), identified by alignment with the Go-binding domain of human APP_{695} (His657-Lys676; as described in Nishimoto et al., 1993). Fusion constructs containing the coding domains of insect Goα, Giα, and Gsα were ligated in-frame at their N-termini with Vn2, consisting of AA 159-239 of Venus Fluorescent Protein plus a 10 amino acid glycine-rich linker region. For an *in vitro* analysis of bimolecular fluorescence complementation (BiFC) induced by reassembly of Vn1- and Vn2-tagged fusion proteins, COS7 cells were plated on poly-lysine coated coverslips (at 20% density) and transiently transfected the following day with either 1000 ng total plasmid DNA or 20 ng plasmid DNA plus 980 ng pGEM-T helper plasmid, using *Trans*IT-LT1 (Mirus Bio LLC). After 18, 24, or 48 hr, the cells were

fixed for 10 min in 4% PFA, followed by incubation in blocking solution (PBS plus 10% normal horse serum) for 30 min. Primary antibodies were diluted in blocking solution and applied to the cells for 1 hr at room temperature. For this analysis, we labeled the cells with anti-nAPPL (1:1000), anti-Goα (1:100), and mouse anti-GFP (Invitrogen/Molecular Probes, A-11120), which recognizes the Vn2 fragment of the holoprotein. After rinsing with PBS, the cells were incubated with Alexa 568- and Alexa 647-conjugated secondary antibodies (diluted 1:1000) for 30 min, rinsed again, and mounted on glass slides with Elvanol for imaging with confocal microscopy. Z-stack images of each cell (5 optical sections per stack) were acquired under linear parameters, using identical laser and acquisition settings. The stacked images were flattened in MetaMorph and adjusted for brightness and contrast, using identical settings for all cells imaged in an experiment. To quantify membrane-associated BiFC levels generated by different combinations of the Vn1 and Vn2 constructs, maximum intensity projections of each stacked image were generated in MetaMorph, and intensity values were determined for equivalent perimeter segments for each cell in Fiji. Values were obtained independently for anti-APPL, anti-Goα, and BiFC (visualized in different wavelengths). The mean values of average pixel intensities were then derived for replicate sets of cells (at least 20 cells per group), and used to evaluate statistical differences between the BiFC signals generated by the Venus-tagged proteins when expressed individually or in combination.

For BiFC analysis of APPL-Goα interactions *in vivo*, constructs containing the coding domains for *Manduca* APPL, APPLΔGo, and Goα were cloned in-frame with Vn1 and Vn2, respectively. The constructs were then ligated into the pUASg (Appl) or pUAST (Goα) vector and used to transform *Drosophila* (BestGene Inc; Chino Hill, CA). Transformant flies homozygous for UAS-APPL-Vn1, UAS-APPLΔGo-Vn1, UAS-Vn2-Goα, or recombined to express combinations of the constructs (UAS-APPL-Vn1 + Vn2-

Goα or UAS-APPLΔGo-Vn1 + Vn2-Goα) were crossed with flies carrying the eye-specific GMR-GAL4 promoter construct (Brand and Perrimon, 1993). Mated flies were maintained at 28°C, and third instar larvae were collected at various stages of development for imaging and analysis. Larval eye discs were isolated in PBS and immediately placed on ice. Discs were fixed for 10 min in PBS plus 4% PFA at 4°C, then blocked for 30 min with 10% normal horse serum in PBS plus 0.1% Triton X-100. To detect the expression of either Vn1 or Vn2 fusion constructs, discs were immunostained with polyclonal GFP antibodies (Aves #GFP1020 or Invitrogen #A11122; 1:1000), which recognize both fragments of Venus fluorescent protein. To amplify BiFC signals specifically induced by the reassembly of Vn1 and Vn2, we used anti-GFP (Sigma-Aldrich #G6539; 1:1000), which only labels the recombined protein. Discs were incubated in primary antibodies for 1.5 hr, then rinsed with PBS-0.1% triton, and incubated with secondary antibodies (diluted in blocking solution) for 30 min at room temperature. DyLight 549 goat-anti-chick antibodies (Jackson ImmunoResearch) were used at 1:200; Alexa-conjugated secondary antibodies (Molecular Probes) were used at 1:1000. Whole discs were mounted in Elvanol, and flattened Z-stack images were obtained by confocal microscopy and ImageJ processing, using the same number of optical sections and laser settings for each disc.

Manipulations of endogenous G protein activity

To test the role of G protein activity in regulating Goα-APPL interactions, lysates were prepared from staged *Manduca* embryos or from GV1 cells (Hiruma and Riddiford, 2004) a *Manduca* cell line of ectodermal origin that endogenously expresses APPL and Goα (as well as other neuronal proteins; Coate et al, 2009). Cells and tissues were homogenized in either chilled NP40 buffer (1%) or RIPA buffer, and clarified by

centrifugation at 13,000 rpm for 10 min. The following reagents were then added to replicate aliquots of the lysates at the following final concentrations: GTPγS (Sigma), 0.01-10 μm; GDPβS (Sigma), 1-20 μm; Mas7 (a mastoparan analog with enhanced activity; Enzo Life Sciences), 50-400 μm; Mas17 (an inactive mastoparan analog; Enzo Life Sciences), 30 μm; and Pertussis Toxin A protomer (Enzo Life Sciences), 1-4 μg/ml plus 1 mM NAD+. After incubation at room temperature for 30 min, the lysates were briefly centrifuged to remove cellular debris and analyzed by coimmunoprecipitation and immunoblotting, as described above. For analysis using the Odyssey Infrared Imaging System (LI-COR Biosciences), immunoblots were labeled with IRDye 680- and 800-conjugated secondary antibodies (from Rockland Immunochemicals and Molecular Probes/Invitrogen). Quantification of band intensities was performed using Odyssey software, and each experimental condition was normalized with respect to untreated control immunoprecipitations (run in parallel on the same immunoblots). Alternatively, immunoblots were processed using the chemiluminescent protocols described above; the blots were then imaged on X-ray film with X-OMAT processing, scanned into TIFF files with Photoshop (Adobe), and relative pixel intensities were calculated for bands of interest using ImageJ. For each treatment condition, relative levels of Goα and APPL were normalized to levels detected in matched control samples (run on the same immunoblots) and imaged with identical parameters. Goα levels were then calculated as a ratio of Goα/APPL levels; each experiment was repeated at least 3 times. For statistical analysis, levels of immunoprecipitated Goα for each experimental condition were normalized to their respective untreated controls. Mean Goα levels for each treatment condition were then compared to matched untreated controls, using Student's two-tailed *t* tests. Each experiment was repeated at least three times.

Embryonic culture and migration assays

Staged *Manduca* embryos were isolated at 52 hpf, shortly before the onset of EP cell migration. Embryos were dissected from their egg shells and extraembryonic membranes and placed in Sylgard-coated chambers filled with either culture medium: 50% Schneider's *Drosophila* medium, 40% MEM with Hank's salts, 9.7 % heat-inactivated normal horse serum, 0.2% 20-hydroxyecdysone, 0.1% insulin, and 0.01% penicillin-streptomycin (pen-strep), pH 7.4; or defined saline: 140mM NaCl, 5mM KCl, 28mM glucose, 5mM HEPES, 4 mM $CaCl_2$, 0.2% 20-hydroxyecdysone, 0.1% insulin and 0.01% pen-strep, pH 7.4 (Horgan and Copenhaver, 1998). A small incision in the dorsal body wall between segments T2 and T3 (a position just anterior to the foregut-midgut boundary) was made to expose the enteric plexus on the developing gut. The premigratory EP cells were then directly treated with experimental reagents targeting APPL or Goα. The incision was then gently closed with glass electrodes, and the embryos were allowed to develop in culture for another 12-18 hr at 28°C, spanning the time of normal EP cell migration and axon outgrowth. In experiments targeting subsequent aspects of axon elongation and terminal branch formation, embryos were opened in culture at 65 hpf (at the end of the migratory period), treated with experimental reagents, and incubated for an additional 24 hr, spanning the normal period of synaptogenesis on the midgut musculature (Wright et al., 1998). Aluminum fluoride (AlF_{4-}) was prepared by diluting premixed solutions of 0.6 M NaF and 0.5 mM $AlCl_3$ (1:40) in culture medium to give a final concentration of 12.5 μM AlF_{4-}; equivalent concentrations of NaCl premixed with $AlCl_3$ served as controls (after Horgan and Copenhaver, 1998). Pertussis toxin (PTX; intact molecule; Gibco/Life Technologies) was preactivated with 1M dithiothreitol and diluted in serum-free culture medium (Horgan et al., 1995). Treatment of the EP cells with anti-nAPPL antibodies (#21506) was

performed by diluting a purified IgG fraction of the antibody in culture medium; equivalent concentrations of control rabbit IgG (Jackson ImmunoResearch) were used as controls.

At the end of each experiment, embryos were dissected completely to expose the ENS, then fixed and immunostained with anti-Fas II to reveal the full extent of EP cell migration and outgrowth (Wright et al., 1999). Anti-Fas II immunoreactivity was detected with biotinylated anti-mouse secondary antibodies (1:200) and the avidin-biotin-HRP protocol from Vector Laboratories (ABC kit; Burlingame, CA). The distributions of postmigratory EP cells and their axons were analyzed using photomicrographic and camera lucida techniques. Ectopic outgrowth was quantified using a grid-based analysis of EP cell processes that had extended into each interband region of the midgut (normally inhibitory to the neurons); ectopic neurons were counted manually. To account for day-to-day variability in culture conditions, values obtained from each experimental preparation were normalized to mean values calculated from replicate sets of matched control preparations included with each experiment. Pairwise statistical differences between control and experimental groups were then calculated using Student's two-tailed *t* tests.

Morpholino antisense oligonucleotides (morpholinos; Gene Tools Inc.) were designed against several regions of the mRNA sequence encoding *Manduca* APPL, and initially tested for their effectiveness and specificity in GV1 cells. Morpholinos were applied to cultured GV1 cells for 48 hr (grown in GV1 medium: 3.32g lactalbumin hydrolysate and 20 ml 50x Yeastolate per liter of Grace's medium, plus 10% heat inactivated FBS and 1% pen-strep). The cells were then lysed in chilled NP40 lysis buffer, and residual APPL levels were analyzed by western blotting methods; the expression of several control proteins (including Fas II and tubulin) were visualized in the same samples to monitor for off-target effects of the morpholinos. The most effective

APPL-specific morpholino (directed against a sequence spanning the initiation codon; CCGCGTTGCTTCCCA-CCAGCCC) was subsequently used to knock down APPL expression in cultured embryos. Morpholinos were diluted in defined saline (1-50 μM) supplemented with 10% heat-inactivated horse serum, 0.5% pen-strep, 0.2% 20-hydroxyecdysone, 0.1% insulin, and 0.2 M L-glutamine. Embryos were opened in culture at 48 hpf, and the morpholinos were delivered into the EP cells with 0.6 % Endo-Porter (Coate et al., 2008). Matched sets of embryos were treated with standard control morpholinos (Gene Tools, Inc.) or Endo-Porter alone. The embryos were then allowed to develop for an additional 24-48 hr at 28^{o}C before fixation and analysis, as described above. Matched sets of cultured preparations were also immunostained with anti-nAPPL to monitor the effectiveness of the morpholinos in inhibiting APPL expression.

RESULTS

Goα colocalizes with endogenous APPL and APP in motile neurons

During formation of the Enteric Nervous System (ENS) in *Manduca*, a population of ~300 neurons (EP cells) undergoes a stereotyped sequence of migration along preformed pathways to form a branching nerve plexus (the EP), which spans the foregut-midgut boundary (FG/MG; Fig. 2.1A-C). After delaminating from a neurogenic placode in the foregut epithelium (Copenhaver and Taghert, 1990), the EP cells first spread bilaterally around the foregut (from 40-55 hpf). During this phase of migration (Fig. 2.1A; 52 hpf) approximately equal subsets of neurons align with one of the eight longitudinal muscle bands that have recently differentiated on the midgut surface ('b' in Fig. 2.1A; only the four dorsal bands are shown). From 55-65 hpf (Fig. 2.1B; 58 hpf), the neurons migrate in a chain-like manner along each of the muscle bands while avoiding adjacent interband regions ('ib'). From 65-75 hpf (Fig. 2.1C; 65 hpf), the neurons continue to elaborate long axons posteriorly along the midgut (Copenhaver and Taghert, 1989a, b). During this process, EP cells actively extend and retract filopodia onto the band and interband muscles but remain aligned with their selected band pathways. Only once migration and axon outgrowth are complete do the neurons eventually sprout lateral branches that innervate the adjacent interband musculature (from 80-100 hpf). However, only a small number of EP cells normally extend processes onto the interband regions near the foregut-midgut boundary (asterisks in Fig. 2.1F; Copenhaver and Taghert,1989b).

In previous work, we showed that a combination of permissive and repulsive guidance factors regulate the guidance of the EP cells along the muscle bands. The Ig-CAM Fasciclin II (Fas II; the insect ortholog of NCAM and OCAM) is expressed by both the EP cells and the muscle band cells, and homophilic signaling interactions mediated

by Fas II play an essential role in promoting migration along these pathways (Copenhaver et al., 1996, Wright et al., 1999). (For clarity, the montages in Fig. 2.1D-F include Fas II immunostaining only in the muscle bands; see methods). In addition, we recently showed that the migratory EP cells express APPL (Fig. 2.1D-F; green), coincident with their expression of Goα (Horgan et al., 1995, Swanson et al., 2005). Given the *in vitro* evidence that APP can interact with Goα (Nishimoto et al., 1993) and our previous data showing that Goα-dependent signaling restricts the extent of EP cell migration (Horgan and Copenhaver, 1998), we investigated whether APPL might function as a transmembrane receptor that functionally interacts with Goα in these migratory neurons.

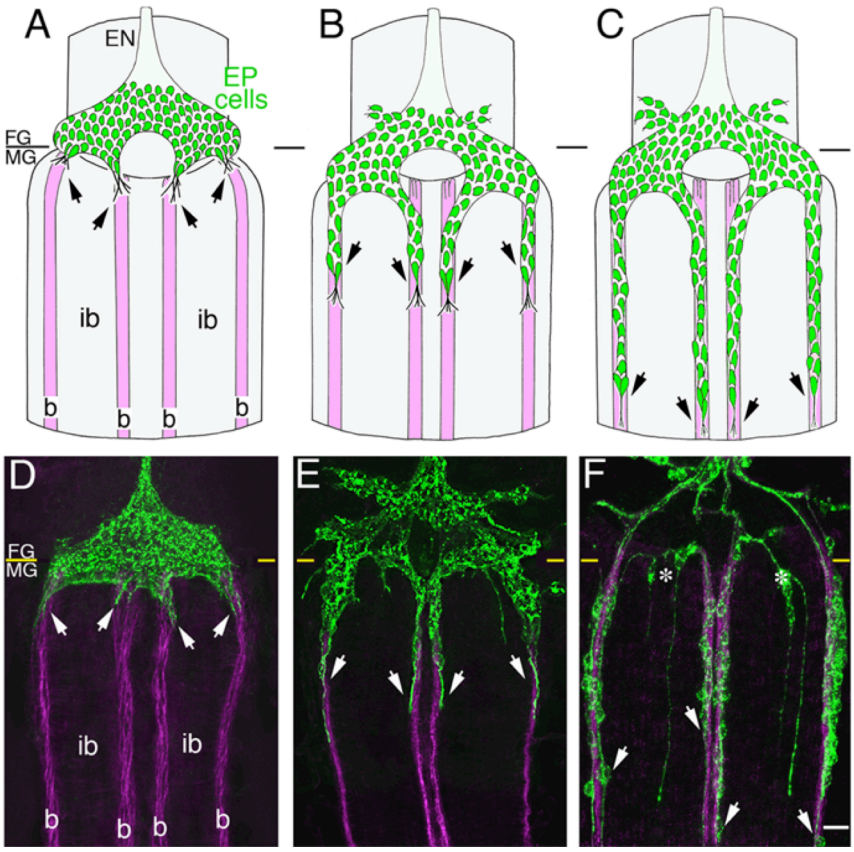

Figure 2.1. *APPL is expressed by migrating EP cells and their motile processes.* **A-C)** Schematic representation of the developmental sequence of EP cell migration (green) along the eight muscle band pathways (magenta) to form the enteric plexus of the ENS in *Manduca* (only the dorsal four muscle bands are shown). **D-F)** Montages of whole-mount preparations of filleted embryos that show the developing ENS from corresponding embryonic stages, immunostained for APPL (green) and TM-Fas II (magenta; Fas II). (For these montaged images, Fas II staining was omitted from the EP cells to clearly show their alignment with the muscle bands; see methods). **A**, **D)** By 55 hpf, the EP cells have spread bilaterally around the surface of the foregut, adjacent to the foregut-midgut boundary (FG/MG); all of the neurons express APPL as they extend filopodia (arrows) preferentially onto the Fas II-positive muscle band pathways ("b"). **B**, **E)** By 58 hpf, subsets of EP cells have begun migrating along each muscle band pathway, while avoiding the adjacent interband regions ("ib"). APPL is strongly expressed throughout the motile cell bodies and within their leading processes that have extended along the bands (arrows). **C**, **F)** By 65 hpf, the EP cells have completed their migration but will continue to grow axonal processes posteriorly along the band pathways for another 15 hr, before eventually innervating the lateral visceral musculature. Throughout this developmental sequence, the EP cells maintain robust levels of APPL expression (particularly in their most motile regions) and remain confined to the muscle band pathways, although a small number occasionally extend processes from the foregut-midgut boundary onto the interband regions (asterisks). Abbreviations: hpf= hours post fertilization; FG/MG = foregut-midgut boundary; EN = esophageal nerve of the foregut; EP cells = Enteric Plexus neurons; b = muscle bands; ib = interband musculature of the midgut. White scale bar: 50 μm.

Past studies have shown that insect APPL contains all of the key structural features that typify APP family proteins in other species (Fig. 2.2A), including conserved E1 and E2 extracellular domains that may interact with potential ligands (Luo et al., 1990, Swanson et al., 2005) and an Aβ domain that has neurotoxic effects when overexpressed as a cleavage fragment (Carmine-Simmen et al., 2009). In addition, the cytoplasmic domain of *Manduca* APPL shares strong similarity with equivalent domains in other APP-related proteins (Fig. 2.2B), including 88% sequence identity with *Drosophila* APPL and 77% identity with human APP_{695} (Swanson et al., 2005). Of particular note is the TPEER region within the putative Go-binding domain ("Go"; Nishimoto et al., 1993) and the NPXY phosphotyrosine binding domain ("Y") (Chen et al., 1990, Hoe and Rebeck, 2008) that are 100% identical between *Manduca* and mammalian APP family proteins, suggesting that these domains regulate conserved signaling functions. As with human APP_{695}, APPL undergoes a dynamic sequence of secretase-dependent cleavage to produce soluble ectodomain fragments, C-terminal fragments (CTFs), and APP intracellular domains (AICDs) (Carmine-Simmen et al., 2009, Bolkan et al., 2012), each of which might affect different aspects of cell motility (Turner et al., 2003, Gralle and Ferreira, 2007). To investigate whether APPL can act as a Goα-associated receptor in migratory neurons, we first examined whether APPL colocalized with Goα at the plasma membrane of the EP cells, consistent with a potential role in signal transduction.

For the current analysis, we used a panel of well-characterized antibodies against the extracellular and intracellular domains of APP and APPL (shown schematically in Fig. 2.2A), including antibodies targeting conserved residues within the putative Go-binding domain. Double immunostaining the developing ENS with anti-nAPPL (against the N-terminal extracellular domain; green) and anti-cAPPL (against the

C-terminal intracellular domain; magenta) verified the presence of the full-length holoprotein at the plasma membrane of migrating neurons (Fig. 2.2C-F, arrowheads) and their leading processes (Fig. 2.2G-J, arrowheads). Also notable in these preparations was the abundance of additional APPL within large perinuclear vesicles, as well as smaller vesicle populations containing either N-terminal (green) or C-terminal fragments (magenta) of the holoprotein (Fig. 2.2C-F). We also found that the subcellular distributions of APPL and its fragments were markedly altered during periods of active migration and outgrowth, during which transmembrane APPL accumulated in regions of active growth (as manifested by the colocalization of N- and C-terminal epitopes at the membrane). These observations support our previous evidence that APPL undergoes a dynamic sequence of trafficking, processing, and post-translational modifications that correlate with specific phases of EP cell differentiation (Swanson et al., 2005). They also are consistent with recent studies on APP trafficking in neuroblastoma cells (Muresan et al., 2009), suggesting that much of the newly synthesized holoprotein may be proteolytically cleaved and sorted to distinct compartments prior to their transport out of the cell body. This process may therefore help regulate the bioavailability of APPL as a transmembrane receptor during phases of active motility (unpublished observations). To determine whether membrane-associated APPL colocalized with Goα in the EP cells, embryos were coimmunostained with antibodies against anti-nAPPL (green) and anti-Goα (magenta). As shown in Fig. 2.2K-N, robust colocalization was detected at the plasma membrane of the migratory neurons (arrowheads) and within their leading processes (Fig. 2.2O-Q, arrowheads). Surface labeling of unpermeabilized embryos with anti-nAPPL and subsequent permeabilization and staining for Goα verified that Goα colocalizes with cell-surface APPL in the EP cells (data not shown). To examine the relationship between APP and Goα expression in developing mammalian neurons,

embryonic rat hippocampal neurons were isolated and fixed after 5 days in primary culture. The neurons were then triple-immunostained with antibodies specific to the extracellular domain (green) and cytoplasmic domain of APP (red/magenta), as well as for Goα (blue/gray scale; Fig. 2.2R-T). As seen for APPL in the EP cells, full-length APP was found to be abundantly expressed within the growth cones of rat hippocampal neurons, where it colocalized with Goα (yellow/white regions, Fig. 2.2R-T). These results indicate that transmembrane forms of APP family proteins are closely associated with endogenously expressed Goα in developing neurons, particularly within regions of active growth and motility, and that this association is conserved in both invertebrate and vertebrate preparations.

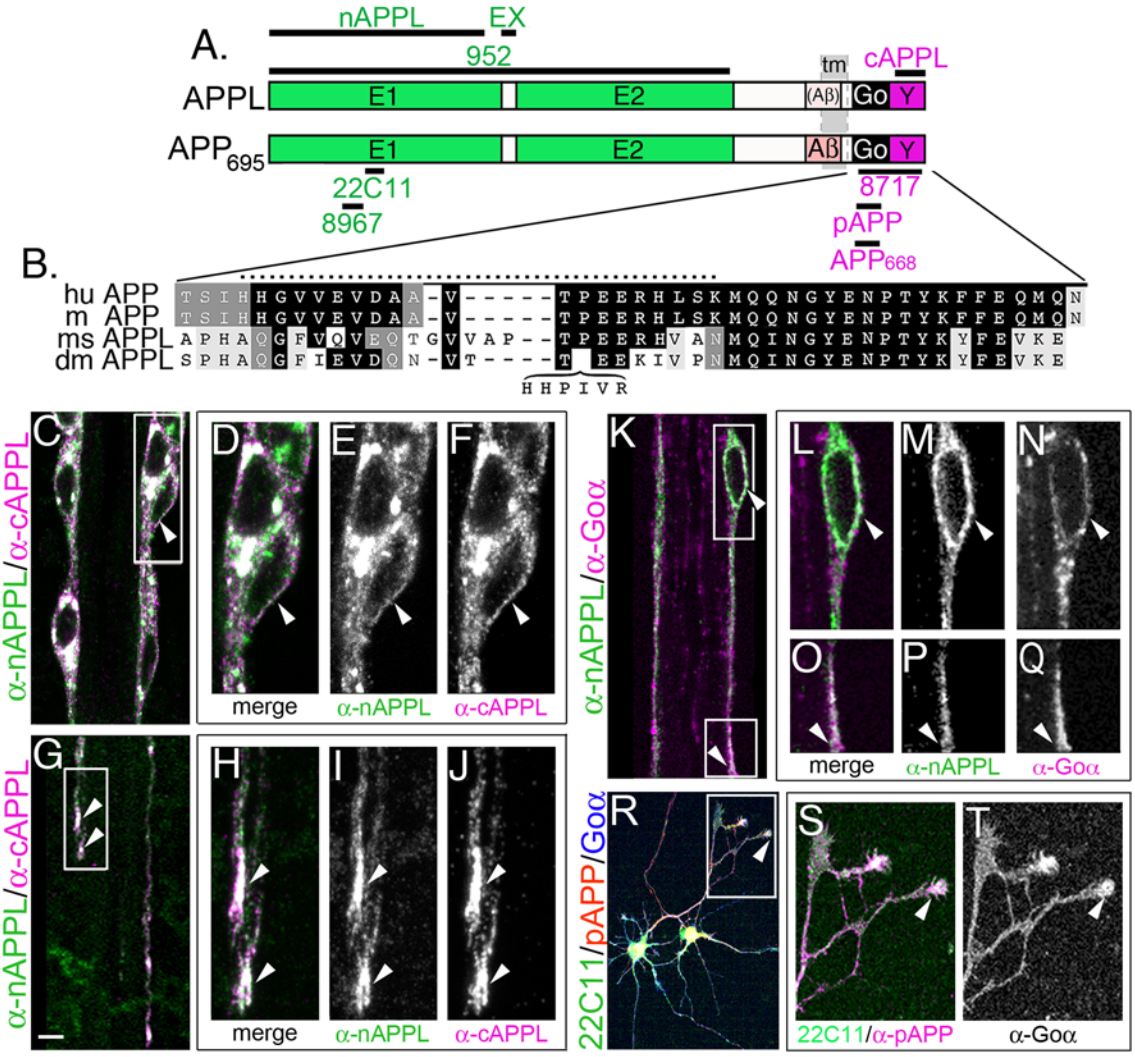
A.
nAPPL
EX
952
tm
cAPPL
APPL
E1
E2
(Aβ)
Go
Y
APP695
Aβ
22C11
8967
8717
pAPP
APP668
B.
hu APP
m APP
ms APPL
dm APPL
HHPIVR
α-nAPPL/α-cAPPL
merge
α-nAPPL
α-cAPPL
α-nAPPL/α-Goα
α-Goα
22C11/pAPP/Goα
22C11/α-pAPP

Figure 2.2

Figure 2.2. *Goα colocalizes with APP family proteins in the motile regions of developing insect and mammalian neurons.* **A)** Schematic diagram of APPL and APP, indicating the conserved extracellular domains (E1 and E2), Aβ domains, and the cytoplasmic Go-binding domain (Go) and internalization domain (Y). Transmembrane domains are shown in gray ("tm"). Epitopes targeted by the different anti-APPL and APP antibodies used in this study are indicated by the labeled black lines. Antibodies targeting APP and APPL extracellular domains are labeled in green and antibodies targeting cytoplasmic domains are labeled in magenta. **B)** Amino acid alignment of the conserved cytoplasmic domains in human (h) APP, mouse (m) APP, *Manduca* (ms) APPL, and *Drosophila* (dm) APPL. Both the putative Go-binding domain (Go) and the internalization domain (Y) within the cytoplasmic (C-terminal) region of APP family proteins are highly conserved across species. Residues that are identical in at least 3 species are shaded in black; residues shared by 2 species are shaded in gray. The dotted black line indicates the putative Go-binding domain identified in APP_{695} (Nishimoto et al., 1993; Okamoto et al., 1995). **C)** EP cells at 65 hpf immunostained with anti-nAPPL (green) and anti-cAPPL (magenta); the white box indicates the region highlighted in **D-F**. Individual channels in **E** (anti-nAPPL) and **F** (anti-cAPPL) are shown as monochrome images. Arrowheads indicate colocalized N- and C-terminal immunostaining (which appears white in **D**) at the plasma membrane, consistent with the presence of full-length transmembrane APPL. Images in **C-F** show compressed images of three optical sections acquired by confocal imaging. **G)** Leading processes of EP cells on the dorsal muscle band pathways, immunostained with anti-nAPPL and anti-cAPPL antibodies; the white box indicates the region highlighted in **H-J**, which includes 3-4 fasciculated growth cones. Arrowheads indicate colocalized N- and C-terminal immunostaining in the motile growth cones (white regions in **H**); individual channels in **I** (anti-nAPPL) and **J** (anti-cAPPL) are shown as monochrome images. Images in **G-J** show compressed images of 10 optical sections. **K)** EP cells coimmunostained with anti-nAPPL (green) and anti-Goα (magenta); white boxes indicate regions highlighted in **L-N** and **O-Q**. Arrowheads in **L-N** indicate the colocalization of APPL and Goα at the plasma membrane of a migrating neuron; arrowheads in **O-Q** indicate colocalization in the EP cell growth cone. Individual channels in **M** and **P** (anti-nAPPL) and **N** and **Q** (anti-Goα) are shown as monochrome images. The images in **K-Q** show single optical sections. **R)** Rat hippocampal neurons immunostained with antibodies against N-terminal APP (green, 22C11), C-terminal APP (red, pAPP), and Goα (blue); the white box indicates the highlighted region shown in **S-T**. **S)** Enlarged view of colocalized nAPP (green) and cAPP (magenta) immunostaining in the neuronal growth cones, indicating the presence of transmembrane APP. **T)** Corresponding image of anti-Goα immunostaining (shown in monochrome), consistent with the colocalization of Goα with full-length APP in mammalian growth cones. Images **R-T** show a compressed image of 10 optical sections. Scale bars: **C**,**G**,**K**, 7 μm; **D-F**, **H-J**, **L-Q**, 3 μm; **R**, 50 μm; **S-T**, 25 μm.

Both APPL and APP endogenously interact with Goα

In previous investigations, coimmunoprecipitation assays were used to show that both human APP and insect APPL can interact with Goα (Brouillet et al., 1999, Shaked et al., 2009), but these studies did not determine whether Goα interacts specifically with full-length APP family proteins or with their C-terminal cleavage products (CTFs and AICDs). Another recent study showed that epitope-tagged C-terminal fragments of APP could interact with a different heterotrimeric G protein (Gsα) when overexpressed in cell culture (Deyts et al., 2012). Given that APP contains a conserved BBXXB domain, which in other receptor classes can promote binding to the alpha subunits of several different G proteins (Okamoto et al., 1990, Wu et al., 1995, Timossi et al., 2004), these results suggest that APP might function as a promiscuous G protein-associated receptor (Deyts et al., 2012).

To address this issue, we immunoprecipitated APPL from *Manduca* embryonic lysates with antibodies specific to both the N- and C-terminal domains of the holoprotein, and probed the resultant immunoblots with antibodies against different G protein subunits (shown schematically in Fig. 2.3A). As shown in Figure 2.3B-C, endogenously expressed Goα could be readily coimmunoprecipitated with both N-terminal and C-terminal-specific APPL antibodies, but not with matched control immunoglobulins (IgG and IgY, respectively). In contrast, APPL did not coimmunoprecipitate with either Giα or Gsα (Fig. 2.3D-E), despite the robust expression of these G proteins in the embryonic nervous system (Copenhaver et al., 1995). Since APPL expression in insects is restricted to neurons (Martin-Morris and White, 1990), these results indicate that full-length APPL selectively interacts with endogenously expressed Goα but not other G proteins within the developing insect nervous system.

Previous experiments in *Drosophila* have shown that flies lacking APPL (*Appl*^{d}) exhibit defects in synaptic differentiation and aberrant adult behavior (Luo et al., 1992, Torroja et al., 1999b), supporting a role for APPL in regulating neuronal growth and target innervation. To complement our studies of APPL-Goα interactions in *Manduca*, we used fly head lysates to show that *Drosophila* Goα could be coimmunoprecipitated with anti-cAPPL antibodies from wild type controls but not *Appl*^{d} flies (Fig. 2.3F), although both fly strains express equivalent levels of Goα (Fig. 2.3F, input). As noted above, Nishimoto et al. identified a candidate Go-binding domain within the cytoplasmic domain of human APP_{695} (His_{657}-Ly_{676}) that was required for APP-Goα interactions in reconstituted liposomes (Nishimoto et al., 1993, Okamoto et al., 1995). To determine whether the conserved Go-binding domain is required for APPL-Goα interactions in the insect nervous system, we used transgenic fly lines expressing modified forms of APPL in the absence of wild type protein. APPL^{sd} lacks the proteolytic cleavage site in APPL (AA 758-791) and consequently is expressed only as a transmembrane protein; APPL$^{sd}\Delta$Cg also lacks a portion of the putative Go-protein binding site (AA 845–855; Torroja et al., 1999b). Using the GMR promoter, UAS constructs of each isoform were expressed in the eyes of *Appl*^{d} flies, and head lysates were immunoprecipitated with anti-Goα. Blotting for anti-cAPPL revealed that Goα interacts with APPL^{sd} but not APPL$^{sd}\Delta$Cg (Fig. 2.3G), although both constructs were expressed at similar levels (Fig. 2.3G, input). *Appl*^{d} fly head lysates were used as a negative control. Probing the immunoprecipitates for Goα and Gβ verified the abundance of heterotrimeric G proteins immunoprecipitated from all of the fly lines used for this analysis (Fig. 2.3G, IP). These results demonstrate that Goα interacts with transmembrane forms of APPL, consistent with its role as a Goα-associated receptor, and that the conserved Go-binding domain within APPL is necessary for its interactions with Goα *in vivo*.

We also investigated whether endogenously expressed Goα interacts with full-length APP in the mammalian nervous system. Using similar methods, we found that Goα could be readily coimmunoprecipitated with both nAPP- and cAPP-specific antibodies from lysates prepared from cortical and hippocampal regions of adult mouse brain, compared to control IgG and normal rabbit serum (Fig. 2.3H), supporting the model that Goα interacts with full-length APP in neurons. In contrast, none of the APP-specific antibodies that we tested were found to coimmunoprecipitate Gsα (Fig. 2.3I), suggesting that Gsα does not normally interact with full-length APP or its C-terminal cleavage products in the brain. Whether elevated expression of APP or its fragments can promote this interaction under pathological conditions remains to be determined.

If APP and its orthologs function as authentic Goα-coupled receptors, they would be expected to interact with heterotrimeric Go(αβγ) complexes in their inactive state (Bourne et al., 1991, Gales et al., 2006), whereas activation of APP signaling should induce their dissociation. Conversely, if APP and APPL function as downstream targets for activated Goα, we would not expect them to associate with the αβγ trimer. As shown in Figure 2.3J, antibodies against both the N- and C-terminal domains of APP coimmunoprecipitated Gβ subunits as well as Goα, similar to previous reports using extracted membrane preparations (Nishimoto et al., 1993). Lastly, based on recent studies suggesting that APP-Goα interactions might be perturbed in AD patients (Shaked et al., 2009), we also used human brain lysates prepared from the cortical regions of healthy control subjects (provided by the Oregon Brain Bank) to show that anti-nAPP antibodies also coimmunoprecipitated human Goα, compared with the low background levels of Goα immunoprecipitated by control IgG (Fig. 2.3K). In combination, these results indicate that both insect APPL and mammalian APP selectively interact with heterotrimeric Go (but not other Gα proteins) under physiological conditions,

consistent with an evolutionarily conserved role for APP-Goα signaling in the developing and mature nervous system.

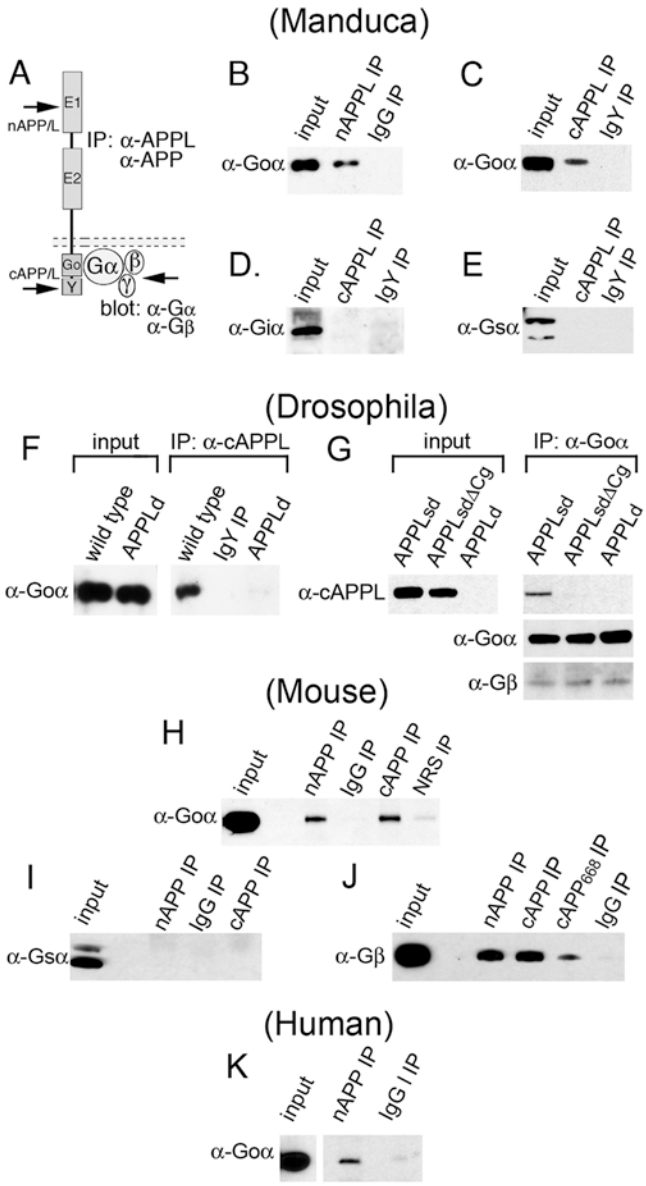
(Manduca)
A
E1
nAPP/L
IP: α-APPL
α-APP
E2
cAPP/L
Go
Y
Gα
β
γ
blot: α-Gα
α-Gβ
B
input
nAPPL IP
IgG IP
α-Goα
C
input
cAPPL IP
IgY IP
α-Goα
D.
input
cAPPL IP
IgY IP
α-Giα
E
input
cAPPL IP
IgY IP
α-Gsα
(Drosophila)
F
input
IP: α-cAPPL
wild type
APPLd
wild type
IgY IP
APPLd
α-Goα
G
input
IP: α-Goα
APPLsd
APPLsdΔCg
APPLd
APPLsd
APPLsdΔCg
APPLd
α-cAPPL
α-Goα
α-Gβ
(Mouse)
H
input
nAPP IP
IgG IP
cAPP IP
NRS IP
α-Goα
I
input
nAPP IP
IgG IP
cAPP IP
α-Gsα
J
input
nAPP IP
cAPP IP
cAPP668 IP
IgG IP
α-Gβ
(Human)
K
input
nAPP IP
IgG I IP
α-Goα

Figure 2.3

Figure 2.3. *Goα interacts with transmembrane APPL and APP in the nervous system.* **A)** Schematic of the experimental protocol used in Figure 2.3: tissue lysates were immunoprecipitated with antibodies specific for either the N- or C-terminal domains of APPL and APP, then immunoblotted with antibodies specific for different G protein subunits. **B-E)** Western blots of *Manduca* embryonic lysates immunoprecipitated with anti-nAPPL or anti-cAPPL and immunoblotted with antibodies against different Gα-subunits. **B)** Embryonic lysate immunoprecipitated with anti-nAPPL and immunoblotted with anti-Goα. Input lane shows endogenous Goα levels in the lysates before immunoprecipitation; IgG IP shows a matched negative control immunoprecipitation. **C)** Embryonic lysate immunoprecipitated with anti-cAPPL and immunoblotted with anti-Goα. Input lane shows endogenous Goα levels in the lysates; IgY IP shows a matched negative control immunoprecipitation. The size of *Manduca* Goα is 41 kDa. **D-E)** Western blots of *Manduca* embryonic lysates immunoprecipitated with anti-cAPPL and immunoblotted for either Giα (**D**) or Gsα (**E**). Input lanes show endogenous Giα and Gsα levels in the lysates before immunoprecipitation. Neither Giα nor Gsα coimmunoprecipitate with anti-cAPPL or with control IgY. The size of Giα is ~41 kDa; Gsα is detected as a doublet at 48 and 52 kDa (Copenhaver et al., 1995). **F-G)** Western blots of immunoprecipitated *Drosophila* head lysates. **F)** *Drosophila* head lysates from wild type and $Appl^{d}$ flies (which lack APPL expression) immunoprecipitated with anti-cAPPL and immunoblotted with anti-Goα. Inputs show equivalent levels of endogenous Goα in both fly lines. Goα was coimmunoprecipitated with anti-cAPPL antibodies from wild type lysates but not with control IgY, nor from $Appl^{d}$ lysates. **G)** Western blot of lysates from $Appl^{d}$ flies overexpressing mutant forms of APPL under the control of the GMR promoter. $Appl^{sd}$ flies ("secretion-deficient) express a transmembrane form of APPL lacking the juxtamembrane domain that is normally cleaved by secretases; $Appl^{sd\Delta Cg}$ flies express secretion-deficient transmembrane APPL that also lacks the putative Go-binding domain. Fly head lysates were immunoprecipitated with anti-Gi/oα and immunoblotted with anti-cAPPL (135 kDa). Input lanes show abundant expression levels of $APPL^{sd}$ and $APPL^{sd}\Delta Cg$; no APPL-related proteins were detected in $APPL^{d}$ flies. $APPL^{sd}$ but not $APPL^{sd}\Delta Cg$ coimmunoprecipitated with Goα, indicating that the Go domain is necessary for APPL-Goα interactions *in vivo*. $Appl^{d}$ flies served as the negative control. Probing with anti-Goα verified that abundant levels of Goα were immunoprecipitated from each of the fly lines. Similar levels of Gβ also coimmunoprecipitated with Gi/o in all three fly lines, indicating equivalent expression of the heterotrimeric G protein complexes. The size of fly Gβ is ~37 kDa. **H-J)** Western blots of mouse brain lysates immunoprecipitated with N- or C-terminal-specific APP antibodies and immunoblotted with antibodies targeting different G protein subunits. **H)** Immunoprecipitated mouse brain lysates labeled with anti-Goα. **Input** shows endogenous Goα levels in the lysate before immunoprecipitation. **Lane 2:** Goα coimmunoprecipitated with anti-nAPP. **Lane 3:** IgG = matched negative control immunoprecipitation. **Lane 4:** Goα also coimmunoprecipitated with anti-cAPP (8717; see Figure 2). **Lane 5**: matched negative control immunoprecipitation with normal rabbit serum (NRS). **I)** Immunoprecipitated mouse brain lysates immunoblotted for Gsα. **Input** shows endogenous Gsα levels in the lysate before immunoprecipitation. **Lanes 2-4** show that Gsα did not coimmunoprecipitate with anti-nAPP, control IgG, nor anti-cAPP. **J)** Mouse brain lysates immunoprecipitated with N- or C-terminal-specific APP antibodies and immunoblotted with α-Gβ. **Input** shows Gβ levels in the lysates before immunoprecipitation. **Lanes 2-4:** Gβ coimmunoprecipitated with both anti-nAPP and anti-cAPP antibodies (8717 and $cAPP_{668}$). **Lane 5:** IgG negative control immunoprecipitation. **K)** Immunoprecipitated human brain lysates immunoblotted for Goα. Input shows endogenous Goα levels in the lysate before immunoprecipitation. Goα was coimmunoprecipitated with anti-nAPP but not with control IgG.

APPL directly binds Goα both *in vitro* and *in vivo*

The model that APPL functions as a Goα-associated receptor requires direct contact between the two proteins at the plasma membrane. To address this issue, we used Bimolecular Fluorescence Complementation (BiFC), a modified "split-GFP" approach whereby complementary fragments of Venus Fluorescent Protein (Vn) are fused to proteins of interest, but they remain non-fluorescent unless brought together by direct interactions between the tagged proteins (Kerppola, 2008, Robida and Kerppola, 2009). For these assays, we fused the N-terminal fragment of Venus Fluorescent Protein (Vn1) to the cytoplasmic domain of *Manduca* APPL (APPL-Vn1) and the complementary C-terminal fragment (Vn2) to Goα (Vn2-Goα). As an initial test of these constructs, we transfected them either singly or in combination into COS7 cells, which do not express detectable levels of mammalian Goα or APP (unpublished observations). After 18-24 hr, we then fixed and immunostained the cells with antibodies specific for APPL and Goα to monitor their expression levels (using Alexa 568 and Alexa 647-coupled secondary antibodies), independent of BiFC-induced fluorescence (visualized in the green channel). As shown in Figure 2.4, COS7 cells expressing either APPL-Vn1 (Fig. 2.4A) or Vn2-Goα alone (Fig. 2.4B) showed strong immunoreactivity for the individual fusion constructs but produced no detectable BiFC signal (Fig. 2.4A_3, B_3). In contrast, cells that coexpressed both APPL-Vn1 and Vn2-Goα exhibited robust BiFC signals throughout their somata and growing processes (Fig 2.4C_3). These results demonstrate that APPL can directly bind Goα in exogenous cells.

Based on our evidence that the Go-binding domain of APPL is necessary for its association with APPL *in vivo* (Fig. 2.3G), we also tested whether this domain was necessary for direct APPL-Goα interactions in our BiFC assays by cotransfecting COS7 cells with Vn2-Goα and APPLΔGo-Vn1 (a form of *Manduca* APPL lacking the Go-binding

domain, AA 762-791; dotted line in Fig. 2.2B). In contrast to the membrane-associated BiFC signals seen in cells that expressed full-length APPL-Vn1 plus Vn2-Goα (Fig. 2.4C_3, arrowheads), cells that coexpressed APPLΔGo-Vn1 plus Vn2-Goα exhibited only minimal BiFC signals that were confined to the Golgi/endoplasmic reticulum (ER) regions (Fig. 2.4D), despite the presence of both Vn-tagged constructs in more peripheral regions of the cells (arrowheads). To directly compare BiFC fluorescence in multiple cells transfected with APPL or APPLΔGo, we identified cells with relatively low levels of each construct (to avoid saturation in the BiFC channel) and quantified the BiFC signal as a ratio to the levels of each construct. Quantification of the relative fluorescent intensities in each channel verified that coexpression of Vn2-Goα with full-length APPL-Vn1 produced significantly stronger BiFC signals than coexpression with APPLΔGo-Vn1 (Table 2.1). These results show that the Go-binding domain previously identified in human APP_{695} is also required for direct interactions between APPL and Goα.

To test whether APPL selectively interacts with Goα but not other related G proteins, we also cotransfected COS7 cells with APPL-Vn1 and Vn2-tagged constructs of Giα or Gsα. For these assays, we fixed the transfected cells after 48 hrs in culture, and then immunostained them with anti-APPL and an anti-GFP antibody that only recognizes the Vn2 domain; this approach allowed us to confirm that all of the Vn2-tagged Gα constructs were expressed at comparable levels. As in the previous experiment, cotransfection of APPL-Vn1 with Vn2-Goα produced strong BiFC signals throughout the cells and their growing processes (Fig. 2.4E_3, arrowheads). In contrast, cotransfection of APPL-Vn1 with Vn2-Giα produced only faint BiFC signals that were predominantly restricted to Golgi/ER regions (Fig. 2.4F_3, arrowheads), despite the presence of both proteins at the plasma membrane and in growing processes (similar to

APPL-Vn1 and Vn2-Goα Fig. 2.4$E_{1\text{-}2}$). Similarly, cells that coexpressed APPL-Vn1 with Vn2-Gsα exhibited no detectable BiFC signals (Fig. 2.4G_3). These results indicate that APPL directly binds Goα but not other related G proteins in cell culture, consistent with the model that APPL selectively interacts with Goα at the plasma membrane.

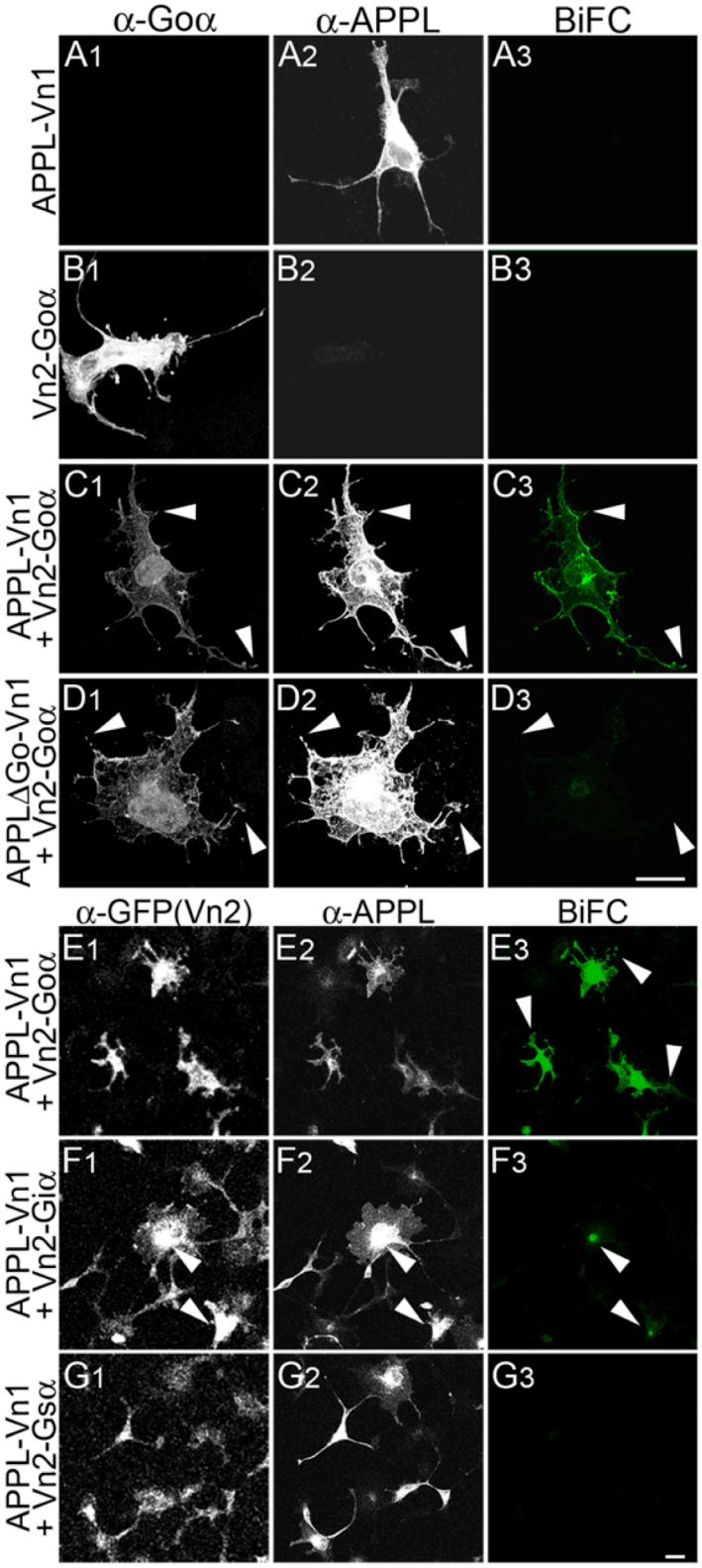
α-Goα
α-APPL
BiFC
APPL-Vn1
A1
A2
A3
Vn2-Goα
B1
B2
B3
APPL-Vn1 + Vn2-Goα
C1
C2
C3
APPLΔGo-Vn1 + Vn2-Goα
D1
D2
D3
α-GFP(Vn2)
α-APPL
BiFC
APPL-Vn1 + Vn2-Goα
E1
E2
E3
APPL-Vn1 + Vn2-Giα
F1
F2
F3
APPL-Vn1 + Vn2-Gsα
G1
G2
G3

Figure 2.4

Figure 2.4. *APPL and Goα directly interact in cell culture.* **A-D)** Representative images of COS7 cells at 18-24 hours post transfection, immunostained with α-Goα (left columns) and α-APPL (middle columns) to detect constructs of interest. Right-hand columns show green fluorescent BiFC signals that were produced by direct interactions between Vn1- and Vn2-tagged fusion proteins. **A-B)** Cell transfected with either APPL-Vn1 alone (panel **A_3**) or Vn2-Goα alone (panel **B_3**) did not emit detectable BiFC signals. **C)** Cell co-transfected with both APPL-Vn1 and Vn2-Goα exhibited BiFC signals at the plasma membrane and throughout growing processes (panel **C_3**, arrowheads). **D)** Cell cotransfected with Vn2-Goα and APPLΔGo-Vn1 (APPL lacking the putative Go-binding domain; AA 762-791) produced only minimal BiFC signals that were restricted to the Golgi/ER regions. No detectable BiFC signals were present at the plasma membrane or growing processes of the cell (panel **D_3**, arrowheads), despite the expression of both constructs in these regions (**D_1- D_2**). **E-G)** Lower magnification images of COS7 cells co-transfected with APPL-Vn1 plus equivalent levels of different Vn2-tagged Gα subunits. 48 hr post transfection, cells were coimmunostained with a Vn2-specific anti-GFP antibody and with α-APPL (to detect APPL-Vn1). **E)** Cotransfection of APPL-Vn1 plus Vn2-Goα produced robust BiFC signals (as in panel **C_3**), indicating direct APPL-Goα binding (arrowheads). **F)** Cotransfection of APPL-Vn1 with Vn2-Giα produced only minimal BiFC signals that were primarily localized within the ER/Golgi regions (panel **F_3**). BiFC signals were not apparent in the plasma membrane or growing processes of the cells, despite the presence of both Vn-tagged constructs in these regions (panels **F_1-F_2**). **G)** Coexpression of APPL-Vn1 and Vn2-Gsα did not result in any detectable BiFC signals (panel **G_3**), although both proteins were expressed throughout the cells (panels **G_1-G_2**). Scale bars: 10 μm.

Table 2.1. Coexpression of APPL plus Goα in COS7 cells produces significantly greater BiFC signals than APPLΔGo plus Goα.

Expressed Proteins	APPL levels	Goα levels	BiFC levels
APPL + Goα	107 ± 9 (ns)	72 ± 5 (ns)	116 ± 13***
APPLΔGo + Goα	119 ± 10	92 ± 10	9 ± 2

Table 2.1. Quantification of expression levels for APPL, APPLΔGo, Goα, and BiFC signals in transfected COS7 cells (expressed in relative units per unit area). Fluorescence intensities were calculated from identical regions of the cell membrane and associated filopodia for each channel (as shown in Fig. 2.4). APPL-Goα interactions produced significantly stronger BiFC signals than APPLΔGo-Goα interactions when expressed at similar levels. Each data set shows mean ± SEM; N = 20 for each sample; ns, no significant difference; ***$p < 0.001$, Student's two-tailed *t* test.

To complement our analysis of APPL-Goα interactions *in vitro*, we also used the UAS-GAL4 system to express APPL-Vn1 and Vn2-Goα within the fly nervous system. For these experiments, we induced expression of UAS-APPL-Vn1 and UAS-Vn2-Goα using the eye-specific GMR-GAL4 promoter construct. Developing eye discs were then collected at progressive stages of development, fixed, and immunostained with a polyclonal anti-GFP antibody that recognized both Vn1 and Vn2 (visualized with Alexa 568-conjugated secondary antibodies), allowing us to monitor their expression levels in addition to the BiFC signals that they produced. When we expressed either APPL-Vn1 (Fig. 2.5A_1) or Vn2-Goα alone (Fig. 2.5B_1), we could readily detect the constructs in developing adult photoreceptors within the eye discs, but (as expected) no BiFC signals were produced (Fig. 2.5A_2, 2.5B_2). In contrast, coexpression of APPL-Vn1 with Vn2-Goα resulted in robust BiFC signals within the photoreceptor membranes and their axonal projections extending into the developing adult brain (Fig. 2.5C). These results demonstrate that APPL and Goα directly bind when coexpressed *in vivo*, similar to our results in COS7 cells.

To explore whether APPL-Goα interactions could be visualized in synaptic regions within the brain, we also examined younger third instar larvae, when GMR-induced expression can also be detected in 12 bilaterally paired larval photoreceptors that project to the brain (Steller H, 1987, Hartenstein, 1988). As shown in Figure 2.5D, BiFC signals produced by coexpression of APPL-Vn1 with Vn2-Goα could be readily detected in larval photoreceptor axons extending through the developing eye disc via Bolwig's nerve and into the larval optic neuropil (lon; Fig. 2.5D_2), where they make synaptic contacts with several classes of interneurons (Tix et al., 1989, Sprecher et al., 2011). In contrast, when we coexpressed UAS-Vn2-Goα with UAS-APPLΔGo-Vn1 (lacking the Go binding domain of APPL) at similar levels, no detectable BiFC signals

were produced (Fig. 2.5E$_2$); again demonstrating that this domain is required for APPL-Goα interactions *in vivo*. At slightly later stages (white pupae), BiFC signals also became apparent within the developing synaptic terminals of adult photoreceptors coexpressing APPL-Vn1 and Vn2-Goα in the lamina cortex (Fig. 2.5F). These results confirm our immunohistochemical evidence that endogenously expressed Goα colocalizes with APP family proteins in developing neurons, providing additional support for the model that APP-Goα signaling may play a functional role in regulating key aspects of neuronal motility.

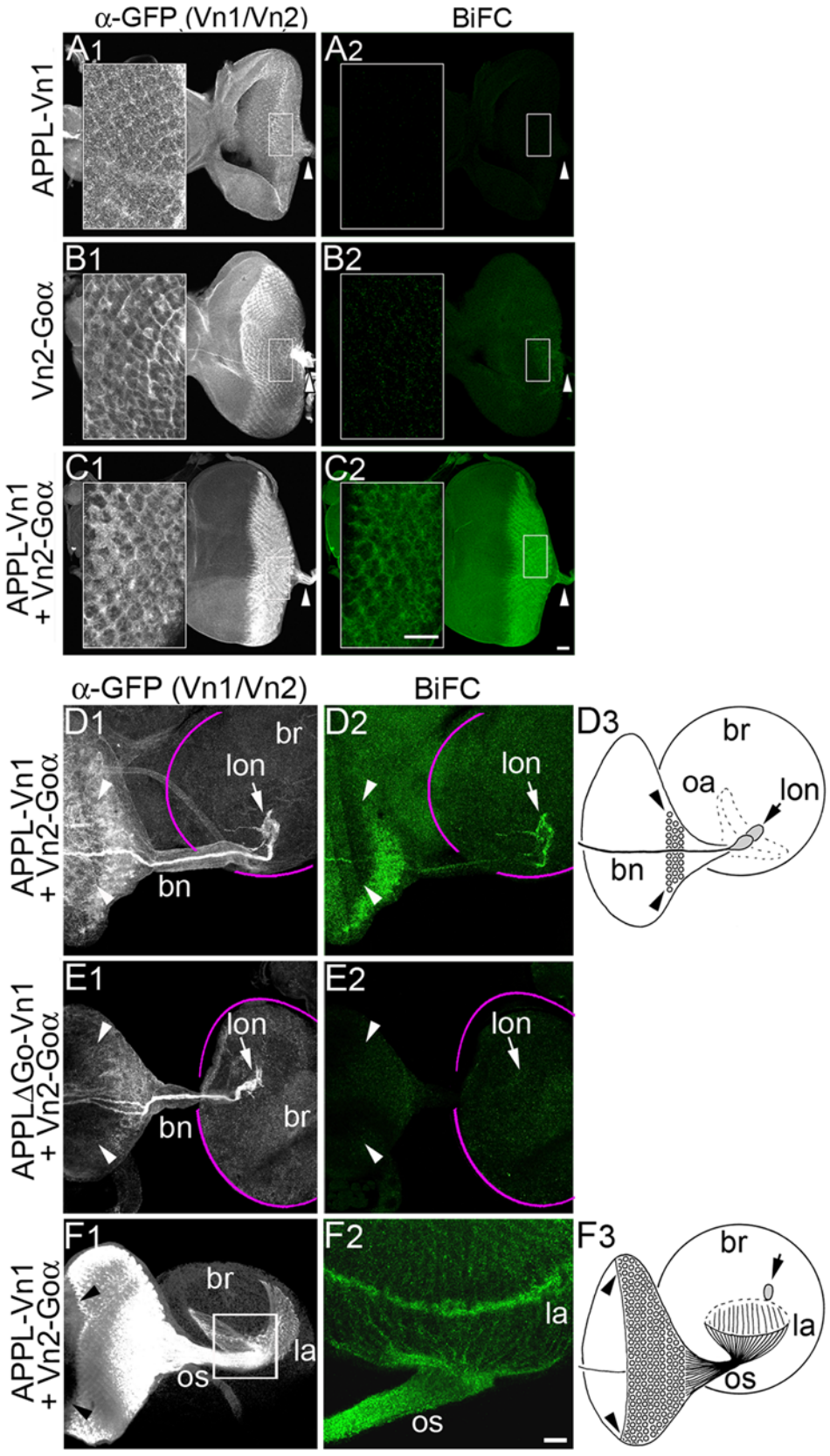
α-GFP (Vn1/Vn2)
BiFC
APPL-Vn1
Vn2-Goα
APPL-Vn1 + Vn2-Goα
A1
A2
B1
B2
C1
C2
D1
D2
D3
E1
E2
F1
F2
F3
br
lon
bn
oa
os
la
APPLΔGo-Vn1 + Vn2-Goα

Figure 2.5

Figure 2.5. *APPL and Goα directly interact in Drosophila photoreceptors and developing synapses.* Isolated eye discs from third instar larvae expressing UAS-APPL-Vn1, UAS-Vn2-Goα, or both constructs (controlled by GMR-GAL4). Discs were fixed and immunostained with α-GFP (Aves #GFP1020) to label both Vn1 and Vn2 epitopes (visualized with Alexa-568 secondary antibodies); BiFC signals produced by APPL-Goα interactions were imaged in the green channel. **A_1**, **B_1)** Eye discs expressing either APPL-Vn1 or Vn2-Goα alone did not exhibit detectable BiFC signals (**A_2**, **B_2**). **C_1)** Coexpression of APPL-Vn1 and Vn2-Goα resulted in robust BiFC signals throughout the fly photoreceptors (**C_2**) and their axonal projections extending into the optic stalk (arrowheads). Small white boxes in the low-magnification images indicate highlighted regions shown in the insets of each panel. **D-E)** Isolated eye disc-brain complexes from mid-third instar *Drosophila* larvae that expressed Vn2-Goα plus either wild type APPL-Vn1 or APPLΔGo-Vn1. Magenta outlines demarcate the proximal brain lobe (br) in each preparation. **D_1,E_1)** Eye disc-brain complexes from mid-third instar larvae coexpressing Vn2-Goα plus mutated or wild type forms of APPL-Vn1. Immunostaining for anti-GFP showed that the Venus-tagged constructs were expressed in the developing adult photoreceptors (adjacent to the morphogenetic furrow; arrowheads) and throughout Bolwig's nerve (bn), which carries the axons of 12 larval photoreceptors through the eye disc into the larval optic neuropil of the brain (lon; arrows). Larval photoreceptors are out of the field of view. **D_2)** The combined expression of APPL-Vn1 and Vn2-Goα produced robust BiFC signals in regions where both proteins were coexpressed (indicative of direct APPL-Goα interactions), including the synaptic projections of the larval photoreceptors in the larval optic neuropil. **E_2)** Coexpression of APPLΔGo-Vn1 plus Vn2-Goα produced no detectable BiFC signals, despite comparable expression levels for both APPL constructs in **D** and **E** (data not shown). **D_3)** Schematic representation of the mid-third instar larval eye disc-brain complex (equivalent to dissected preparations in **D-E**), illustrating the orientation of Bolwig's nerve (bn) and the lon. Arrowheads indicate the morphogenetic furrow; dotted outline in the brain (br) indicates the adult optic anlage (Swanson et al.), forming adjacent to the lon. **F)** Eye disc-brain complex from a white pupa expressing APPL-Vn1 plus Vn2-Goα. **F_1)** Immunostaining with anti-GFP revealed the expression of the Venus-tagged constructs in developing adult photoreceptors, their projecting axons in the optic stalk (os), and their differentiating synaptic terminals within the lamina cortex (la) of the brain. **F_2)** Magnified image of the boxed region in **F_1** (compressed image of 16 optical sections) to highlight the presence of BiFC signals in the photoreceptor axons within the os and their synaptic terminals in the la. **F_3)** Schematic representation of the eye disc-brain complex at the white pupal stage (equivalent to preparation in **F_1**) illustrating the orientation of the os and la regions; small oblong circle (gray) indicates the position of the residual lon (not visible in **F_1-F_2**). Scale bars: **A-C**, 25 μm in panels; 15 μm in inset boxes; **D-F_1**, 30 μm ;10 μm in **F_2**.

APPL-Goα interactions are regulated by Goα activity

A prediction from the model that APPL functions as an authentic G protein-coupled receptor (GPCR) is that APPL should preferentially bind inactive Goα as part of a heterotrimeric complex, whereas activation of Goα should promote its dissociation from APPL (Fig. 2.6A). To address this issue, we use our coimmunoprecipitation assays to determine whether stimulating G protein activity affected basal APPL-Goα interactions. As an initial test, we prepared lysates from *Manduca* GV1 cells (which endogenously express both proteins) and verified that APPL and Goα could be readily coimmunoprecipitated with anti-cAPPL antibodies (Fig. 2.6B, Lane 1; histogram values in Fig. 2.6B were calculated by normalizing coimmunoprecipitated Goα levels relative to untreated controls). In contrast, treating replicate samples with GTPγS, a non-hydrolyzable GTP analog that activates all G proteins (Stryer and Bourne, 1986), reduced APPL-Goα interactions in a concentration-dependent manner (Fig. 2.6B, Lanes 2-4). Treating lysates with GDPβS, which inhibits G protein activation, slightly increased Goα-APPL interactions (Fig. 2.6B, Lane 6). These results indicate that APPL preferentially binds inactive but not active Goα, consistent with the hypothesis that APPL may function as a Goα-associated receptor rather than a downstream target of Goα signaling.

A potential caveat to the foregoing experiments is that GDP/GTP analogs can modulate the activity of both heterotrimeric and monomeric G proteins (Stryer and Bourne, 1986) and therefore might affect APPL-Goα interactions both directly and indirectly. We therefore performed a similar analysis with reagents that selectively target Goα, using lysates prepared from *Manduca* embryos at 60-70 hpf (during the active period of EP cell migration and outgrowth). Lysates were immunoprecipitated with anti-cAPPL, and the immunoblots labeled with both anti-Goα (Fig. 2.6C, upper gel) and anti-

nAPPL (Fig. 2.6C, lower gel); the doublet labeled by the double arrows in Fig. 2.6C indicates the immature and mature forms of full-length APPL (Swanson et al., 2005). For these experiments, relative levels of coimmunoprecipitated Goα were normalized to APPL levels in each sample, and then quantified as a ratio compared to untreated controls. Because insect APPL is exclusively expressed by neurons (Luo et al., 1990; Swanson et al., 2005), this approach provided a means of testing how Goα activity affects its association with endogenous APPL in the developing nervous system. As shown in Figure 2.6C (Lanes 1-2), treatment with GTPγS dramatically reduced the amount of Goα that could be coimmunoprecipitated with APPL, compared to untreated controls. Likewise, treatment with the Goα activator Mas 7 (a potent analog of Mastoparan) caused a substantial reduction in APPL-Goα interactions at all concentrations (Fig. 2.6C, Lanes 3-4; and data not shown). Although Mas 7 will also activate Giα (Higashijima et al., 1990), our evidence that APP family proteins associate with Goα but not other G proteins (Fig. 2.3) suggest that the effects of Mas 7 were specific to Goα in this assay. In contrast, treatment with PTX caused a dramatic increase in the amount of Goα that coimmunoprecipitated with APPL (Fig. 2.6C, Lanes 5-6). Since PTX inhibits insect Goα but not Giα (which lacks the C-terminal cysteine targeted for ADP-ribosylation; Thambi et al., 1989), these results indicate that the inactivation of Goα specifically inhibits its dissociation from APPL. None of these treatments significantly altered APPL levels (Fig. 2.6C. double arrowheads), indicating that the observed changes in APPL-Goα interactions were not caused by accelerated cleavage or degradation of the holoprotein. Figure 2.6D summarizes the combined results of multiple experiments using these methods, showing that both GTPγS and Mas 7 caused significant decreases in coimmunoprecipitated Goα. In contrast, treatment with PTX caused a concentration-dependent increase in APPL-Goα interactions, ranging from a

slight enhancement at 1 μg/ml to highly significant increases at 2-4 μg/ml (Fig. 2.6D, and data not shown). In some preparations, GDPβS also caused an increase in the level of coimmunoprecipitated Goα, although this response was more variable and did not reach statistical significance at the concentrations used for this assay. In combination, these experiments support the model that stimulation of APPL signaling within neurons will induce the activation and release of Goα, similar to conventional GPCRs. They also suggest that under normal conditions, a low level of APPL activation coincides with EP cell migration and outgrowth, consistent with a role for APP family proteins in regulating motile responses to endogenous guidance cues.

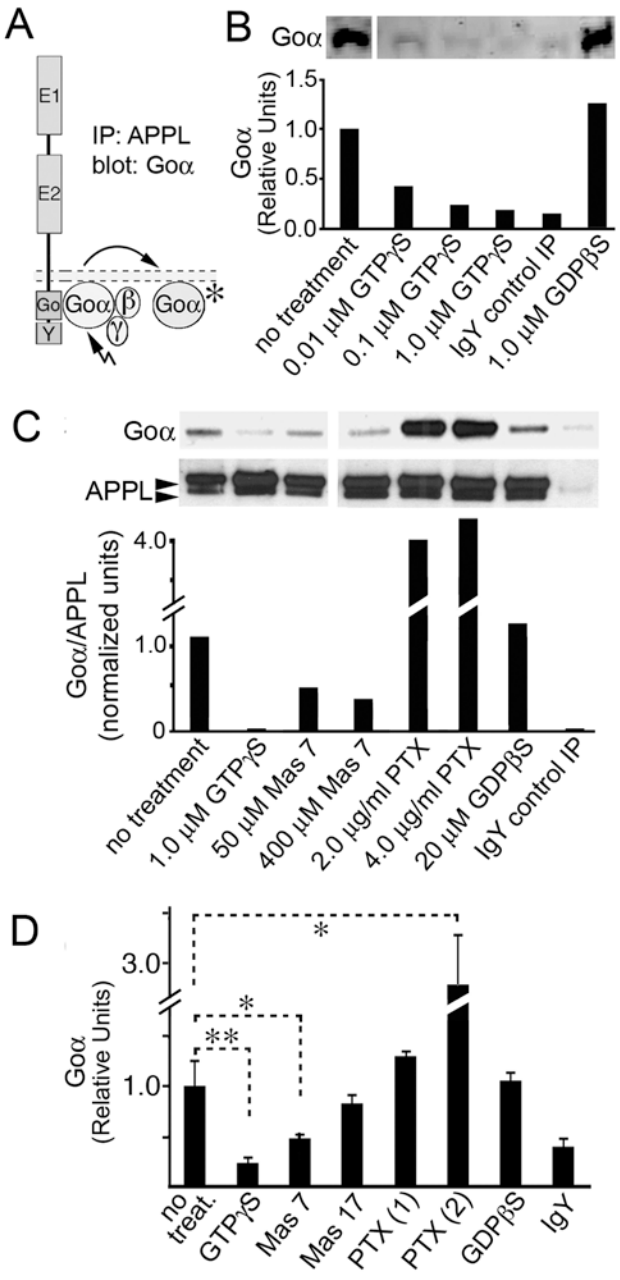
A
E1
E2
IP: APPL
blot: Goα
Go
Goα
β
γ
Goα
*
Y
B
Goα
Goα (Relative Units)
1.5
1.0
0.5
0.0
no treatment
0.01 μM GTPγS
0.1 μM GTPγS
1.0 μM GTPγS
IgY control IP
1.0 μM GDPβS
C
Goα
APPL
Goα/APPL (normalized units)
4.0
1.0
0
no treatment
1.0 μM GTPγS
50 μM Mas 7
400 μM Mas 7
2.0 μg/ml PTX
4.0 μg/ml PTX
20 μM GDPβS
IgY control IP
D
Goα (Relative Units)
3.0
1.0
*
*
**
no treat.
GTPγS
Mas 7
Mas 17
PTX (1)
PTX (2)
GDPβS
IgY

Figure 2.6

Figure 2.6. *APPL-Goα interactions are regulated by Goα activity.* **A)** Schematic of the model that inactive Goα binds APPL as part of a heterotrimeric complex with Gβγ. Activation of Goα (normally due to the exchange of bound GDP for GTP) promotes its dissociation from APPL, whereas inhibiting Goα prevents this dissociation, resulting in an increase in basal APPL-Goα interactions. **B)** Replicate cultures of *Manduca* GV1 cells (which endogenously express APPL and Goα) were treated as indicated, then lysed, immunoprecipitated with anti-APPL, and immunoblotted with anti-Goα. Relative levels of coimmunoprecipitated Goα were normalized to "no treatment" control run in parallel (**Lane 1**). Stimulating G protein activity with GTPγS (a non-hydrolyzable activator of G proteins) led to a concentration-dependent reduction in the amount of Goα that coimmunoprecipitated with APPL (**Lanes 2-4**). IgY = matched negative control immunoprecipitation (**Lane 5**). Treatment with GDPβS (a nonhydrolyzable G protein inhibitor) caused a modest increase in APPL-Goα interactions (**Lane 6**). **C)** Lysates from staged groups of embryos (60-65 hpf) were treated as indicated, immunoprecipitated with anti-APPL, and immunoblotted with anti-Goα. Gel shows a representative western blot of coimmunoprecipitated Goα (upper blot) and APPL (lower blot; labeled with anti-nAPPL). Double arrow indicates the immature (smaller) and mature (larger) forms of full-length APPL. Goα levels were calculated as a ratio of immunoprecipitated full-length APPL in the same sample, and ratios were normalized to untreated controls (**Lane 1**). Treatment with 1.0 μM GTPγS decreased APPL-Goα interactions (**Lane 2**). Treatment with Mas 7 (to activate Giα/Goα) decreased APPL-Goα interactions in a concentration-dependent manner (**Lanes 3-4**). In contrast, inhibiting Goα with PTX enhanced APPL-Goα interactions (**Lanes 5-6**). Treatment with 20 μM GDPβS caused only a minor increase in coimmunoprecipitated Goα levels (**Lane 7**). IgY = negative control immunoprecipitation (**Lane 8**). **D)** Combined analysis of multiple experiments in which *Manduca* embryonic lysates were treated with G protein-specific reagents, then immunoprecipitated with anti-cAPPL and immunoblotted with anti-Goα. Each manipulation was repeated in at least three independent experiments and normalized to their respective untreated controls in the same assay. Treatment with both GTPγS and Mas 7 significantly reduced APPL-Goα interactions. Mas 17, an inactive mastoparan analog, had no significant effect, compared to controls. PTX induced a concentration-dependent increase in APPL-Goα interactions. Although treatment with GDPβS caused a slight increase in APPL-Goα interactions in some experiments, overall this effect was not significant at the concentrations tested. IgY represents the species-matched negative control immunoprecipitations performed in each assay. Pairwise statistical analyses were performed between the control and each experimental group using Student's two-tailed *t* tests, *$p < 0.05$; **$p < 0.01$. Error bars indicate SEM.

APPL and Goα signaling regulate common aspects of neuronal migration

To test whether APPL-Goα signaling regulates specific aspects of neuronal motility *in vivo*, we used our well-characterized embryo culture assay for neuronal migration in *Manduca* (Horgan et al., 1995; Coate et al., 2008). Developmentally synchronous embryos were opened in culture to expose the ENS before the onset of the migration (at 52-53 hpf; Fig. 2.7A), and the EP cells were directly challenged with experimental reagents targeting either Goα or APPL. The embryos were allowed to develop in culture for an additional 24 hr, and then fixed and immunostained with anti-Fas II to quantify the full extent of EP cell migration and axon outgrowth. As shown in Figure 2.7B, embryos treated with control medium during this period exhibited a normal pattern of migration and outgrowth that was predominantly restricted to the midgut muscle bands ("b"), with relatively few neurons and processes extending onto the interband regions ("ib"). Treating the EP cells with AlF_4- to selectively stimulate heterotrimeric G protein activity (Sternweis and Gilman, 1982) curtailed their subsequent migration and outgrowth (Fig. 2.7C, E), similar to the effects of both GTPγS (which stimulates all G proteins) and mastoparan (specific for Goα and Giα; Horgan et al., 1994, 1995). In contrast, inhibiting Goα with PTX resulted in a distinctive pattern of ectopic migration and outgrowth by the EP cells onto the interband regions (Fig. 2.7D, F-G), as well as a moderate increase in their average distance traveled along the normal band pathways (Fig. 2.7E). To confirm the specificity of this effect, we also treated premigratory neurons with the A-Protomer of PTX (which lacks the lectin-like activity of the B-oligomer; Mangmool and Kurose, 2011), using alpha toxin to enhance cell penetration (as previously described; Horgan et al., 1995). As shown in Figure 2.7F-G, this treatment induced a more dramatic increase in the number of ectopic neurons and neurites that extended into the interband regions, as well as a moderate but significant

increases in migration and growth along the band pathways (Fig. 2.7E). Treatment with alpha toxin alone caused no significant effects (not shown). These results are consistent with our previous evidence that Goα activity normally restricts the extent of EP cell migration in a Ca^{2+}-dependent manner (Horgan and Copenhaver, 1998).

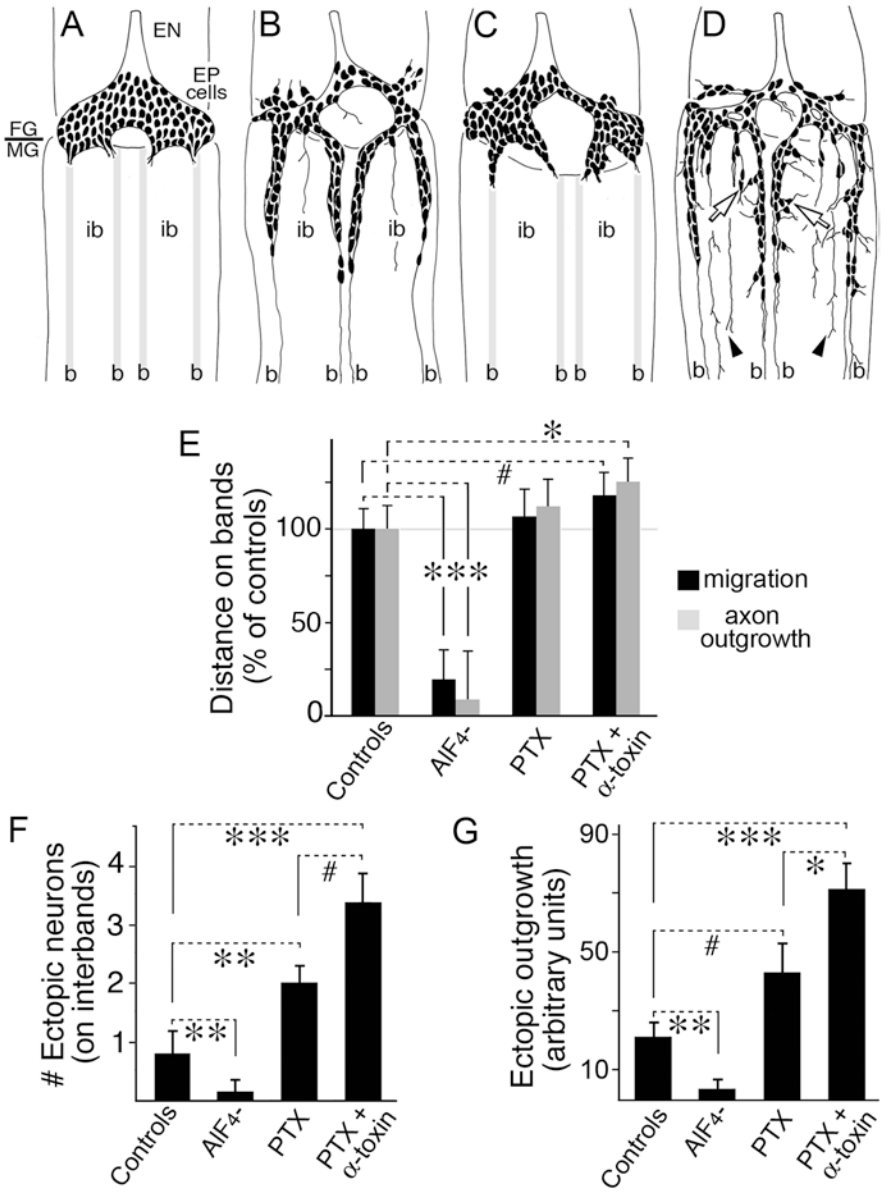
A
EN
EP cells
FG
MG
ib
b
B
C
D
E
Distance on bands (% of controls)
migration
axon outgrowth
Controls
AlF4-
PTX
PTX + α-toxin
F
Ectopic neurons (on interbands)
G
Ectopic outgrowth (arbitrary units)

Figure 2.7

Figure 2.7. *Inhibiting Goα activity in the EP cells induces ectopic migration and outgrowth.* **A-D)** Representative camera lucida drawings of *Manduca* embryos in which the EP cells were treated prior to migration onset with reagents targeting Goα, grown in culture for another 24 hr, then fixed and immunostained with anti-Fas II to reveal the full extent of migration and outgrowth in the developing ENS. **A)** Control embryo immunostained at the onset of an experiment (52 hpf) to show the initial positions of the premigratory EP cells adjacent to the foregut-midgut boundary (FG/MG). By this stage, subsets of neurons had begun to extend exploratory filopodia onto their future muscle band pathways (b) but had not commenced their migratory dispersal. **B)** Embryo opened at 52 hpf and treated with control culture medium throughout 24 hr of development showed the normal pattern of migration and outgrowth along the muscle bands, with only a few processes growing onto the interband musculature (ib). **C)** Treatment with 12.5 μM AlF_4- (an activator of heterotrimeric G proteins) caused almost complete inhibition of migration and outgrowth, stalling the neurons at the foregut-midgut boundary. **D)** Treatment with 100 ng/ml PTX (a specific inhibitor of Goα in insects) induced a distinctive pattern of ectopic migration (open arrows) and outgrowth onto the interband regions (black arrowheads). **E)** Average distances of neuronal migration and axon outgrowth along band pathways for each treatment group (normalized to matched sets of control embryos in each experiment). **F)** Quantification of the average number of neurons per embryo that exhibited ectopic migration into each interband region for each treatment condition. **G)** Quantification of the average extent of ectopic axon outgrowth in the interband regions of embryos treated with various reagents. In **E-G** pairwise statistical analyses were performed between each experimental group and their corresponding controls, using Student's two-tailed *t* tests, *$p < 0.05$; $^{\#}p < 0.02$; **$p < 0.01$; ***$p < 0.001$. N= at least 10 per condition. Error bars indicate SEM.

Based on reports that APP family proteins can regulate neuronal migration in other systems (Herms et al., 2004; Young-Pearse et al., 2007) and our evidence that APPL endogenously interacts with Goα in the developing ENS, we tested whether altering APPL expression in the EP cells induced similar defects in their migratory behavior. We first evaluated a panel of morpholinos targeting the coding domain of *Manduca* APPL mRNA for their effectiveness in knocking down APPL expression in GV1 cells. As shown in Figure 2.8A, one of these morpholinos (MO-APPL2) caused significant reductions in APPL levels that were both concentration-dependent and specific, almost completely eliminating APPL protein levels (Fig. 2.8B) without affecting Goα or tubulin expression (used as off-target controls; Fig. 2.8A, B). Staged embryos were then opened in culture at 48 hpf (7 hr before migration onset) and treated with either MO-APPL2 or control morpholinos for 24 hr, using Endo-Porter to facilitate their transport into developing neurons (Coate et al., 2008). Compared to the infrequent ectopic events seen in embryos treated with control morpholinos (Fig. 2.8C), knocking down APPL expression in the EP cells resulted in a pattern of excessive migration and outgrowth onto the interband regions (Fig. 2.8D, G-H), a phenotype strikingly similar to the ectopic growth induced by PTX treatment (Fig. 2.7D). Because our methods for visualizing the EP cells (with anti-Fas II immunostaining) precluded a simultaneous analysis of APPL expression, it was not possible to directly correlate the extent of ectopic growth by individual neurons and their residual APPL levels. Nevertheless, quantifying these effects for the entire population of EP cells indicated that inhibiting APPL expression resulted in the same distinctive pattern of ectopic growth and migration caused by inhibiting Goα activity.

Although several candidate proteins have now been shown to interact with APP family proteins in different contexts (Ho and Sudhof, 2004, Osterfield et al., 2008, Rice et

al., 2012) authentic ligands that regulate their intrinsic signaling activity have yet to be identified. As an alternative strategy, we used our anti-nAPPL antibody (targeting the extracellular domain of APPL) to block endogenous interactions between APPL and its putative binding partners to test whether APPL-dependent signaling is required for their normal pattern of migration and outgrowth. Accordingly, staged embryos were opened in culture shortly before the onset of migration (52-23 hpf), and the EP cells were directly treated with medium containing either anti-nAPPL or control IgG. Imaging these preparations after 24 hr revealed the same pattern of ectopic growth and migration (Fig. 2.8E) caused by PTX treatment and APPL-specific morpholinos (Fig. 2.8G-H), whereas neither of these treatments had a significant effect on the extent of migration and axon growth along the band pathways (Fig. 2.8F). Thus, inhibition of either Goα or APPL activity produced an identical phenotype within the developing ENS, in which the migratory neurons and their processes traveled inappropriately into regions that were normally inhibitory to neuronal growth.

The dramatic effects caused by perturbing APPL signaling in our embryonic culture assays were particularly striking, compared to the relatively subtle phenotypes induced by the genetic deletion of APPL. In flies lacking APPL, the initial formation of the nervous system was surprisingly normal (Luo et al., 1992), although these animals displayed more subtle defects in axonal targeting and postsynaptic synaptic growth (Ashley et al., 2005, Mora et al., 2013), and they exhibited aberrant responses to both neurodegenerative insults and traumatic brain injury (Leyssen et al., 2005, Wentzell et al., 2012). Flies lacking APPL also exhibited behavioral and learning deficits that could be rescued by re-expression of APPL or human APP (Luo et al., 1992). These results are consistent with the model that APPL-dependent interactions modulate multiple aspects of neuronal motility throughout life. By comparison, genetic deletion of Goα in

Drosophila caused more extensive abnormalities in neuronal growth and guidance, including errors in axonal guidance, fasciculation, and target innervation (Fremion et al., 1999), suggesting that additional guidance factors besides APPL normally contribute to the homeostatic control of Goα in the nervous system. In this manner, the local control of Goα activity in motile neurons may provide a convergent mechanism for integrating their responses to a range of attractive and repulsive stimuli (He et al., 2006, Bromberg et al., 2008). The dramatic patterns of ectopic growth caused by our acute manipulations of APPL signaling in the ENS may therefore reflect a lack of compensatory modulation of Goα over the relatively short time course of our embryonic culture assays.

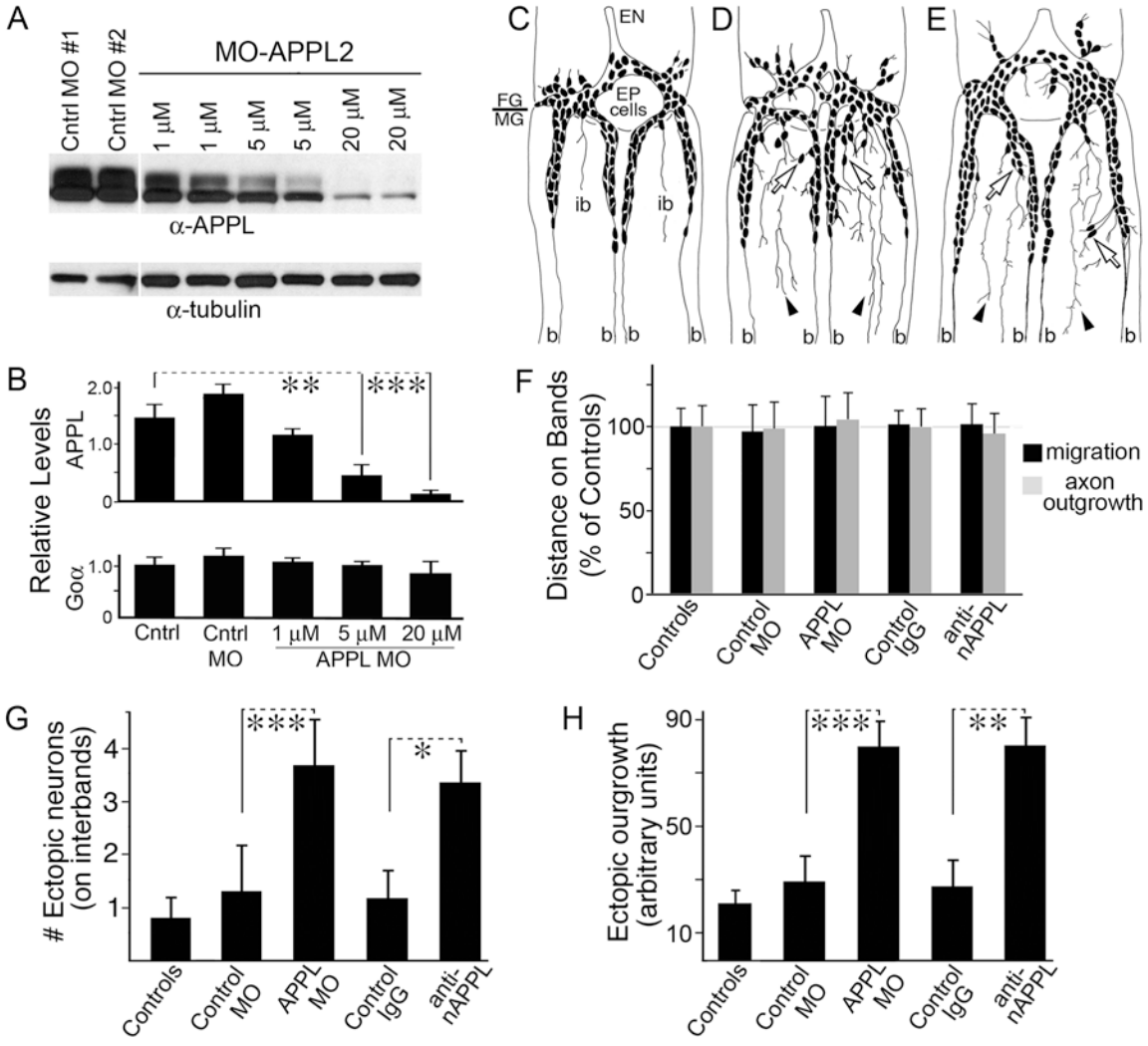
A
Cntrl MO #1
Cntrl MO #2
MO-APPL2
1 μM
1 μM
5 μM
5 μM
20 μM
20 μM
α-APPL
α-tubulin
C
EN
FG
MG
EP cells
ib
ib
b
D
E
B
Relative Levels
APPL
Goα
2.0
1.0
0
**
***
Cntrl
Cntrl MO
1 μM
5 μM
20 μM
APPL MO
F
Distance on Bands (% of Controls)
100
50
0
migration
axon outgrowth
Controls
Control MO
APPL MO
Control IgG
anti-nAPPL
G
Ectopic neurons (on interbands)
4
3
2
1
***
*
H
Ectopic ourgrowth (arbitrary units)
90
50
10
**

Figure 2.8

Figure 2.8. *Disrupting APPL signaling in the EP cells induces ectopic migration and outgrowth*. **A)** Western blot of *Manduca* GV1 cells treated with APPL-specific morpholinos (MOs) for 48 hrs, then lysed and immunoblotted with anti-APPL to demonstrate the selective knock down of APPL expression. Immunoblotting the same gel with anti-tubulin served as a control for non-specific effects of the MOs. **Lanes 1-2**: replicate GV1 cell lysates treated with 20 μM standard control MOs (plus 0.6% Endo-Porter). **Lanes 3-8**: replicate lysates treated with 0.6% Endo-Porter plus increasing concentrations of APPL MOs. **B)** Quantification of replicate experiments demonstrating the effectiveness of the APPL MOs at different concentrations (normalized to tubulin levels); treatment with 5 and 20 μM APPL significantly inhibited APPL protein levels. Quantification of Goα levels in the same samples (also normalized to tubulin) showed that Goα was unaffected by the morpholino treatments. **C-H)** Inhibiting APPL signaling in the EP cells phenocopies the effect of inhibiting Goα activity on ectopic migration and outgrowth. **C-E)** Camera lucida drawings of *Manduca* embryos in which the EP cells were treated prior to migration onset with reagents targeting APPL signaling, allowed to develop in culture for another 24-48 hr, then fixed and immunostained with anti-Fas II to reveal the full extent of migration and outgrowth. **C)** Control embryo treated with culture medium exhibited a normal pattern of migration and outgrowth (same preparation shown in Fig. 7B). **D)** Treatment with APPL-specific morpholinos (50 μM) induced the same overall pattern of ectopic migration and outgrowth caused by inhibiting Goα activity. **E)** Treatment with anti-nAPPL (1 μg/ml) also induced a similar phenotype. Open arrows in **D-E** indicate ectopic neurons in the interband regions; black arrowheads indicate ectopic processes. **F)** Average distances of neuronal migration and axon outgrowth along the band pathways for each treatment group (normalized to matched sets of control embryos in each experiment). **G)** Quantification of the average number of neurons that exhibited ectopic migration onto the interband regions for each treatment condition. **H)** Quantification of the average extent of ectopic axon outgrowth per interband region for each treatment condition. *$p < 0.05$; $^{\#}p < 0.02$; **$p < 0.01$; ***$p < 0.001$; Student's two-tailed *t* tests. N= at least 10 per condition. Error bars indicate SEM.

In combination with previous evidence that local activation of Goα in the EP cells induces Ca^{2+}-dependent filopodial retraction (Horgan and Copenhaver, 1998), we propose that APPL (and its vertebrate orthologs) can function as unconventional Goα-associated receptors that regulate the motile behavior of developing neurons (Fig. 2.9). By this model, transmembrane APPL normally traffics to the leading processes of developing neurons, where it assembles into a signaling complex with Goα. Interactions between APPL on exploratory filopodia and unidentified ligands on adjacent cells induce the local activation and release of Goα, which in turn promotes Ca^{2}-dependent filopodial retraction. Global stimulation of this pathway should therefore induce a collapse/stall response in migration (as caused by activators of Goα), whereas inhibition of either APPL or Goα should permit ectopic, inappropriate migration and outgrowth (as illustrated by the foregoing manipulations). In this manner, APPL and its vertebrate orthologs might contribute to the dynamic positioning of neurons and their processes within the developing nervous system, and in regions of synaptic plasticity in the adult brain.

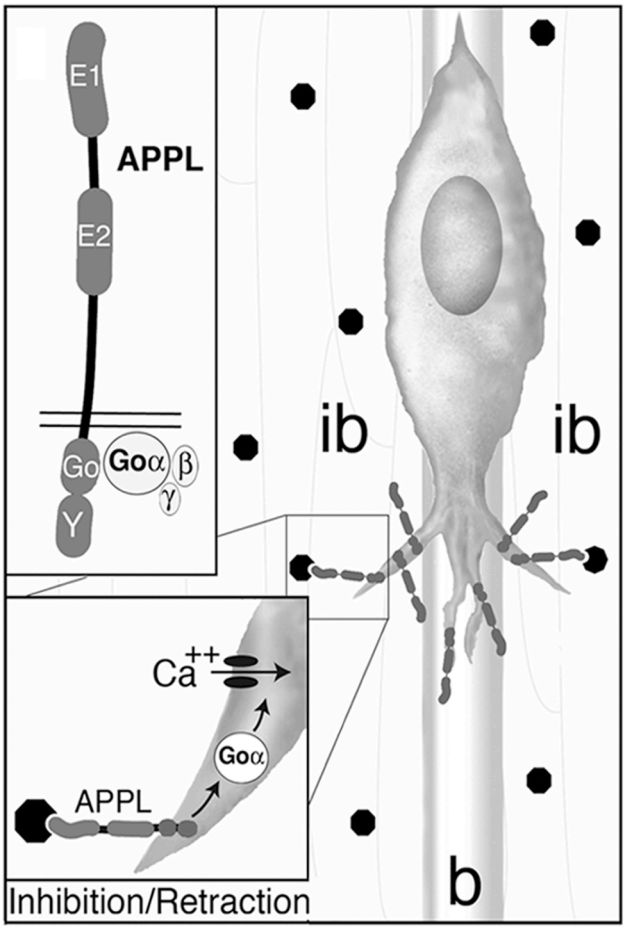

Figure 2.9. *A model for the role of APPL-Goα signaling in the control of neuronal migration within the developing ENS.* Transmembrane APPL is expressed in the motile processes of migrating EP cells, where it colocalizes with Goα. When exploratory filopodia extend off the band pathway (b) onto the adjacent interband regions (ib), they encounter ligands (as yet unidentified; black octagons) that induce APPL-dependent activation of Goα. In turn, local activation of Goα within the leading process induces Ca^{2+} influx via voltage-independent channels (Horgan and Copenhaver, 1998), resulting in filopodial retraction, thereby restricting inappropriate outgrowth and migration into these regions.

DISCUSSION

APP family proteins as unconventional Goα-coupled receptors

Evidence that APP can function as a G protein-associated receptor originated from studies by Nishimoto and colleagues (Nishimoto et al., 1993; Okamoto et al., 1995), who used reconstituted phospholipid vesicles to show that clustered APP can activate Goα via a 20 AA sequence within its cytoplasmic domain. However, the physiological role of APP as an authentic regulator of Goα activity has remained unclear. We have now used several different approaches to show that endogenously expressed APPL (in insects) and APP (in mammals) interact with Goα in the nervous system. Simultaneous immunolabeling with antibodies against both the N- and C-terminal domains of APP and APPL indicated that the full-length forms of these proteins colocalize with Goα in regions of active motility, including the leading processes of migrating neurons and the growth cones of elongating neurites (Fig. 2.1-2.2). Likewise, our coimmunoprecipitation analysis showed that endogenously expressed full-length APPL and APP both interact with Goα, in contrast to other related Gα-subunits (including Giα and Gsα; Fig. 2.3). Using genetically modified *Drosophila* lines, we demonstrated that the conserved Go-binding domain within APPL is required for this interaction (Fig. 2.3G), providing new support for the model proposed by Nishimoto and colleagues. A pharmacological analysis of APPL-Goα interactions in lysates from *Manduca* cells and embryos demonstrated that activation of Goα induced its dissociation from APPL, whereas inhibiting Goα enhanced APPL-Goα interactions (Fig. 2.6), consistent with the effects of similar manipulations targeting conventional GPCRs (Mangmool and Kurose, 2011).

Lastly, we adapted BiFC protocols to show that APPL directly interacts with Goα (but not other Gα subunits) in transfected COS7 cells (Fig. 2.4) and within the fly nervous system (Fig. 2.5). Consistent with our coimmunoprecipitation assays, we found

that the production of BiFC signals by APPL-Goα interactions required the conserved Go-binding domain in APPL (Figs. 2.4-2.5). These results provide the first demonstration that APPL and Goα can directly bind *in vivo*, and they support the model that APP family proteins represent a distinct class of unconventional (single-transmembrane) Goα-coupled receptors (Patel, 2004).

APP family proteins and the control of neuronal migration

Although the normal functions of APP and its orthologs remain controversial, considerable evidence indicates that they can regulate multiple aspects of neuronal motility. Developmentally expressed APP (in mammals) and APPL (in insects) are upregulated in regions of active growth and migration (Luo et al., 1990, Clarris et al., 1995, Torroja et al., 1999a, Sabo et al., 2003, Swanson et al., 2005, Young-Pearse et al., 2007), while both the transmembrane holoproteins and their cleaved ectodomain fragments are capable of modulating cell adhesion responses, neurite arborization, and synaptogenesis (Qiu et al., 1995, Torroja et al., 1999a, Leyssen et al., 2005, Soba et al., 2005). In particular, several recent reports have indicated that APP may play an important role in controlling neuronal migration within the mammalian brain. However, different experimental strategies have produced conflicting results, possibly due in part to the overlapping activities of the related proteins APLP1 and APLP2 (Heber et al., 2000). Analogous to the rather subtle defects seen in flies lacking APPL, genetic deletion of APP alone produced no major abnormalities in mouse brain development, although these animals subsequently exhibited a variety of postnatal defects in dendritic growth, synaptic plasticity, and spatial learning (Sugaya et al., 1996, Dawson et al., 1999, Phinney et al., 1999). Even in mice lacking all three APP family proteins, many aspects of brain development were found to be essentially normal, except for a striking pattern of

heterotopias resembling cobblestone lissencephaly (Herms et al., 2004), caused by excessive, inappropriate neuronal migration in the developing cortex (Devisme et al., 2012). Similar defects were also reported in mice lacking both Fe65 and Fe65L1 (Guenette et al., 2006), cytoplasmic adapter proteins that regulate APP trafficking and processing and may control the bioavailability of the holoprotein (McLoughlin and Miller, 2008, Dumanis et al., 2012). These results support the model that signaling by APP and its orthologs normally restricts the extent of neuronal migration in the mouse brain, analogous to our results in *Manduca*. As with APPL in the insect nervous system, we postulate that other guidance cues besides the APP family regulate Goα activity within motile neurons in the developing mammalian brain, providing a mechanism for integrating local growth responses to a variety of environmental stimuli. Given our evidence that endogenously expressed APP and Goα both colocalize and interact in mammalian neurons, it will be interesting to test whether the synaptic defects caused by the loss of APP family proteins can be linked to alterations in Goα-dependent signaling pathways.

In contrast to the heterotopias induced by genetic deletion of APP and its orthologs, interfering with APP expression in neuronal precursors by RNA interference resulted in the premature arrest of migration by their progeny (Young-Pearse et al., 2007), suggesting that APP normally promotes migration in response to permissive guidance cues in the developing cortical plate (Young-Pearse et al., 2008; Rice et al., 2012). Recent evidence demonstrating that members of the APP family also regulate the mitotic behavior of cortical progenitors (independent of their role in migration) may provide an explanation for these disparate results (Shariati et al., 2013). Since insect APPL is not expressed by developing neurons until after their terminal mitosis (Luo et al.,

1990; Swanson et al., 2005), our manipulations in the embryonic ENS have specifically addressed its function during the migratory period of development.

By exploiting the comparative simplicity of *Manduca* as a model system, we have shown that APPL plays an important role in regulating the directionality of motile neurons within the nervous system. Knocking down APPL expression in the EP cells with morpholinos eliminated their normal inhibitory response to the interband regions of the ENS, resulting in a distinctive pattern of inappropriate migration and outgrowth (Fig. 2.8D, G-H). Similarly, treating the migratory neurons with antibodies against the extracellular domain of APPL induced the same ectopic phenotype (Fig. 2.8E), presumably by interfering with endogenous interactions between APPL and its functional ligands (as yet unidentified). An alternative explanation is that treatment with anti-APPL antibodies might have accelerated the internalization or clearance of APPL from the surface of the migrating neurons, which would produce the same effect. By comparison, EP cells that remained on the muscle bands in these preparations migrated correctly (Fig. 2.8D-F), indicating that APPL is not required for their response to permissive cues associated with their normal pathways (including Fas II: Wright et al., 1999). Intriguingly, APPL has also been postulated to restrict inappropriate nuclear migration by developing photoreceptor neurons in *Drosophila*, albeit via a more indirect signaling mechanism (Pramatarova et al., 2008). Whether overstimulation of APPL signaling in the EP cells will induce premature termination of migration (similar to Goα hyperactivation) remains to be determined. Nevertheless, these results support the model that APPL functions as a guidance receptor that transduces neuronal responses to local inhibitory cues, preventing developing neurons from growing into inappropriate regions of the nervous system.

The role of APP-Goα interactions in neural development and disease

Work on a number of model systems has demonstrated an important role for Goα in the control of neuronal growth and motility. Goα is the most abundant heterotrimeric G protein in the brain (Strathmann and Simon, 1990, Chen et al., 1999); it is enriched in growth cone membranes and migrating neurons (Chang et al., 1988, Strittmatter, 1992, Horgan et al., 1994, Bates and Meyer, 1996), and it regulates neurite outgrowth (He et al., 2006, Bromberg et al., 2008). In cultured chick neurons, PTX-sensitive Go/i proteins have been shown to transduce "collapse" responses in growth cones that encounter certain inhibitory cues, in part by promoting Ca^{2+}-dependent filopodial retraction (Igarashi et al., 1993, Nakayama et al., 1999). The misregulation of this pathway may also affect regeneration responses within the mammalian CNS (Bates and Meyer, 1996). Previously, we showed that Goα stimulation in the EP cells inhibits their motility and causes premature stalling within the developing ENS (recapitulated in Fig. 2.7C), a response that is transduced via activation of voltage-independent Ca^{2+} currents (Horgan and Copenhaver, 1998). In contrast, inhibiting Goα resulted in the same characteristic pattern of inappropriate migration and outgrowth caused by interference with APPL-dependent responses (Fig. 2.8D-E).

Based on our evidence that Goα and APPL colocalize within the leading processes of the EP cells; that they are functionally coupled and directly interact via the Go-binding domain in APPL; and that inhibiting either Goα or APPL signaling produces the same distinctive phenotype of ectopic migration and outgrowth, we hypothesize that APPL functions as a Goα-coupled receptor that regulates neuronal motility in a variety of contexts. Moreover, our evidence that transmembrane APP selectively associates with Goα in mammalian neurons (Fig. 2.2R-T, 2.3H-K) suggests that this interaction is evolutionarily conserved. In the developing nervous system, this signaling pathway

would provide a previously unrecognized mechanism for restricting inappropriate migration and outgrowth, a response that might also play a role in synaptic remodeling (complementing the model proposed by Ashley et al., 2005). In the context of AD, several intriguing studies have suggested that the misregulation of APP-Goα signaling may also play a role in progressive neurodegeneration. The neurotoxic effects of FAD-associated mutations in APP were previously shown to hyperactivate Goα in cell culture, whereas blocking Goα signaling could prevent the apoptotic effects of disease-associated APP isoforms (Okamoto et al., 1996; Yamatsuji et al., 1996). More recently, studies using human brain samples revealed that both elevated G protein activity and decreased APP-Goα interactions correlated with the severity of AD symptoms (Reis et al., 2007; Shaked et al., 2009; Sola Vigo et al., 2009), while *in vitro* assays showed that Aβ peptides could disrupt APP-Goα interactions, resulting in the hyperactivation of Goα and aberrant Ca^{2+} influx (Reis et al., 2007, Shaked et al., 2009). These results are also consistent with evidence that the dysregulation of neuronal Ca^{2+} may be an important factor in initiating the neurodegenerative responses that typify AD (Khachaturian, 1987, LaFerla, 2002). Further investigation of the normal processes controlled by APP-Goα signaling (including Ca^{2+}-dependent synaptic growth and remodeling) may therefore provide the framework for testing whether the misregulation of this pathway contributes to a variety of age-related neurological conditions.

CHAPTER 3

Ligand-induced stimulation of APP regulates Go-dependent aspects of neuronal development

Modified from an in-progress manuscript

ACKNOWLEDGEMENTS

We thank Ms. Tracy Swanson for generating the Mscontactin-Fc constructs described in this chapter, and Mr. Jonathon Zweig for providing technical assistance in experiments using hippocampal neurons. Ms. Barbara Smoody and Dr. Gary Banker (Jungers Center, OHSU) provided primary cultures of embryonic rat hippocampal neurons. Suspensions of mouse hippocampi were kindly provided by Dr. Joseph Quinn and Mr. Christopher Harris (Department of Neurology, Portland Veterans Administration Medical Center, and Layton Center for Aging and Alzheimer's Disease Research, OHSU), with funding from NIH P30 AG8017. Ms. Aurelie Snyder and Dr. Stefanie Kaech (Advanced Light Microscopy Core, Jungers Center, OHSU) assisted with image analysis and quantification for experiments in hippocampal neurons. Support for this work was provided by NIH RO1 AG025525 and R21 NS080036 (to PFC), and by a grant from the Oregon Partners for Alzheimer's Research (to JMR).

ABSTRACT

Amyloid precursor protein (APP) is a transmembrane protein that has been postulated to regulate multiple aspects of neuronal motility by functioning as a receptor. However, the identity of its upstream ligands and the mechanisms by which APP signaling is induced *in vivo* remain elusive. Using established protocols for activating APP in mammalian neurons with antibodies, I have demonstrated that APP signaling causes Go-dependent growth cone retraction and collapse in cultured neurons. As a complementary strategy, I also investigated whether contactins (a group of candidate APP ligands) could regulate neuronal migration in a manner consistent with APP signaling. Using an established assay for neuronal migration in the hawkmoth, *Manduca*, I provide evidence that *Manduca* contactin (Mscontactin) may play a role in regulating the positioning of migrating neurons, consistent with Mscontactin functioning as an APPL ligand. Based on preliminary evidence that APP regulates key aspects of neuronal migration and axon outgrowth, I hypothesize that contactins function as upstream activators for APP family proteins, inducing Goα-dependent growth cone collapse that ultimately restricts neuronal migration and axon outgrowth.

INTRODUCTION

Amyloid precursor protein (APP) has been postulated to function as a receptor (Kang et al., 1987) that may regulate distinct aspects of neuronal migration, such as neurite outgrowth (Perez et al., 1997, Small et al., 1999), cell adhesion (Breen et al., 1991, Soba et al., 2005), synapse formation (Wang et al., 2005, Priller et al., 2006), and neuronal positioning (Herms et al., 2004, Young-Pearse et al., 2007, Pramatarova et al., 2008). Numerous candidate ligands for APP have been identified based on their ability to bind the extracellular domain of APP, regulate aspects of APP-associated cellular responses, and/or alter APP bioavailability. These candidates include pancortin (Rice et al., 2012, Rice et al., 2013), F-spondin (Ho and Sudhof, 2004), Reelin (Hoe et al., 2006, Hoe et al., 2009b), and members of the contactin family (Ma et al., 2008, Osterfield et al., 2008). Screens for APP-binding partners conducted by the Flanagan (Osterfield et al., 2008) and Copenhaver laboratories (unpublished data) revealed that contactins could bind the extracellular domain of amyloid precursor family proteins. Based on evidence that APP and contactins can regulate similar aspects of neurite outgrowth *in vitro*, specific contactins have been postulated to function as upstream ligands for APP (Osterfield et al., 2008).

Although the identity of endogenous ligands for APP within the brain is still controversial (Zheng and Koo, 2011), numerous studies have demonstrated that anti-APP antibodies can bind the extracellular domain of APP and stimulate APP-dependent pathways *in vitro*. In phospholipid vesicles, application of the APP antibody 22C11 enhanced Goα-GTPγS binding when the heterotrimeric G protein was expressed in combination with APP, but not when it was coexpressed with mutant forms of APP lacking their cytoplasmic Go-binding domain (APPΔGo) (Okamoto et al., 1995, Okamoto et al., 1996). These data suggest that 22C11-induced clustering of APP mimics the

effects of an agonist, thereby activating APP-Goα signaling. In culture, applying APP antibodies to rat neuroblastoma cells that were transfected to stably overexpress APP caused cytotoxicity that could be prevented by the Goα/Giα inhibitor PTX. Combined with evidence that APP interacts with Goα but not Giα, these results suggest that overstimulation of APP signaling can trigger cell death via unregulated Goα activation (Sudo et al., 2000).

Although prolonged hyperactivation of APP-Goα signaling may induce neurotoxicity *in vitro*, whether this transduction pathway mediates physiological functions in neurons is not known. When 22C11 antibodies were applied to rat cortical neurons at 14-21 days *in vitro* (DIV) and analyzed 24 hours post-treatment (prior to the onset of widespread cell death), both neurite degeneration and somal shrinkage were observed (Rohn et al., 2000). These results suggest that APP-Goα signaling may initially regulate neurite retraction responses but can subsequently harm neurons if left unchecked. In support of this model, when cultured hippocampal rat neurons were treated with sub-lethal levels of 22C11 (100 ng/mL), they exhibited reduced numbers of dendritic spines, decreased post-synaptic density markers, and increased Aβ (Lefort et al., 2012). These data suggest that hyperstimulation of APP causes synaptic dysfunction, neurite degeneration, and eventually cell death (Lefort et al., 2012). Whether APP regulates neurite outgrowth or synaptic formation during neuronal development, and whether it does so in a Goα-dependent manner, remains unknown.

To determine the role of APP in developing neurons, we applied extracellular APP antibodies to rat and mouse primary cultured hippocampal neurons during the initial establishment of their axon polarity (stage 3 neurons; Kaech and Banker, 2006). Our results identify a function for APP in mediating growth cone collapse, a response that requires downstream activation of Go (or Gi). To investigate whether this same signaling

pathway might mediate neuronal migration or axon outgrowth *in vivo*, we made fusion constructs of a candidate APP ligand, *Manduca* contactin (Mscontactin; the sole ortholog of mammalian contactins in *Manduca*), in-frame with the Fc dimerization domain of human IgG. When we applied Mscontactin-Fc fusion proteins to the developing enteric nervous system (ENS) in *Manduca* embryos, we observed stalling behavior in migrating neurons. Based on our previous study suggesting that APP regulates neuronal migration and outgrowth in the nervous system by functioning as a Goα-associated receptor (Ramaker et al., 2013), we hypothesize that Mscontactin-induced stimulation of APP-Goα signaling regulates the guidance of neuronal migration and axon outgrowth in developing neurons.

METHODS

Hippocampal cultures

Hippocampal neuron cultures were kindly prepared by the Banker laboratory, according to previously published protocols (Kaech and Banker, 2006, Kaech et al., 2012). Briefly, hippocampi were dissected from E20 male and female rat pups, digested with Trypsin (Invitrogen), and triturated into a single-cell suspension. Neurons were plated on 18 mm glass coverslips coated with poly-L-lysine at a density of 20,000-25,000 cells per coverslip and grown above astroglial feeder layers in neurobasal medium (Gibco, Life Technologies), supplemented with B27 and glutaMAX (Gibco, Life Technologies) for 24 hours. For experiments using mouse neuronal cultures, single-cell suspensions from P0 mouse hippocampi were kindly provided by Dr. Joseph Quinn and Mr. Christopher Harris and cultured, as described above.

APP antibody treatment

12-well culture dishes were pre-filled with 500 μL of each treatment reagent diluted in culture media, and equilibrated to 37^{o}C for 10 min, prior to adding coverslips containing cultured neurons. The following reagents were used for specific experiments: 1-2 μg/mL 22C11 (mouse anti-APP), targeting the extracellular domain AA 66-81 of human APP_{695} (Millipore #MAB348); 1-2 μg/mL IgG control (Jackson Laboratories #1-000-003); 50 μm Mas 7 (a mastoparan analog with enhanced activity, Enzo Life Sciences #BML-G420-0001); 50 μm Mas 17 (an inactive mastoparan analog, Enzo Life Sciences #BML-G421-0001); 100-1000 ng/mL pertussis toxin, “PTX” (List Biological Laboratories #179A); 20-100 μg/mL chick anti-ext APP, “nAPP #3”, (targeting the extracellular domain AA 433-452 of human APP_{770}, Aves laboratories); and as a matched control, 20-100 μg/mL chick anti-cyt APP, “cAPP” (targeting the intracellular

domain AA 753-770 of human APP_{770}, Aves laboratories). At 1 DIV, coverslips containing cultured neurons were transferred neuron-side-up into the pre-filled wells and incubated for 5 hours at 37°C. For pretreatment with pertussis toxin (PTX), coverslips were initially placed in wells containing PTX for 90 min, then were transferred to a new well with experimental reagents plus PTX, and inhibited for an additional 5 hours.

To fix cultured neurons, equal volumes of 8% Paraformaldehyde (PFA) in ddH_2O and 2x PHEM buffer (120 mM PIPES, 50 mM HEPES, 10 mM EGTA, 2 mM MgCl2, 6% sucrose (wt/vol), pH 7.4) were combined and preheated to 37°C. PFA:PHEM was gradually added drop-wise onto the coverslips while the growth medium was removed. Neurons were fixed for 45 min, then rinsed with PBS and stored at 4°C until use.

Immunohistochemistry of primary neurons

For immunostaining, neurons were permeabilized for 10 min with PBS-0.1% triton (PBST), and then blocked with 5% fish skin gelatin (Sigma #G7754) in PBST (blocking solution) for 30 minutes. All incubations were performed at room temperature (RT), and neurons were gently rinsed three times with PBS after each step. To visualize polymerized actin filaments, phalloidin-tetramethylrhodamine B (phalloidin-TRITC, Sigma #P1951) was diluted 1:100 in block and applied to coverslips for 20 min to stabilize actin filaments, prior to immunohistochemical staining. Primary antibodies targeting beta-III tubulin “Tuj-1” (R&D Systems #MAB1195) were diluted 1:100 in blocking solution and applied for one hour, followed by a 30 minute application of FITC-conjugated IgG2A secondary antibodies (Jackson ImmunoResearch #115-095-206) diluted in blocking solution. Neurons were post-fixed with PFA:PHEM for 45 minutes at RT. Additional primary and secondary antibodies, if used, were applied sequentially, followed by postfixation after each secondary antibody. For protocols using phalloidin, phalloidin-TRITC was reapplied to coverslips for 20 minutes at the end of the antibody

incubation period. DAPI (Sigma #D9564) was diluted in PBST to a final concentration of 36 μM and applied for 10 min. Coverslips were rinsed with PBS and then briefly rinsed with double-distilled water (ddH2O) before mounting on glass microscope slides using Elvanol (Banker G, 1998). Neurons were imaged on a Nikon compound microscope (Optiphot2-UD), using a DXM1200F digital camera and Nikon ACT-1 software; subsequent cropping and adjustments of brightness and contrast were performed with Adobe Photoshop software.

Quantification of growth cone morphology

To quantify growth cone morphology, the coverslips were scored blind to the treatment conditions. Using a Zeiss Apotome microscope, 55 neurons from each treatment group were imaged in the 555 channel (to visualize rhodamine phalloidin-labeled actin). Only stage 3 neurons that could be clearly distinguished from other neurons and whose axons did not contact other cells were chosen for this analysis. Images were compiled with Zeiss Zen software. Axonal growth cones were classified as "extended" if they widened at the tip and had veils between filopodial protrusions. Growth cones were classified as "collapsed" when they had little to no lamellipodial veils between filopodia, and classified as "retracted" when they exhibited a thinning of the axonal process and retraction debris.

For statistical analysis, the frequency of growth cones with extended, collapsed, or retracted morphologies within each experiment were compared across all treatment groups, using row-by-column contingency tables. If significant differences between groups were identified, pairwise chi-squared tests were subsequently performed to compare each treatment group with media controls. Additionally, for experiments employing PTX pretreatment, pairwise chi-squared tests were conducted to compare neurons treated with each concentration of nAPP antibody with the matched sets of

neurons that were pretreated with PTX. For experiments using multiple pairwise comparisons, the Bonferroni correction was applied to establish the p-value associated with significance.

Contactin Fusion Protein

A fragment of *Manduca sexta* contactin (Mscontactin) containing four fibronectin III-like (FN-III) domains was obtained from embryonic cDNA, using primers 5' CTT CTC ACA CAC AAC TGC GGA TTG 3' and 5' ATT GTA ATG CGA TAA GTG ACC 3'. This transcript was used as a template for PCR using primers engineered with Pme I (+ contactin signal sequence) and Sbf I sites and subcloned in-frame with a C-terminal Fc tag into the Pme I/Sbf I sites of our previously engineered pcDNA3-MCS-Fc expression vector. The resulting plasmid was transiently transfected into 293T cells using Trans-IT LT1 Transfection Reagent (Mirius). The media from the cells containing the secreted Mscontactin-Fc protein was collected after 1 week, purified on a Protein A column, and subsequently dialyzed into defined saline + 4 mM $CaCl_2$.

Embryo culture

Manduca sexta embryos were collected from a laboratory colony and raised at 25^{o}C. At 50 hours post fertilization (hpf; equivalent to 50% of embryogenesis), embryos were dissected from their eggshells and positioned dorsal-side up in sterile Sylgard chambers (Coate et al., 2008) filled with warmed culture medium (50% Schneider's *Drosophila* medium, 40% MEM with Hank's salts, 9.7% heat-inactivated normal horse serum, 0.2% 20-hydroxyecdysone, 0.1% insulin, and 0.01% penicillin-streptomycin (pen-strep), pH 7.4). Glass electrodes were used to make a small incision in the dorsal epithelium, exposing the premigratory EP cells. Experimental reagents were bath applied, the incision closed, and embryos incubated at 31^{o}C for 24 hours. At the

completion of each experiment, media containing the experimental reagents was replaced with normal culture medium and the embryos were dissected along the midline to completely expose the developing ENS. Embryos were fixed in 4% PFA in PBS for 1 hour and rinsed with PBS.

For immunostaining to visualize the EP cells, fixed embryos were permeabilized with PBS-0.1% Triton-X 100 (PBST), and blocked with 10% normal horse serum (NHS) in PBST+0.01% sodium azide (insect blocking solution). Embryos were incubated for 1 hour at room temperature (RT) with mouse anti-Fasciclin II (Fas II, C3 monoclonal) and diluted 1:20,000 in blocking solution (Wright et al., 1999). To detect anti-Fas II, embryos were incubated in biotinylated anti-mouse secondary antibodies (Jackson), diluted 1:200 in blocking solution, followed by an avidin-biotin reaction to amplify the signal (Vector Laboratories). Preparations were reacted with 1.4 mM diaminobenzine (DAB) in 0.001% H_2O_2 and then mounted in a glycerol-based media on microscope slides. To quantify changes in cell migration, camera lucida and photomicrographic techniques were used to measure the distance that each EP cell migrated from the FG/MG boundary. The average distance of migration was calculated for each band pathway, and Student's two-tailed *t* test was performed to compare means between the control and treatment group.

For immunofluorescence histochemistry, anti-Fas II primary antibodies were detected with goat-anti-mouse secondary antibodies conjugated to the fluorochrome Alexa Fluor 555 (Invitrogen), diluted 1:1000. For preparations treated with Mscontactin-Fc (or control Fc), the preparations were also immunostained with rabbit anti-human Fc antibodies, detected with goat-anti-rabbit Alexa Fluor 488 secondaries. Whole embryos were mounted on glass slides using Elvanol and imaged with an Olympus FluoView 300 laser scanning confocal head mounted on an Olympus BX51 microscope (located in the Live Cell Imaging Facility, Center for Research on Occupational and Environmental

Toxicology). ImageJ was used to create maximum intensity projections from Z-stack confocal images, and Photoshop software was used to compile images.

RESULTS

Antibody-induced APP signaling causes growth cone collapse and retraction

Previous experiments showed that treating cultured neurons for 24 hours with low concentrations (0.1-100 ng/mL) of the APP antibody 22C11 (targeting an epitope in the extracellular domain) resulted in synaptic dysfunction, while higher concentrations of the antibody caused neurite degeneration and cell death (Rohn et al., 2000). These studies suggest that misregulation of APP signaling might play a role in neurodegenerative pathology. However, the physiological functions of APP remain unidentified. To determine the effect of APP signaling on developing neurons, I treated cultured mouse hippocampal neurons with 22C11 at 1 DIV. By this time, about half of the cultured neurons have typically reached “stage 3” of their differentiation, having established a single, well-defined axon that is substantially longer than the other dendritic processes (Dotti et al., 1988). Most of the remaining neurons are still at “stage 2”, possessing multiple shorter processes and lacking an established axon. Characteristic of stage 3 neurons, each axon possesses a well-defined growth cone that undergoes periods of extension and stalling. During active periods of extension, growth cones consist of a wide central domain with numerous filopodial extensions, plus prominent lamellipodial veils between adjacent filopodia (Kaech and Banker, 2006).

To stimulate APP signaling in cultured neurons, 22C11 antibodies (2 μg/mL) were applied to 1 DIV cultures for 5 hours, after which neurons were immunostained to visualize actin and microtubules in their processes. Neurons were then scored blind to the treatment conditions: 55 stage 3 neurons were selected at random from each treatment group for imaging, and their axonal growth cones were scored as extended, collapsed, or retracted (representative images, Fig. 3.1A-C). In contrast to normal growth cones that had wide, extended tips with veils between the filopodia (see arrows, Fig.

3.1A), collapsed growth cones were stubby, with little or no veils between filopodia (Fig. 3.1B). Retracted growth cones had a more severe phenotype, with a thinning axon tapered at the tip (Fig 3.1C).

As neurons explore their environment, they constantly extend and retract their growth cones. Consistent with the normal dynamic movements of growth cones, neurons treated with media alone exhibited a mix of extended, collapsed, and retracted growth cones. Our experiments examining the effects of APP stimulation therefore tested whether different treatment conditions shifted the proportion of axonal growth cones with different morphologies. Compared to cultures treated with control media, neurons treated with 22C11 had a significantly decreased proportion of neurons with extended growth cones and corresponding increases in the proportion of growth cones with collapsed and retracted morphologies. Whereas 25/55 of the sampled neurons treated with control media displayed extended morphologies, only 13/55 neurons treated with 22C11 exhibited extended morphologies, corresponding to increases in both collapsed and retracted morphologies following 22C11 treatment ($p=0.001$). By comparison, the ratios of growth cone morphologies in cultures treated with control IgG were not significantly different than controls ($p=0.58$), although they were also not significantly different than cultures treated with 22C11 ($p=0.15$) (Fig. 3.1D). In agreement with previous work demonstrating that 22C11 can bind the extracellular domain of APP and trigger APP-dependent responses (Okamoto et al., 1995, Okamoto et al., 1996, Rohn et al., 2000, Sudo et al., 2000, Lefort et al., 2012), these results suggest that APP signaling triggers growth cone collapse and retraction.

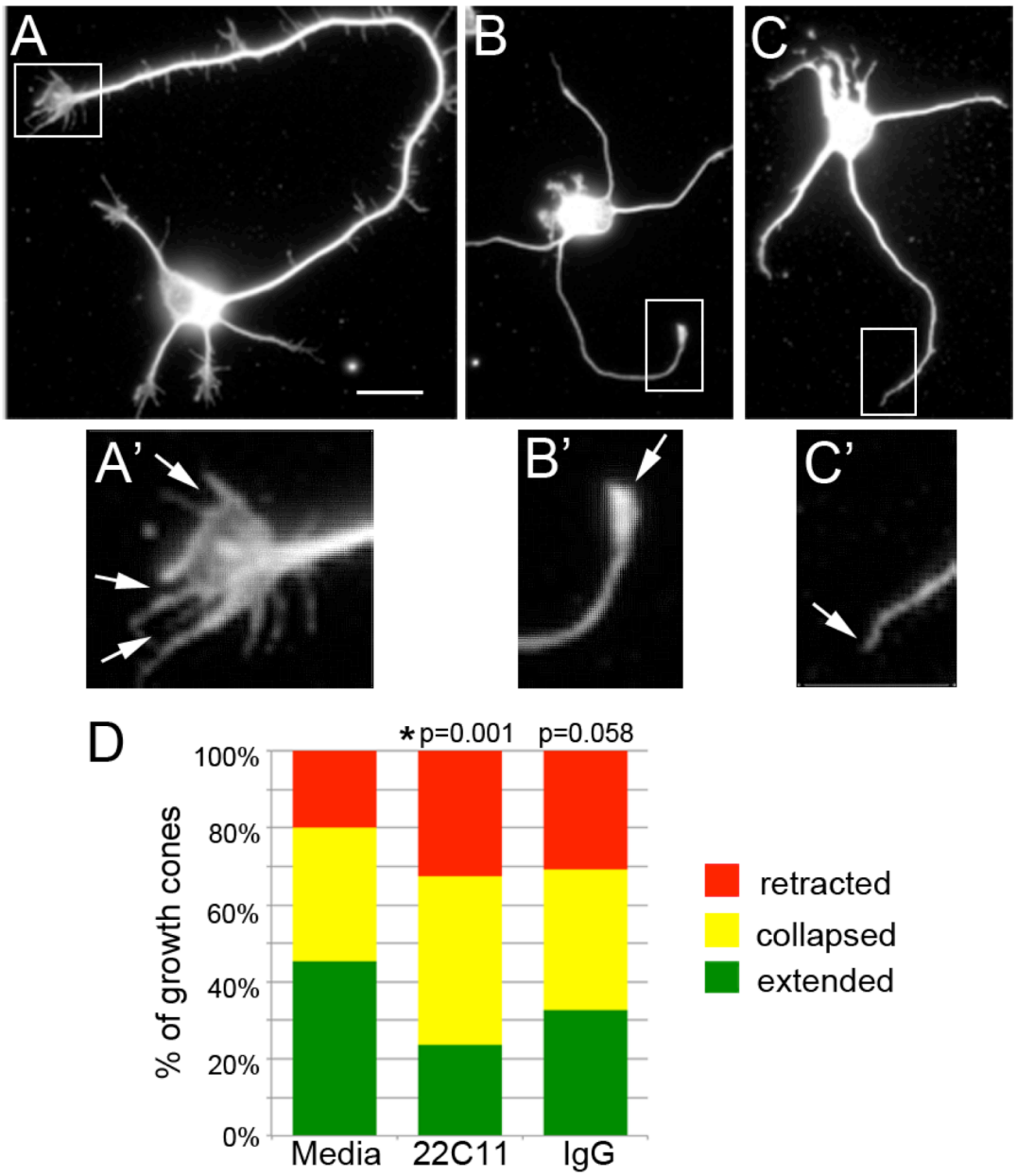

Figure 3.1. *Antibody-induced APP signaling causes growth cone collapse and retraction in cultured neurons.* **A-C)** Examples of stage 3 neurons with each of the three characteristic growth cone morphologies. Neurons were labeled with phalloidin to visualize polymerized actin. Boxed regions are enlarged in panels **A'-C'. A)** An extended growth cone, with a wide tip and veils between filopodia. **A')** Arrows point to extensive lamellipodial veils between filopodia. **B-B')** A collapsed growth cone, with little to no veils between filopodia (arrow). **C-C')** A retracted growth cone, with a thin-tipped process (arrow). **D)** Quantification of growth cones morphologies, characterized as extended, collapsed, or retracted following each treatment condition. Cultured mouse hippocampal neurons were treated at 1 DIV for 5 hours with media alone, 2 μg/mL 22C11, or 2 μg/mL IgG. Stage 3 neurons from each treatment condition were imaged and their axonal growth cone scored. Images in A-C provided by SKP of Jungers Center Advanced Light Microscopy Core, OHSU. Scale bar: 30 μM in overviews, 10 μm in insets. Pairwise chi-squared tests were used to compare the proportion of growth cone morphologies for each treatment group compared to the media control.

Antibody-induced growth cone collapse is Go-dependent

In previous studies, neuroblastoma cells overexpressing human APP were treated with a panel of APP antibodies, all of which induced neurotoxicity in 80-90% of cells after 72 hours (Sudo et al., 2000). Notably, this panel included 22C11 (targeting AA 66-81), Alz90Ab (targeting AA 511-608), and α1680 (targeting AA 1-591), verifying that the effect was specific for APP (Sudo et al., 2000), and suggesting that APP antibodies can induce signaling by binding to either the E1 or E2 domain of APP. Therefore, I tested whether a recently developed set of anti-APP antibodies (Aves Laboratories) could also induce growth cone collapse in our assays, and if so, whether this response required Go activity.

Rat hippocampal neurons were grown in culture for 24 hrs, and then treated with one of the APP antibodies and/or Go-specific reagents for 5 hrs. After fixation, neurons were stained for Tuj-1 to label microtubules (Fig. 3.2, shown in green) and phalloidin to label polymerized actin (Fig. 3.2, shown in magenta and enlarged in the grayscale inset). In the absence of treatment, the majority of neurons had extended growth cones, with prominent lamellipodial veils between filopodial protrusions (Fig. 3.2A, quantified in Fig. 3.2I), while proportionately fewer had collapsed or retracted growth cones. Treating neurons with the Go/iα activator Mas 7 resulted in a dramatic increase in the number of collapsed and retracted growth cones, and also noticeably disrupted both actin and microtubule integrity (Fig. 3.2B). Of the anti-APP antibodies tested in this assay, only nAPP #3 (targeting the E2 domain of APP; Fig. 3.2H) induced a similar response, resulting in a concentration-dependent increase in the proportion of axonal growth cones that exhibited collapsed or retracted morphologies, compared to control cultures (Fig. 3.2C, I). Although neither of these effects reached statistical significance (set at $p<0.005$ with Bonferroni correction for 11 pairwise comparisons), the trends support the model

that APP-Go activation induces growth cone collapse/retraction responses in developing neurons.

Consistent with a role for APP in inducing Go-dependent growth cone collapse and retraction, pretreating neurons with the Goα/iα inhibitor PTX for 90 min significantly reduced the number of growth cones with collapsed and retracted morphologies compared nAPP #3 treatment alone ($p<0.001$,Fig 3.2D, I). As expected, when neurons were treated with control antibodies targeting the cytoplasmic domain of APP (cAPP), the majority retained expected growth cone profiles, with the proportion of extended growth cones closely mirroring the media control (Fig. 3.2E, I). Treatment with PTX treatment alone resulted in a significant increase in the number of extended growth cones in a concentration-dependent manner ($p<0.001$, Fig. 3.2F-G, I). Given previous data that APP interacts with Goα but not Giα in cultured neurons, these results suggest that APP induces growth cone collapse and retraction through Go-dependent mechanisms. These results are also consistent with studies from other laboratories, which showed that local Goα activation in motile growth cones induced filopodial retraction, collapse responses, and the termination of axon growth (Igarashi et al., 1993, Horgan et al., 1995).

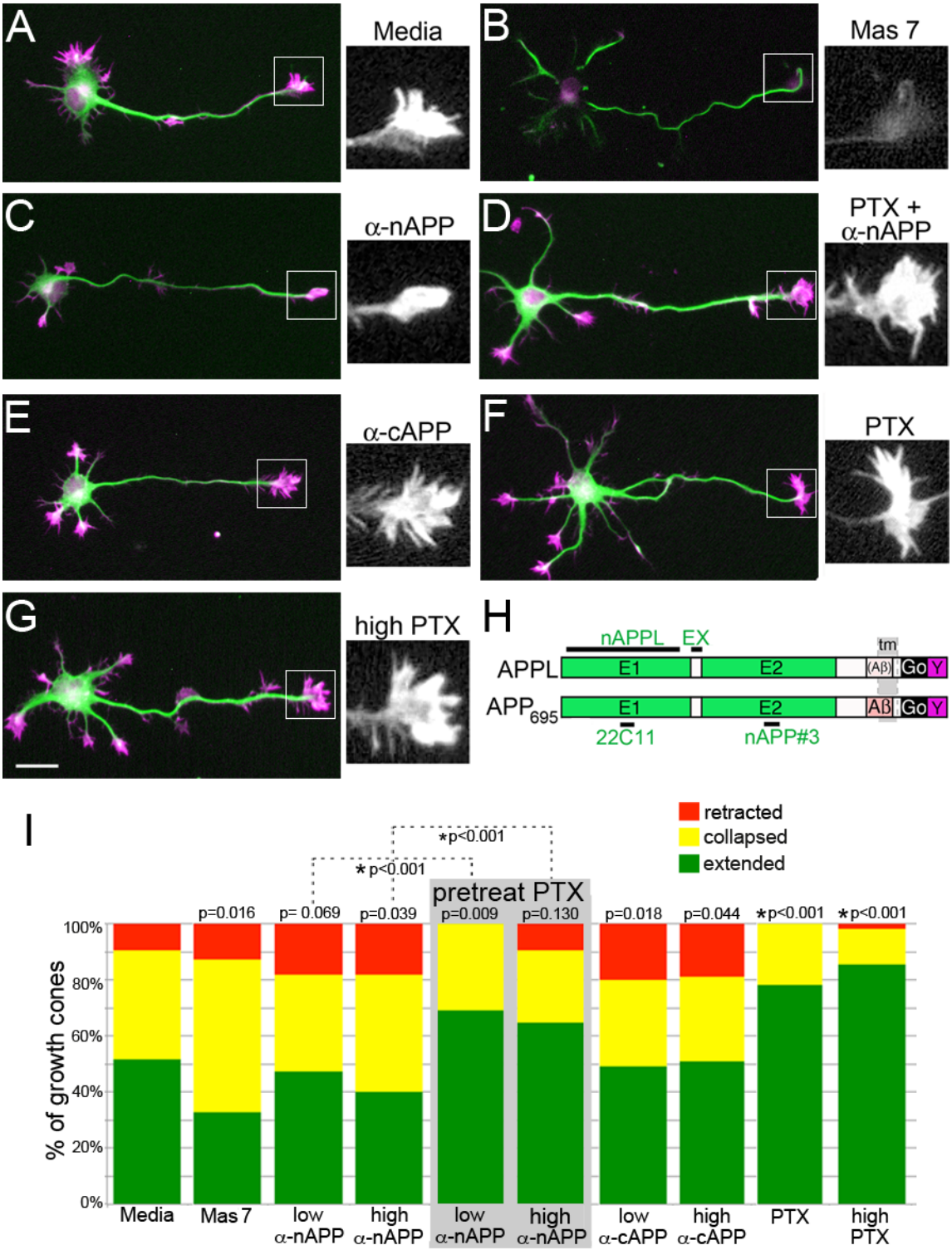
A
Media
B
Mas 7
C
α-nAPP
D
PTX +
α-nAPP
E
α-cAPP
F
PTX
G
high PTX
H
nAPPL
EX
tm
APPL
E1
E2
(Aβ)
Go
Y
APP695
Aβ
22C11
nAPP#3
I
retracted
collapsed
extended
*p<0.001
*p<0.001
pretreat PTX
p=0.016
p= 0.069
p=0.039
p=0.009
p=0.130
p=0.018
p=0.044
*p<0.001
*p<0.001
% of growth cones
100%
80%
60%
40%
20%
0%
Media
Mas 7
low α-nAPP
high α-nAPP
low α-nAPP
high α-nAPP
low α-cAPP
high α-cAPP
PTX
high PTX

Figure 3.2

Figure 3.2. *APP-induced growth cone collapse is Go-dependent.* **A-G)** Representative neurons from each treatment condition showing growth cone morphology that became more prevalent after that treatment. At 1 DIV, primary rat hippocampal neurons were treated for 5 hours with APP antibodies targeting the E2 domain or Go-specific reagents, then labeled with phalloidin (magenta) and anti-tubulin (green). Boxed areas in each image are magnified in the adjacent insets, showing phalloidin in grayscale. Scale bar: 30 μm in overviews and 6 μm in insets. **A)** Representative neuron treated with media alone, displaying an extended growth cone morphology. **B)** Mas 7 treatment severely disrupted actin and microtubule integrity, and resulted in increased numbers of neurons with collapsed (and retracted) growth cones. **C)** Treatment with nAPP #3 increased the proportion of neurons with collapsed (shown) and retracted morphologies. **D)** Treating neurons with PTX prior to nAPP #3 treatment rescued nAPP-induced collapse/retraction, enhancing the number of neurons with extended growth cone morphologies. **E)** An extended growth cone morphology exhibited by most neurons treated with control cAPP antibodies. **F)** Treatment with 100 ng/mL PTX enhanced the number of neurons with an extended morphology. **G)** PTX at 1000 ng/mL resulted in even more neurons with extended growth cones. **H)** Schematic representation of APP and APPL, with black lines demarking regions targeted by each extracellular antibody. 22C11 and nAPP #3 antibodies were used in experiments employing rodent neurons and nAPPL and EX were used in experiments using *Manduca* embryos (see next section). “E1” and “E2” are highly conserved extracellular domains in APP and APPL. “TM” demarks the transmembrane region, while the Go-binding domain “Go” and internalization domain “Y” comprise the cytoplasmic region. **I)** Quantifying the number of neurons with each growth cone morphology demonstrates that 5 hours of treatment with anti-nAPP antibodies increased the number of retracted and collapsed growth cones while pretreatment with PTX prevented this effect. P-values were obtained by comparing each treatment condition to the media control using pairwise chi-squared tests. Pairwise chi-tests comparing nAPP #3 treatment with and without PTX pretreatment were also performed. *Statistical significance with Bonferroni correction, $p<0.005$.

Inducing APPL signaling *in vivo*

I also attempted to adapt our protocols for antibody-induced APP signaling to analyze APPL functions in *Manduca* embryos. For this study, we initially generated affinity-purified antibodies against the E1 domain of *Manduca* APPL ("nAPPL"). As noted in Chapter 2, applying nAPPL antibodies to developing EP cells phenocopied the effect of knocking down APPL with morpholinos (Chapter 2), arguing that these antibodies functioned by blocking endogenous APPL signaling. As an alternative strategy, I preclustered nAPPL antibodies with anti-Fc antibodies, a strategy that has been used to induce receptor clustering and activation in other assays (Cerretti et al., 1995, Stein et al., 1998). After 24 hours in culture, the extent of neuronal migration and axon outgrowth along each of the band pathways was analyzed using the methods described above. However, cross-linked APPL antibodies did not alter the extent of cell migration or axon outgrowth in embryos compared to controls (data not shown), suggesting that the preclustering simply reduced the blocking effect of these antibodies. As a third approach, I also tested *Manduca* with APPL "EX" antibodies, generated against a region within APPL flanked by the E1 and E2 domains (for schematic, see Fig. 3.2H). As with our experiments using nAPPL antibodies, treating the EP cells with clustered APPL-EX antibodies was unsuccessful at inducing a migration phenotype.

In an effort to produce a more robust assay, I adjusted multiple aspects of the protocol, altering ratios of anti-APPL:anti-FC, increasing the concentration of antibodies, and shortening the time course of analysis, but none of these approaches were effective in producing an APPL-dependent migration phenotype. Therefore, as an alternative approach, I sought to induce APPL signaling *in vivo* by stimulating APPL with its endogenous ligand.

Mscontactin causes neuronal positioning defects in *Manduca* embryos

In order to identify potential binding partners for APP in the developing brain, the Flanagan laboratory biotinylated developing chick optic tectas, incubated them with alkaline phosphatase-fused sAPP probes (sAPP-AP), and immunoprecipitated lysates with antibodies against the AP tag (Flanagan and Cheng, 2000). Western blotting and mass spectrometry were used to identify members of the contactin family as candidate binding partners for APP (Osterfield et al., 2008). Subsequently, multiple contactin isoforms have been shown to bind APP in different assays (Ma et al., 2008, Osterfield et al., 2008) and to act in common pathways with APP to regulate neuronal development (Ma et al., 2008) and axon outgrowth (Osterfield et al., 2008). These data are consistent with the model that contactins may function as ligands for APP, regulating aspects of neuronal migration and outgrowth via APP-dependent signaling.

Contactins are members of the immunoglobulin-related cell adhesion molecule (IgCAM) superfamily. Mammals express six different contactins in the nervous system, all of which are greater than 1000 amino acids, and contain six immunoglobulin domains, four fibronectin type-III (FN-III) repeats, and a C-terminal glycosylphosphatidylinositol (GPI) anchor. Although similar in structure, all six contactins have been ascribed unique roles in development, in part due to their distinct expression patterns in the nervous system (Hosoya et al., 1995). Contactin 1 (contactin) and 2 (TAG-1) promote distinct aspects of paranodal/nodal architecture. Contactin 3 (BIG-1) and 4 (BIG-2) promote neurite outgrowth (Osterfield et al., 2008). Contactin 5 (NB-1) interacts with APLP1 at presynaptic terminals of cultured neurons and has been postulated to mediate synaptic formation (Shimoda et al., 2012). Contactin 6 (NB-2) promotes oligodendrocyte formation by acting as a ligand for Notch (Hu et al., 2006). Contactin 2, 3, 4, and 5 can each bind APP *in vitro* (Ma et al., 2008, Osterfield et al., 2008), suggesting that these proteins might function as APP ligands to mediate a

number of APP-dependent functions in different contexts. Like the APP family, contactins are also evolutionarily conserved. Whereas vertebrates express six contactin genes, only one has thus far been identified in insects. Recent studies have shown that vertebrate contactins can be detected in both neuronal and glial cell types, while *Drosophila* contactin is expressed embryonically by epithelial cells and glial cells but has not been detected in neuronal cells (Falk et al., 2002).

In the *Manduca* embryo, we have identified one contactin gene (Mscontactin), which we have subsequently cloned. Based on evidence from the Flanagan laboratory that the FN-III domains of contactin interact with the E1 domain of APP (Osterfield et al., 2008), we created a fusion construct containing the four FN domains of Mscontactin, in-frame with human Fc (Mscontactin-Fc). The construct was produced in transfected HEK 293T cells, purified by precipitation with Protein A beads, and resuspended in *Manduca* culture medium for our experiments.

As noted in Chapter 2, we previously showed that inhibiting Goα activity in *Manduca* embryos caused the migratory EP cells to grow inappropriately in interband regions between their usual pathways, which are normally inhibitory to migration. This behavior is in striking contrast to the normal pattern of migration and outgrowth by EP cells, which typically remain in close apposition to the longitudinal muscle bands that form permissive migratory pathways. We also found that inhibiting APPL expression (with APPL morpholinos) or APPL signaling (with blocking antibodies) caused phenotypes that were similar to the effects of inhibiting Goα activity. These observations suggest that an endogenous ligand may normally bind APPL to prevent neurons from growing into the interband regions. In combination with our recent data demonstrating that APPL and Goα directly interact *in vivo*, we hypothesized that Mscontactin might

trigger APPL-dependent Goα activation, which in turn would negatively regulate neuronal migration and outgrowth.

Based on the evidence that mammalian contactins function as APP ligands, I tested whether our Mscontactin constructs could alter EP cell migration in a manner consistent with APPL activation. Just prior to migration onset, Mscontactin-Fc fusion proteins (20-400 μg/mL) were bath applied to the developing ENS of cultured embryos. After 24 hours (spanning the normal duration of migration and outgrowth), the embryos were fixed and immunostained for Fas II to visualize the distribution of the EP cells and their processes in the developing ENS. In embryos treated with control media, neuronal development proceeded normally, in that neurons became dispersed evenly along the midgut muscle bands (Fig. 3.3A). In embryos treated with Mscontactin-Fc, however, neurons became incorrectly positioned along the muscle bands. Although a few of the EP cells migrated normal distances, many of the neurons stalled prematurely, resulting in the neurons aggregating near the anterior portion of the band pathways (Fig 3.3B). Compared to the average distance of EP cell migration in control treated embryos, Mscontactin-Fc treatment reduced the distance of EP cell migration, although the results did not reach statistical significance (Fig. 3.3C). Notably, the occasional growth of EP cells and their processes onto the interband regions (a common feature of untreated control preparations) was generally absent from embryos treated with Mscontactin-Fc, suggesting an enhancement of the normal inhibitory responses that prevent the neurons from traveling into these regions. These results support a role for Mscontactin in regulating neuronal migration in the developing ENS of *Manduca* embryos. Whether APPL is specifically required for the effects of Mscontactin on migration, and whether this response is mediated via the activation of Goα signaling still needs to be investigated.

If Mscontactin normally regulates APPL-dependent aspects of neuronal migration in the developing ENS, I would expect it to be expressed in inhibitory interband regions, where it can activate APPL-dependent responses in exploratory filopodia that wander off their pathways. To date, an antibody targeting *Manduca* contactin is not available. Therefore, as an alternative approach, I used antibodies targeting the Fc fusion protein to determine whether Mscontactin-Fc constructs could bind the EP cells. Following the protocols described above, embryos were treated with 20-400 μg/mL of either Mscontactin-Fc or Fc alone. After culturing the embryos for 24 hours, preparations were immunostained with anti-Fc (to detect bound Fc proteins) and anti-Fas II (to label EP cells and axons). When embryos were treated with control Fc, anti-Fc antibodies produced only low-level background staining throughout the ENS (Fig 3.3D). In contrast, in embryos treated with Mscontactin-Fc, anti-Fc labeled both the EP cells and their axons (arrowheads), consistent with the model that Mscontactin binds APPL on motile neurons. In addition, Mscontactin-Fc also labeled a subset of midline interband cells (Fig. 3.3E), which (like the lateral interband muscles) are inhibitory to migration. Since contactin family members are known to bind both homophilically (as well as heterophilically to other receptors, including APP), these results suggest that contactin may be expressed by both the lateral interband cells and inhibitory midline cells. Upon generation of an antibody, this expression pattern needs to be validated.

Based on the above data, I hypothesize that as EP cells migrate, they express APPL on their exploratory growth cones. When a neuron wanders into the inhibitory interband region, APPL interacts with Mscontactin, inducing APPL-dependent Goα activation. Local Goα activation would then trigger filopodial retraction, preventing migration and outgrowth into this region (See model, Fig. 3.3F). Based on evidence that contactins can bind APP and that they can both regulate aspects of neuronal positioning,

I hypothesize that Mscontactin is an APPL ligand, inducing APPL-Goα retraction responses in the developing nervous system.

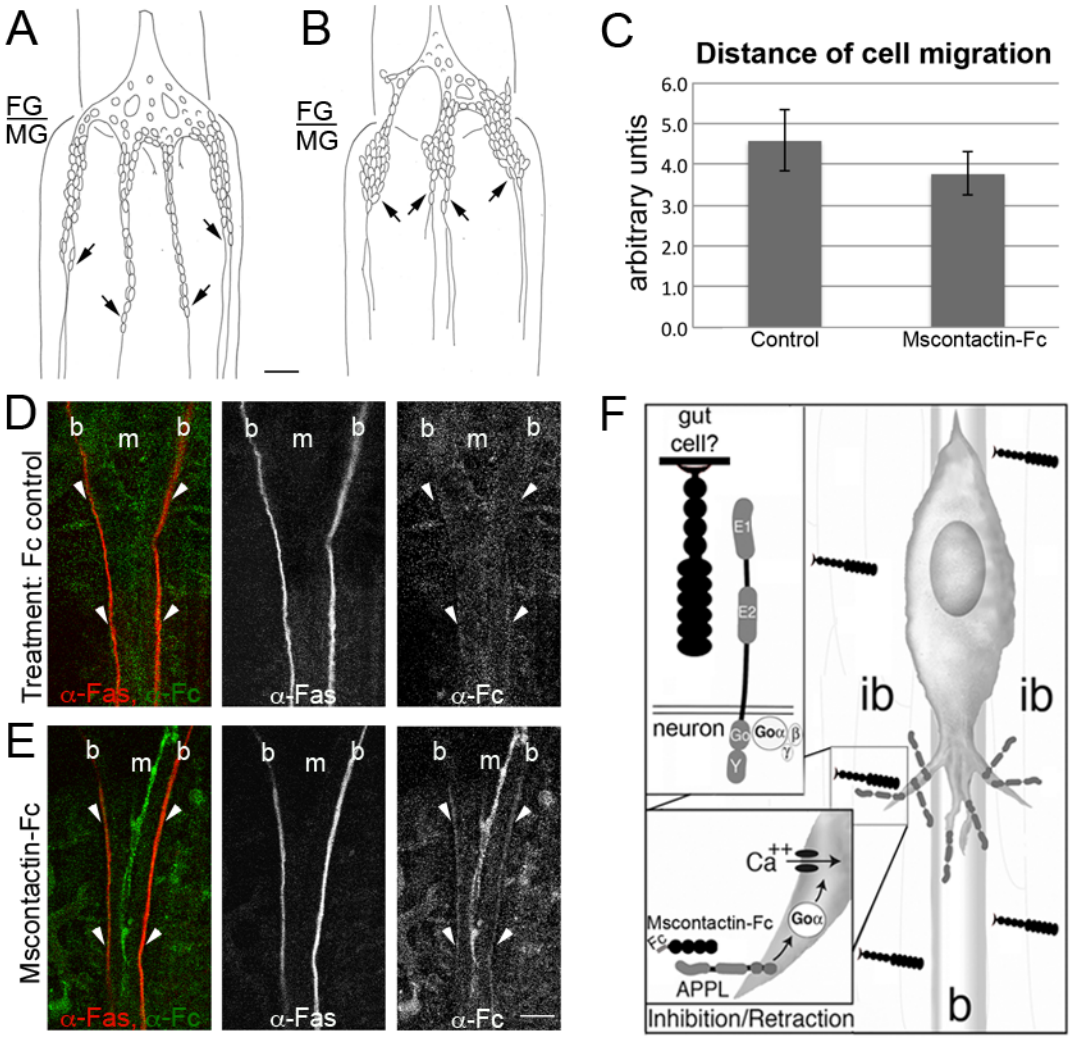
A
FG
MG
B
FG
MG
C
Distance of cell migration
arbitrary untis
6.0
5.0
4.0
3.0
2.0
1.0
0.0
Control
Mscontactin-Fc
D
Treatment: Fc control
b
m
b
α-Fas, α-Fc
α-Fas
α-Fc
E
Mscontactin-Fc
F
gut
cell?
E1
E2
neuron
Gc
Goα
β
γ
Y
ib
ib
Ca++
Mscontactin-Fc
Goα
APPL
Inhibition/Retraction
b

Figure 3.3

Figure 3.3. *Mscontactin-Fc causes defects in neuronal positioning in Manduca embryos*. **A-B)** Camera lucida drawings of *Manduca* embryos in which, prior to onset of migration, EP cells were treated with Mscontactin-Fc fusion constructs, allowed to develop in culture for 24 hours, and then fixed and immunostained with anti-Fas II to visualize EP cells and their axons. Images depict the pattern of EP cells near the FG/MG boundary, but the full extent of axon extension is not shown. Scale bar: 50 μm. **A)** In control embryos, migration proceeded normally, with neurons dispersing evenly along muscle bands (arrows) and axons extending posteriorly along the musculature. **B)** Treatment with Mscontactin-Fc caused neurons to stall and bunch together (arrows), rather than dispersing evenly along the pathways. **C**) Quantification of the average distance of EP cell migration along each of the band pathways. N=4 for control group and N=16 for treatment group. Error bars indicate SEM. **D-E)** Embryos treated with either Fc alone or Mscontactin-Fc constructs were immunostained for anti-Fas II (red) to label the EP cells and axons on their muscle band pathways, and immunostained for anti-Fc (green) to detect the fusion construct. Matched grayscale images of anti-Fas II immunostaining are shown in the middle panels and matched grayscale images of anti-Fc immunostaining are shown in the right hand panels. Each image represents one confocal section, showing the midline ('m') interband region and axons projecting along two of the band pathways ('b'). Arrowheads point to the axons. Scale bar: 15 μm. **D)** Anti-Fas II staining labels the fasciculated axons of EP cells in a *Manduca* embryo treated with control Fc constructs. Only background levels of Fc immunoreactivity are detected in the ENS and adjacent gut musculature. **E)** Anti-Fas II immunostaining labels two groups of fasciculated axons extending along muscle band pathways in a *Manduca* embryo treated with Mscontactin-Fc. Anti-Fc immunostaining reveals bound Mscontactin-Fc on the axons (consistent with their expression of APPL), as well as in a subset of midline interband muscles and more diffusely on the lateral interband muscles (both inhibitory to migration). **F)** Model for the role of Mscontactin-APPL signaling in the developing ENS. I hypothesize that Mscontactin is expressed in regions nonpermissive to EP growth (including the interband muscles), such that when exploratory filopodia extend into these regions, Mscontactin binds to and activates APPL on the neurons, which in turn induces Goα-dependent filopodial retraction and inhibits migration and outgrowth into these regions. Inset: Treating embryos with Mscontactin-Fc fusion constructs would be expected to mimic ligand-induced activation of APPL, resulting in Go-dependent reductions in neuronal migration, consistent with the experimental results.

DISCUSSION

Gain-and loss-of-function studies in animal model systems have provided insight into the role of APP signaling *in vivo*. Mice lacking all three APP family genes (APP, APLP1 and APLP2) displayed defects in brain development related to abnormal neuronal migration. Specifically, groups of neurons in the developing cortical plate migrated beyond their normal termination zones, forming heterotopias of ectopically positioned cells. Likewise in *Manduca*, knocking down APPL with morpholinos caused ectopic migration into inhibitory regions. Both of these results suggest that APP negatively regulates neuronal migration and outgrowth. Consistent with the role of APP as a Goα-coupled receptor, inhibiting Goα activation caused a similar phenotype as inhibiting APPL in the developing ENS, suggesting that APPL regulates migration and outgrowth through Goα-dependent mechanisms. However, assays to determine whether APP stimulation (for example, with Mscontactin-Fc) leads to Goα-dependent changes in neuronal motility *in vivo* had not been attempted.

Evidence that APP undergoes ligand-induced activation

APP has been postulated to function as a Goα-associated receptor *in vitro*, but the mechanisms by which this single transmembrane receptor can trigger Goα activation are not known. In phospholipid vesicles, applying anti-APP antibodies (including 22C11) induced Goα activity, suggesting that APP normally activates Goα in response to endogenously expressed ligands in the nervous system. As an alternative, APP antibodies may have bound to cell-surface APP, blocking a different endogenous signaling pathway that normally inhibits Goα activity. This alternative seems unlikely, given that APP antibodies were previously shown to enhance Goα activation both in cell

culture experiments and in experiments conducted in phospholipid vesicles, in the absence of any additional signaling partners. Likewise, in prior studies, panels of APP antibodies (including one targeting the E1 domain, a second targeting the E2 domain, and a third generated against the entire ectodomain) were each capable of inducing cytotoxic responses in neuroblastoma cells overexpressing APP (Sudo et al., 2000), arguing that the effects of APP antibody treatment were indeed APP-dependent. Based on other studies showing that antibodies against membrane receptors could induce dimerization and clustering, it was postulated that APP-dependent responses were induced via APP activation in these assays. However, whether APP dimerization actually occurred and how it led to the activation of downstream pathways were not investigated.

Previous studies have also identified pathological roles for APP signaling in neurons. Applying APP antibodies to cultured neurons decreased synaptic density, led to neurite degeneration, and enhanced cell death (Rohn et al., 2000, Lefort et al., 2012). However, whether these effects were Go-dependent, and whether APP-Goα signaling could regulate normal aspects of motility in developing neurons were not determined.

In the current studies, I have demonstrated that antibody-induced APP signaling causes Go-dependent growth cone retraction and collapse in cultured embryonic rat neurons. Our demonstration that two different APP antibodies induced similar growth cone responses supports the conclusion that these effects were APP-dependent. However, definitive proof of this model will require knocking down APP in the neurons before anti-APP antibodies are introduced. Our data also provides new evidence that APP signaling may play a physiological role in controlling the behavior of developing neurons, as well as the pathological responses induced in transfected neuroblastoma cells (Sudo et al., 2000).

In addition, our pharmacological studies support a role for Goα as the downstream effector of APP signaling. However, since both Mas 7 and PTX can affect the activity of other members of the Gi/o family of G proteins (Higashijima et al., 1988), future studies will be needed to show that knocking down Goα specifically blocks the effects of APP activation in this assay. Likewise, treating cultured hippocampal neurons with Fc constructs of mammalian contactin 3 and contactin 4 could be used as an alternate method for stimulating APP activity, as noted below.

A role for contactin as a ligand in regulating neuronal migration

APP has been postulated to function as a receptor that regulates aspects of neuronal migration and outgrowth in the nervous system, but whether endogenous ligands actually regulate its function *in vivo* remains controversial. Several extracellular molecules and membrane-bound molecules (including GPI-linked contactins) have been identified as potential APP ligands, based on their ability to bind the APP extracellular domain, their expression patterns, and their ability to alter aspects of neuronal development (Osterfield et al., 2008). Using the developing *Manduca* nervous system as an assay for neuronal development, we previously demonstrated that APPL and Goα activity both function in a pathway that prevents neuronal migration and outgrowth onto the nonpermissive interband regions. We therefore hypothesized that activation of this pathway would not only prevent inappropriate outgrowth, but possibly inhibit normal migration and outgrowth as well.

To determine whether Mscontactin could alter migration or outgrowth by inducing APPL-Goα signaling, I first determined whether Mscontactin-Fc constructs could regulate important aspects of motility in this model system. In contrast to the normal pattern of migration that results in a dispersed arrangement of EP cells along their

muscle band pathways, treatment with Mscontactin-Fc resulted in defective cell positioning along muscle band pathways. Rather than EP cells being evenly dispersed along the bands, more distal regions were devoid of neurons, while more proximal regions were occupied by abnormally aggregated groups of neurons (Fig. 3.3). Mscontactin-Fc treatment also reduced the overall extent of neuronal migration by about 20% compared to Fc-treated controls. Although these results were not statistically significant (in part due to the low sample size of these experiments), they are consistent with a role for Mscontactin in regulating neuronal migration. Future experiments will be performed to increase the sample size for each condition, and to determine whether higher concentrations of Mscontactin-Fc treatment cause a more severe phenotype. If APPL normally restricts inappropriate migration and outgrowth (as suggested by our model), globally activating APPL signaling should induce a general inhibition of migration and outgrowth, consistent with our observations. However, since permissive cues on the bands should still support migration along these pathways, neurons treated with Mscontactin-Fc are essentially receiving mixed cues for migration, resulting in inappropriate positioning. In the *Manduca* ENS, the final position of each migrating neuron is probalistic, depending on its proximity to a muscle band pathway and by dispersal cues from its neighbors. Therefore, defects in neuronal migration may also be affected by defective signaling between adjacent neurons on the same band pathways, resulting in phenotypes in which neurons stall prematurely and accumulate inappropriately on the proximal regions of the band pathways.

Given the migration phenotype that resulted from our Mscontactin-Fc treatments in cultured embryos, I will next test whether APPL is necessary for this defect by treating embryos with Mscontactin-Fc while simultaneously knocking down APPL with antisense morpholinos. Although I could also treat embryos with a combination of Mscontactin-Fc and our blocking antibodies specific for APPL (described in Chapter 2), this approach

might be complicated by competition for binding sites on APPL. Subsequent tests using PTX to inhibit Goα activation (or Goα-specific morpholinos to inhibit its expression) will further delineate whether Go is downstream of Mscontactin-APPL signaling in this pathway.

Based on established evidence for the role of APPL and Goα in ENS development, I hypothesize that ligands/binding partners that normally activate APPL (including Mscontactin) should be expressed by adjacent cell types that might regulate the behavior of the EP cells. One such candidate group of cells are the ensheathing glia that surround the EP cells as they migrate (Copenhaver, 1993; Wright 2000). Based on earlier reports that *Drosophila* contactin is expressed by glia but not neuronal cells (Falk et al., 2002), I am therefore interested to determine whether *Manduca* glial cells also express contactin. In the developing ENS, the ensheathing glia ultimately surround the EP cell bodies (located on the anterior regions of the midgut), but not the posteriorly projecting axons. Consistent with this model, when APPL signaling was disrupted in *Manduca*, aberrant migration and outgrowth occurred predominantly in the anterior region of the midgut (coinciding with the extent of glial ensheathment). These observations are consistent with a model whereby expression of APPL ligands by the ensheathing glia normally prevents migration and outgrowth into these regions.

Alternatively, APPL ligands might be expressed by the interband muscles, whereby neurons that extend processes onto these regions are induced to retract. My preliminary studies using Mscontactin-Fc to label the developing ENS support this latter scenario (as noted above). However, I will need to use additional methods to define the expression pattern of Mscontactin in the developing ENS. Unfortunately, antibodies against Mscontactin are not currently available, and our initial attempts to visualize Mscontactin expression by in situ hybridization were unsuccessful, even though we

could detect Mscontactin mRNA in embryonic lysates by RT-PCR methods. Future studies will therefore require the development of improved probes to detect Mscontactin in the developing ENS.

An alternative to the model that APPL functions as a receptor for Mscontactin is that APPL functions as a ligand and contactin as the receptor. This alternative model was presented by Osterfield et. al. who postulated that APP and contactin 4, both of which are expressed by vertebrate neurons, can interact in *cis* to promote neurite outgrowth (Osterfield et al., 2008). When they examined axon outgrowth in explanted retinal ganglian cells, application of exogenous sAPP (or just the E1 portion of the APP ectodomain) potentiated outgrowth, whereas addition of contactin 4-Fc constructs inhibited growth. From these observations, they concluded that the E1 domain of APP was a sufficient ligand to induce growth through contactin 4, whereas soluble contactin 4-Fc functioned in a dominant-negative fashion by binding APP, thereby preventing normal growth. Notably, using *Manduca* ENS development as an assay, we have observed that the application of sAPPL-AP (the ectodomain of APPL fused to an alkaline phosphatase probe) causes ectopic outgrowth, whereas Mscontactin-Fc leads to stalling and inappropriate neuronal positioning. Based on our model that APP normally functions to inhibit outgrowth (rather than promoting it), our data suggest that treatment with sAPPL might block endogenous Mscontactin-APPL signaling, whereas Mscontactin-Fc functions as a ligand to induce APPL signaling.

These contrasting roles ascribed to contactins and APP family proteins in different models can be resolved by future studies designed to elucidate the role of APP-contactin signaling in neuronal migration and axon outgrowth. For example, using cultured rat hippocampal neurons, I can test whether treatment with contactin 4-Fc can induce growth cone collapse similar to the effects of APP antibodies, which would support the model that both treatments promote retraction by mimicking ligand binding.

Performing the experiment in the absence of endogenous APP would then distinguish whether APP is downstream of contactin in mediating growth cone responses. Lastly, based on our pharmacological data that Gi/Go proteins are required for the collapse/retraction responses induced by APP activation, I can now use this signaling pathway as an assay for determining whether contactin 4 (or other candidate APP ligands) regulate the behavior of motile growth cones in a well-defined experimental context.

CHAPTER 4

APP family proteins undergo developmentally-regulated modifications that may affect their functions in the nervous system

ACKNOWLEDGEMENTS

We thank Ms. Barbara Smoody and Dr. Gary Banker (Jungers Center, OHSU) for providing primary cultures of embryonic rat hippocampal neurons. Dr. Stefanie Kaech (Advanced Light Microscopy Core, Jungers Center, OHSU) assisted with confocal imaging, providing training and technical assistance. Ms. Tracy Swanson performed coimmunoprecipitation and western blotting protocols. Confocal imaging was supported by NIH P30 NS061800. Support for this work was provided by NIH RO1 AG025525 and R21 NS080036 (to PFC), and by a grant from the Oregon Partners for Alzheimer's Research (to JMR).

INTRODUCTION

APP has been postulated to regulate neuronal motility and maintenance in the nervous system by functioning as a transmembrane receptor at the surface of neurons. In Chapter 2, I showed that APPL interacts with Goα in motile neurons, where it likely functions as a Goα-coupled receptor that prevents inappropriate neuronal migration and axonal outgrowth. Previous studies from the Copenhaver laboratory have suggested that during EP cell migration, APPL undergoes developmentally regulated trafficking and processing (Swanson et al., 2005). However, how this regulated pattern of post-translational modification and turnover is associated with APPL-Goα signaling is not known. To investigate whether the transport and cleavage of APPL might function as a mechanism that regulates APPL-Goα signaling, I used immunohistochemistry to examine the expression pattern of APPL and its cleavage products over the course of neuronal development.

In contrast to conventional GPCRs, which can activate their coupled G proteins when they undergo a conformational change in their membrane-spanning units, the mechanisms by which single transmembrane receptors like APP activate their associated G proteins are not known. To explore whether phosphorylation of APP might also regulate its association with Goα, I took advantage of phospho-specific APP antibodies to perform immunohistochemical and coimmunoprecipitation analyses in mammalian neurons. These studies show that Goα preferentially interacts with nonphosphorylated forms of APP, rather than phosphorylated forms (Thr_{668} and Tyr_{682}), revealing a potential role for APP phosphorylation in modulating APP-Goα signaling.

METHODS

Coimmunoprecipitations and Western blotting

Manduca embryos collected at 65 hours post fertilization (hpf) were frozen on dry ice and lysed in 1% NP40 buffer (150 mM NaCl, 50 mM Tris, pH 8). The samples were diluted in Laemmli buffer, then separated on 4-12% gradient polyacrylamide gels (Criterion; Bio-Rad), and transferred to nitrocellulose. Blots were immunostained with anti-cAPPL antibodies (generated against the sequence YENPTYKYFEVKE within the cytoplasmic domain of *Manduca* APPL, as described in Swanson et al., 2005), diluted 1:2500 in tris-buffered saline plus 0.1% Tween-20 (Polysorbate) and 5% Carnation dry milk. Primary antibodies were incubated for 1 hr at room temperature (RT) and detected with secondary antibodies coupled to Horseradish Peroxidase (HRP; Jackson ImmunoResearch), used at 1:10,000. Western blots were visualized using the West Pico or West Femto substrates (Thermo-Fisher) and detected using standard chemiluminescent protocols.

For coimmunoprecipitation assays using mouse brains, frozen tissue samples were provided by Dr. Joseph Quinn and Christopher Harris (Department of Neurology, Portland Veterans Administration Medical Center, and Layton Center for Aging and Alzheimer's Disease Research, OHSU). Brains were divided in half under liquid nitrogen, and extracted in NP40 lysis buffer. Each lysate was centrifuged at 16,000 rpm for 10 min, and the supernatants were pre-cleared with Protein A/G beads (Santa Cruz Biotechnology). The supernatants were then immunoprecipitated with 10-12 μg of the following antibodies for 1-3 hrs at RT or overnight at 4°C: mouse anti-22C11 (Millipore #MAB348, targeting AA 66-81 of human APP); rabbit anti-nAPP (Sigma-Aldrich #8967, targeting amino acids 46-60 of human APP_{695}); rabbit anti-phospho668 APP, "p(Thr_{668}) APP", (Sigma-Aldrich #SAB4300153, targeting phospho-specific 668 within AA 666-670

of human APP_{695},); rabbit anti-668 APP, "(Thr_{668}) APP" (Sigma-Aldrich #SAB4300464, targeting nonphosphorylated AA 666-670 of human APP_{695}); rabbit anti-phospho757 APP, "p(Tyr_{682}) APP" (Abgent #AP3027a, targeting phosphorylated AA 682 of human APP_{695} and phosphorylated AA 757 of APP_{770},); and rabbit anti-cAPP (Sigma-Aldrich #A8717, targeting AA 676-695 of human APP_{695},). Purified IgG (10-12 μg, Jackson Laboratories #1-000-003) was used as a negative control.

After incubating lysates with primary antibodies, samples were incubated with prewashed Protein A beads for 1 hr, then pelleted by centrifugation. Immunoprecipitated protein complexes were eluted by boiling the beads in SDS sample buffer for 1 min, and eluted proteins were separated on 4-12% Criterion polyacrylamide gels and transferred to nitrocellulose. Immunoblotting was carried out as described above, using the following primary antibodies: rabbit anti-nAPP (1:100, 22C11, Millipore #MAB348); anti-Goα (1:100-1:250; Horgan et al., 1995); and anti-Gβγ (1:75, BD Transduction Laboratories).

Immunohistochemistry

Manduca embryos were collected at 55, 58, and 65 hpf (corresponding to periods of filopodial extension, cell migration, and axon outgrowth, respectively), and dissected in defined saline (140mM NaCl, 5mM KCl, 28mM glucose, 40mM CaCl2, and 5mM HEPES, pH 7.4) to expose the developing ENS. Embryos were then fixed in 4% paraformaldehyde (PFA; Sigma/Aldrich) in phosphate-buffered saline (PBS) for 1 hr at RT, and rinsed in PBS plus 0.1% Triton X-100 (PBST). Prior to immunostaining, the preparations were incubated for 1 hr in *Manduca* blocking solution (10% normal horse serum plus 0.1% sodium azide in PBST). Embryos were incubated at RT for 1 hr with the following primary antibodies diluted in blocking solution: anti-nAPPL, (1:5000, #21506, targeting the AA 1-197 of the E1 ectodomain in *Manduca* APPL, described in

Ramaker et. al., 2013), followed by a 1 hr incubation with anti-cAPPL antibodies (1:2500, described above). Primary antibodies were detected with anti-rabbit 488 (Molecular Probes/Life Technologies, 1:1000) and anti-chick DyLight 549 (Jackson ImmunoResearch, 1:400) secondary antibodies. Whole-mount embryos were mounted on microscope slides using Elvanol (Banker and Goslin, 1998) and preparations were imaged with an Olympus FluoView 300 laser scanning confocal head mounted on an Olympus BX51 microscope (located in the Live Cell Imaging Facility, Center for Research on Occupational and Environmental Toxicology), or with an inverted Zeiss LSM710 confocal microscope (located in the Advanced Imaging Center of the Jungers Institute, OHSU). Maximum intensity projections of flattened Z-stack confocal images were generated using MetaMorph or ImageJ software, and images were merged using Photoshop software.

For my immunohistochemical analysis of rat neurons, coverslips containing primary cultures of embryonic hippocampal neurons were kindly provided by Dr. Gary Banker and Ms. Barbara Smoody (prepared according to Dotti et al., 1988). Briefly, neurons were isolated from hippocampi of E19 male and female rat pups and plated at a density of 20,000-25,000 on 18 mm glass coverslips coated with poly-L-lysine. Coverslips were grown at 37^{o}C above astroglial feeder layers in neurobasal medium (Gibco, Life Technologies), supplemented with B27 and glutaMAX (Gibco, Life Technologies). After 1 and 5 days *in vitro* (DIV), neurons were fixed with 4% PFA in PBS for 15 min at RT. Neurons were subsequently permeabilized for 10 min with 0.1% PBST, and preblocked for 15 min with 5% fish skin gelatin in PBST. The following primary antibodies were applied for 1 hr at RT (described above): mouse anti-22C11 (1:20); chick anti-cAPPL (1:2500); rabbit anti-p(Thr$_{668}$) APP (1:200); rabbit anti-(Thr$_{668}$) APP (1:200); and affinity-purified anti-Goα (1:50, Horgan et al., 1995). Secondary antibodies conjugated to Alexa Fluor 488, 568 or 647 (Molecular Probes/Life

Technologies) were used at a final dilution of 1:1000. Coverslips were mounted in Elvanol and imaged as described above.

Quantification and statistical analysis

To quantify the number of large perinuclear vesicles that immunostained positive for both n- and cAPPL in migrating EP cells, confocal images were collected from regions corresponding to trailing and leading cells within each embryo. Using Fiji software, maximum intensity projections containing three optical sections were produced and the image calculator "AND" function was used to create images containing only pixel values common in both the 488 (nAPPL) and 555 (cAPPL) channels. The images were then converted to binary mode, and the watershed segmentation function was applied. Within each image, regions of interest (ROIs) were obtained to isolate individual EP cells, and large perinuclear vesicles containing accumulated APPL were quantified using the "analyze particle" command. To normalize the accepted particle size across images, particle size was set as 1/100 of the average area for all EP cells in that image. Circularity was set from 0.05-1 and quantification was performed for each EP cell both as the number of vesicles per cell and the percent area of large APPL-containing vesicles based on total cell area. Both methods of analysis produced strikingly similar results; accordingly, the number of vesicles per EP cell was used for subsequent reporting purposes. Student's two-tailed *t* tests were used to compare the average number of vesicles in trailing versus leading cells at each developmental stage. At least three embryos were included at each stage, with a total of 10-20 EP cells averaged in each group.

RESULTS AND DISCUSSION

APPL undergoes regulated transport and cleavage in neurons

Previous work by the Copenhaver laboratory revealed that Goα and APPL were both expressed by migrating EP cells in the developing ENS (Swanson et al., 2005, Ramaker et al., 2013). Notably, the expression of both proteins commenced just prior to migration onset and persisted throughout embryogenesis (Horgan et al., 1994, Horgan et al., 1995, Swanson et al., 2005). Within the migratory neurons, APPL and Goα were present throughout the EP cell bodies and their motile processes, where interactions between the two proteins are postulated to regulate aspects of cell migration and axon outgrowth (Chapter 2).

Like mammalian APP, insect APPL is initially expressed as a transmembrane protein but then undergoes secretase cleavage, producing a number of smaller fragments that may each function in distinct aspects of neuronal motility (Turner et al., 2003, Gralle and Ferreira, 2007, Poeck et al., 2012, Wentzell et al., 2012). Previous studies in the Copenhaver laboratory used western blots of lysates containing the *Manduca* ENS to show that levels of full-length APPL and its secreted N-terminal ectodomain fragments (sAPPLs) varied through progressive stages of embryonic development (Swanson et. al. 2005). At 40 hpf, when APPL expression could first be detected in EP cells, high levels of sAPPLs were present in lysates, whereas only low levels of full-length APPL could be detected. As development proceeded, levels of full-length APPL progressively increased, reaching their highest levels between 70 and 85 hpf, coincident with periods of axon outgrowth (Swanson et al., 2005). Likewise, the subcellular distribution of APPL changed over the course of development, consistent with its transport to regions of motility during axonal outgrowth (Swanson et al., 2005). These observations suggest that APPL expression and cleavage are precisely regulated

in developing neurons. However, that particular study utilized anti-cAPPL antibodies for its immunohistochemical analysis and therefore did not distinguish between full-length APPL and its cleaved fragments. In related studies, another group investigated the distribution of full-length APP versus its cleavage fragments in neuroblastoma-derived CAD cells, and concluded that most endogenous APP is cleaved by secretases soon after its expression, whereby different fragments of the holoprotein traffic via distinct vesicle populations to distal regions of growing cells (Muresan et al., 2009). Therefore, to determine whether regulated trafficking and cleavage of APP family proteins might also provide a mechanism for regulating APP-Goα signaling in neurons, I first focused on the pattern of APPL expression and processing in *Manduca*.

To verify that *Manduca* APPL undergoes secretase cleavage during embryogenesis, I collected embryos at 65 hpf (during axonal outgrowth) and immunoblotted lysates with antibodies targeting the cytoplasmic domain of APPL (cAPPL; see Fig. 4.1D). This analysis revealed that in addition to the presence of full-length APPL, which was present in both mature (glycosylated) and immature forms, secretase cleavage also produced C-terminal fragments (CTFs) and APPL intracellular domains (AICDs) (Fig. 4.1E). Additional western blotting analysis with anti-nAPPL (antibodies targeting the extracellular domain) verified the presence of ectodomain fragments (data not shown). These results confirm earlier studies showing that APPL undergoes secretase cleavage in *Manduca* EP cells, similar to the pattern of secretase cleavage observed in human APP and *Drosophila* APPL (Carmine-Simmen et al., 2009; Bolkan et al., 2012; and our unpublished observations*).*

Given the abundant levels of APPL cleavage products that were present in *Manduca* embryos during embryonic development, I utilized antibodies against both the extracellular and cytoplasmic domains of APPL to determine their distribution patterns during key periods of neuronal development. Antibodies targeting the extracellular

domain of APPL (nAPPL) were visualized using Alexa-488 conjugated secondary antibodies and are shown in green, while antibodies targeting the cytoplasmic domain (cAPPL) were visualized with Alexa-568-conjugated secondary antibodies and are shown in magenta (Fig. 4.1A-C). The presence of green or magenta immunoreactivity alone therefore corresponds to N- or C-terminal fragments of APPL, whereas their colocalization (which appears white in Fig. 4.1A-C) indicates either the presence of the holoprotein or possibly the colocalization of N- and C-terminal fragments (e.g. in the same vesicle). The epitopes targeted by the antibodies used in this experiment, as well as the cleavage products detected by each antibody, are schematically illustrated in Figure 4.1D.

Immunostaining *Manduca* embryos at 55 hpf (just prior to migration onset, when the EP cells extend filopodia onto their future pathways) revealed that N- and C-terminal epitopes have very distinct expression patterns in developing EP cells (Fig. 4.1 A). Whereas nAPPL epitopes were primarily expressed in cell bodies, cAPPL epitopes were predominantly expressed in filopodia. The distinct localization of N- and C-terminal epitopes is consistent with previous studies in CAD cells, suggesting that APP fragments are generated in the cell body soon after the holoprotein is expressed, and are then transported to separate intracellular regions (via distinct vesicle populations) and may perform distinct functions (Muresan et al., 2009). However, within the leading processes of the EP cells and their elongating axons, I found that both N- and C-terminal epitopes were strongly colocalized (visualized as white staining; Fig 4.1A, arrows). These results suggest that at least some full-length APPL is transported to the most motile regions of these neurons prior to being cleaved by secretases, localizing the transmembrane holoprotein to positions where it can function as a Goα-coupled receptor that regulates responses to inhibitory guidance cues (as discussed in Chapters 2-3).

During the subsequent period of EP cell migration (58 hpf; Fig 4.1B), APPL continued to be robustly expressed by the locomoting neurons. Notably, both N- and C-terminal fragments colocalized in growth cones (arrows), indicating that the full-length receptor is expressed in these motile regions. In contrast, N-terminal fragments (green) were distributed throughout all regions of the cells, compared to C-terminal fragments (magenta), which were also abundant in axons. These results support a model whereby full-length APPL may be transported to the leading growth cone, where it undergoes rapid secretase cleavage to produce N- and C- terminal cleavage products. Whereas nAPPL ectodomain fragments would be released into the extracellular space, cAPPL fragments (including CTFs and AICDs) may undergo retrograde axonal transport, consistent with the model that AICDs may also function as regulators of gene transcription (Cao and Sudhof, 2001, Nakaya and Suzuki, 2006). Alternatively, APPL may be cleaved prior to its transport, resulting in vesicles packaged with both N- and C-terminal fragments, as well as vesicle populations containing segregated cleavage products (Muresan et. al, 2009).

After EP cells have terminated their migration and have begun to extend axons posteriorly along the muscle bands (65 hpf, Fig. 4.1C), APPL again displays a similar expression pattern. Both N- and C-terminal epitopes were found to be highly expressed in growth cones (arrows), consistent with the expression of full-length APPL in these regions. In contrast, cAPPL fragments were distributed throughout the axons, whereas nAPPL expression was more abundant in cell bodies. Interestingly, postmigratory EP cells exhibited large perinuclear accumulations of colocalized N- and C-terminal epitopes, similar to the pattern seen in premigratory neurons (Fig. 4.1A), again consistent with the model that stationary neurons divert much of the newly expressed full-length protein to this intracellular compartment. However, the resolution of these images did not allow me

to distinguish whether these vesicles primarily consisted of full-length APPL or colocalization of N- and C-terminal APPL fragments.

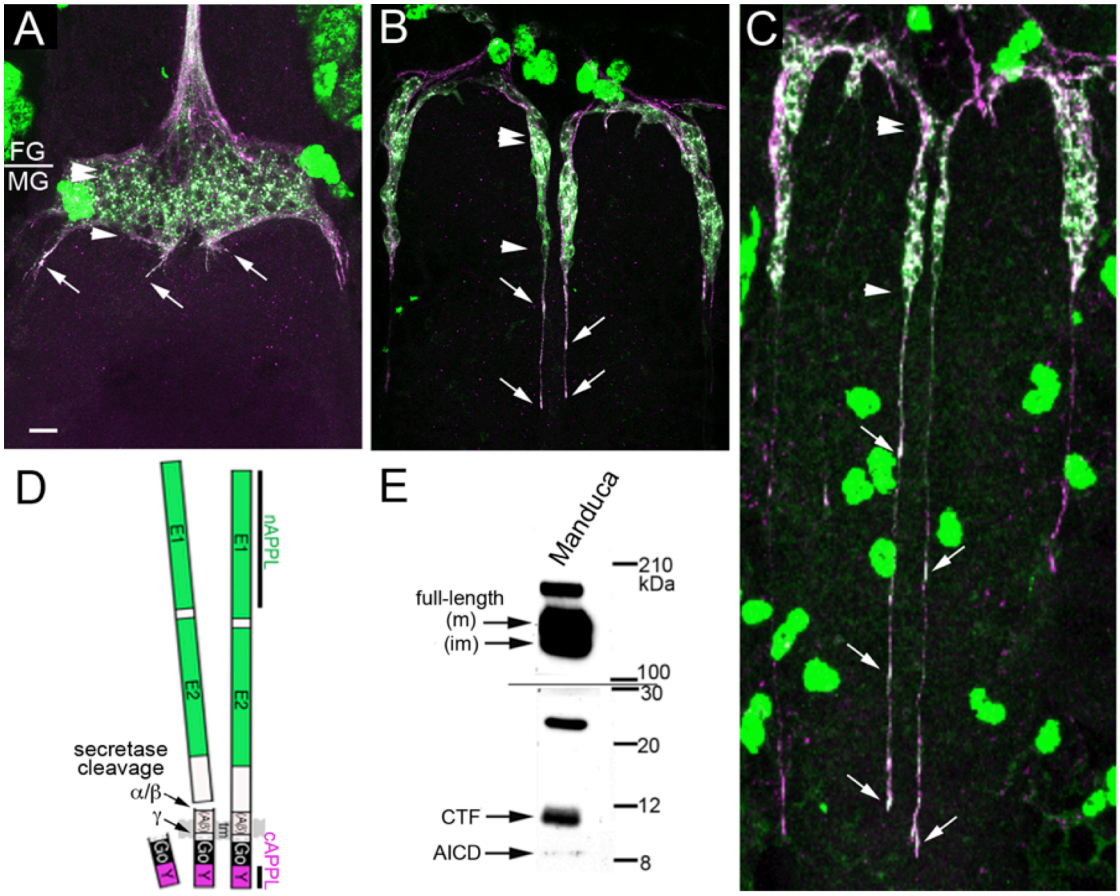
A
FG
MG
B
C
D
E1
E2
nAPPL
secretase
cleavage
α/β
γ
Aβ
tm
Go
Y
cAPPL
E
Manduca
210
kDa
full-length
(m)
(im)
100
30
20
CTF
12
AICD
8

Figure 4.1

Figure 4.1. *APPL undergoes regulated transport and cleavage in neurons.* **A-C)** Whole-mount *Manduca* embryos immunostained with antibodies recognizing nAPPL (green) and cAPPL (magenta). Regions of overlapping green and magenta (visualized in white) represent either full-length APPL or closely colocalized N- and C-terminal fragments. Cleaved ectodomain fragments are also rapidly engulfed by scavenging macrophage hemocytes, which survey the developing ENS and immunostain strongly for nAPPL alone (green). Double and single arrowheads indicate the positions used for analysis in age-matched embryos in Figure 4.2. Scale bar: 25 μm. **A)** At 55 hpf, premigratory EP cells have extended filopodia onto the muscle band pathways of the ENS midgut. nAPPL (green) is highly expressed in cell bodies, whereas cAPPL (magenta) is highly expressed in filopodial processes. Both N- and C-terminal epitopes (merged in white) are localized in the leading tips of their motile processes (arrows). **B)** At 58 hpf, migrating EP cells express high levels of nAPPL in cell bodies. Both N- and C-terminal epitopes accumulate in large perinuclear vesicles (merged in white) and in growth cones (arrows). In addition, whereas cAPPL epitopes are apparent in the growing axons, nAPPL epitopes are predominantly expressed in cell bodies. **C)** At 65 hpf, EP cells have completed migration but continue to extend long axons posteriorly along each band pathway. Whereas the EP cell bodies contain high levels of nAPPL (green) and axons contain high levels of cAPPL (magenta), n- and cAPPL epitopes are coexpressed in growth cones (white merge), suggesting that full-length APPL continues to localize to regions of active motility (arrows). **D)** Schematic illustration of full-length APPL and the cleavage products that result from α/β and γ cleavage. APPL ectodomain fragments are recognized by nAPPL antibodies (shown in green). CTFs and AICDs are recognized by cAPPL antibodies (shown in magenta). Full-length APPL is recognized by the colocalization of N- and C-terminal APPL antibodies (detected as white). **E)** Lysates from *Manduca* embryos at 65 hpf. Immunoblotting with cAPPL antibodies demonstrates that APPL undergoes secretase cleavage in developing embryos. Anti-cAPPL recognizes both mature (m) and immature (im) forms of full-length APPL (also labeled with anti-nAPPL antibodies; not shown), as well as the smaller CTFs and AICDs.

Expression of APPL in *Manduca* embryos is developmentally regulated

Previous studies using cultured rat cortical neurons (at 5 DIV) showed that nAPP is not uniformly distributed throughout neurons, but is highly expressed in cell bodies and distributed in a punctate pattern throughout dendrites and axons (Allinquant et al., 1994). By testing a number of different permeabilization protocols, these authors concluded that most APP localizes to intracellular vesicles, compared to strikingly low levels of full-length APP at the membrane (Allinquant et al., 1994). Given evidence from the previous study that full-length APPL is associated with regions of motility, I wished to determine whether APPL expression is developmentally regulated *in vivo.* Because individual growth cones cannot be distinguished within the developing ENS (due to their fasciculation on each of the band pathways), I focused instead on the cell bodies of individual neurons, analyzing the changing intracellular accumulation of APPL in motile versus stationary neurons.

To investigate the intracellular expression pattern of full-length APPL at different developmental stages, embryos were collected at 55, 58, and 65 hpf and immunostained with antibodies targeting extracellular and intracellular APPL, as described above. Confocal imaging protocols were used to obtain flattened Z-stacks of each EP cell, and the number of large vesicles that immunostained positive for both N- and C-terminal APPL (indicative of full-length protein) was quantified for each cell. To compare the accumulation of APPL in stationary versus motile neurons, EP cells were selected based on their location relative to the FG/MG boundary. (The approximate positions of trailing and leading cells at each stage are marked with arrowheads in the age-matched embryos in Figure 4.1A-C). Consistent with a developmental role for APPL in controlling neuronal motility, the subcellular localization of full-length APPL in premigratory neurons (55 hpf) was distinct from that seen in neurons extending processes onto the band pathways (Fig. 4.2A). In premigratory neurons, a substantial amount of full-length APPL

accumulated within a set of large perinuclear vesicles (arrows, Fig. 4.2A_1). In contrast, actively migrating neurons exhibited full-length protein in their leading processes (high resolution image not shown), whereas they contained considerably less APPL in the large perinuclear vesicle compartments (arrows, Fig. 4.2A_2). Quantifying the number of these large perinuclear vesicles containing APPL verified that premigratory neurons (including “trailing cells”) had significantly more APPL diverted in this compartment than was seen in actively migratory neurons (“leading cells”) within the same preparation (Fig. 4.2D, p=0.002).

Consistent with the model that postmigratory neurons divert full-length APPL to a particular set of intracellular vesicles, stationary neurons near the FG/MG boundary of embryos at 58 hpf exhibited a substantial amount of full length APPL within large perinuclear vesicles (arrows, Fig. 4.2B_1). By contrast, leading cells, which at 58 hpf are still actively migrating, rarely exhibited accumulations of APPL in perinuclear compartments (Fig. 4.2B_2). Notably, the number of large perinuclear APPL-containing vesicles was significantly higher in stationary cells compared to the infrequent accumulation of APPL in large vesicles in motile cells (Fig 4.2D, p=0.001)

Finally, at 65 hpf, a stage when most EP cells have completed their migration and have transitioned to a period of axonal outgrowth, the amount of APPL that accumulated in perinuclear vesicles was substantially reduced in both trailing and leading cells (Fig. 4.2C, quantification in D-E). This pattern is consistent with the model that motile neurons transport full-length APPL from their cell bodies to regions of motility, which at this stage consists of their axonal growth cones. In contrast, the stationary neurons that are no longer actively growing may instead divert most full-length APPL into intracellular compartments for processing and degradation. It will be interesting in future studies to counterstain EP cells for antibodies against different compartment markers to determine the identity of these intracellular compartments.

Interestingly, in all groups of neurons, I observed surprisingly little colocalization of n- and cAPPL epitopes at the plasma membrane of the cell bodies, as would be expected if full-length APPL is targeted to the cell surface immediately after its expression. Alternatively, interactions between full-length APPL and various adapter molecules might potentially mask the epitopes recognized by our cAPPL antibody. This alternative model is supported by my unpublished data, in which I found that nAPPL could be detected on the surface of fixed, unpermeabilized EP cells in regions lacking cAPPL immunoreactivity (data not shown). Future studies utilizing additional C-terminal-specific APPL antibodies (recognizing different epitopes) or using exogenously expressed APPL with distinct N- and C-terminal epitope tags will be instrumental in resolving this issue.

In contrast to the distinct distributions of N- and C-terminal fragments of APPL throughout the EP cell bodies, the considerable overlap in their expression within the large perinuclear vesicle compartments and within motile growth cones was particularly striking. Although I cannot rule out the possibility that these regions contain closely apposed n- and cAPPL cleavage products, the uniform overlap of N- and C-terminal epitopes within these regions suggests the presence of the full-length protein. Notably, neighboring regions of the same neurons display striking segregation of N- and C-terminal epitopes, demonstrating that at this resolution, I am able to detect large populations of vesicles containing different APPL-derived cleavage products. This expression pattern supports our preferred model whereby full-length APPL is transported to motile regions of actively migrating neurons, whereas in stationary neurons, APPL is diverted to perinuclear vesicles. In this manner, the developmentally regulated expression and transport of APPL in developing neurons may play an important role in regulating its function as a modulator of neuronal responses.

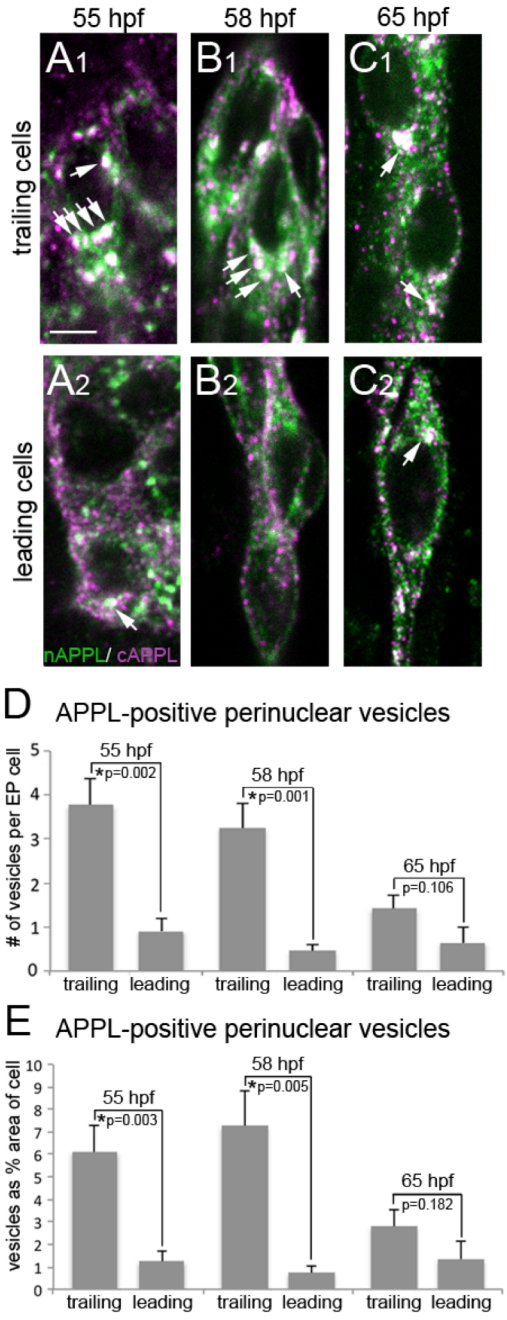
55 hpf
58 hpf
65 hpf
A1
B1
C1
trailing cells
A2
B2
C2
leading cells
nAPPL/ cAPPL
D
APPL-positive perinuclear vesicles
# of vesicles per EP cell
55 hpf
*p=0.002
58 hpf
*p=0.001
65 hpf
p=0.106
trailing leading trailing leading trailing leading
E
APPL-positive perinuclear vesicles
vesicles as % area of cell
55 hpf
*p=0.003
58 hpf
*p=0.005
65 hpf
p=0.182
trailing leading trailing leading trailing leading

Figure 4.2

Figure 4.2. *The distribution pattern of APPL is developmentally regulated in migratory EP cells.* **A-C)** High resolution images showing a stack of three confocal sections focusing on motile EP cells in *Manduca* embryos at 55, 58, and 65 hpf. The arrowheads in Figures 4.1A-C show equivalent regions in age-matched embryos from which these images were collected. (Double arrowheads correspond to the position of trailing cells at each developmental stage and single arrowheads point to leading cells.) Merged images show nAPPL immunostaining in green and cAPPL immunostaining in magenta, whereas their overlap (merged as white) indicates full-length protein. Scale bar: 5 μm. **A)** At 55 hpf, large vesicular accumulations of both N- and C-terminal APPL (colocalization visualized in white) are abundant in premigratory EP cells (arrows, $\mathbf{A_1}$). In contrast, leading cells that have begun migrating and extending filopodia onto the muscle band pathways have significantly fewer large perinuclear vesicles with colocalized n- and cAPPL (arrow, $\mathbf{A_2}$). **B)** At 58 hpf, trailing cells exhibit significantly more n- and cAPPL colocalized (white) in large intracellular vesicles (arrows, $\mathbf{B_1}$) compared to leading cells ($\mathbf{B_2}$), which have very few n- and cAPPL-positive perinuclear vesicles. **C)** At 65 hpf, both the trailing ($\mathbf{C_1}$) and leading ($\mathbf{C_2}$) neurons, which are postmigratory but undergoing axon elongation, have fewer large perinuclear compartments that stain positive for both N- and C-terminal APPL compared to other stages. The number of vesicles in trailing cells is not significantly different than that of leading cells at this stage. **D)** Quantification of the average number of large n- and cAPPL-positive perinuclear vesicles per EP cell, based on their position along the migratory pathway and developmental stage. **E)** Quantification of the average area of n- and cAPPL-positive perinuclear vesicles as percentage of total cell area. P-values were obtained using Student's two-tailed *t* tests for each pairwise comparison. N= at least 10 per condition. Error bars indicate SEM.

***Manduca* APPL and rat APP exhibit similar patterns of developmental expression during development.**

To determine whether the patterns of expression and transport that I observed for APPL are similar to the developmental regulation of mammalian APP, I compared progressive stages of axon outgrowth within the developing ENS of *Manduca* with that of cultured primary rat hippocampal neurons. Figure 4.3 shows APPL immunostaining at two developmental stages in *Manduca,* corresponding to cell migration (Fig. 4.3A) and axonal outgrowth (Fig. 4.3B; similar to the stages shown in Fig. 4.1B and C). For comparison, APP expression was analyzed in stage 3 cultured neurons, corresponding to a period in which neurons first establish axonal polarity and extend a well-defined axon (1 DIV; Fig. 4.3C), and subsequently during stage 5, when neurons undergo an extended period of axonal and dendritic growth (5 DIV; Fig. 4.3D).

Similar to the pattern of APPL expression in *Manduca*, mammalian neurons express high levels of nAPP fragments (green) in the cell bodies and cAPP fragments (magenta) throughout their axons. Additionally, n- and cAPP are highly colocalized in growth cones of cultured rat hippocampal neurons (arrows), suggesting that full-length APP (like APPL) is transported to regions of active motility, consistent with it playing a role in controlling neuronal behavior. As in *Manduca*, rapid cleavage of APP at the growing processes followed by retrograde transport of C-terminal fragments may account for high levels of cAPP immunoreactivity found throughout the axon. Conversely, high levels of nAPP in the cell bodies may correspond to fragments produced by secretase cleavage either before or after full-length APP is transported to more distal regions (Muresan et. al., 2009). In future studies, I plan to use both cultured rat neurons and *Manduca* embryonic cultures to test the functional role of APP/APPL processing in regulating Goα-dependent signaling events in the control of neuronal motility

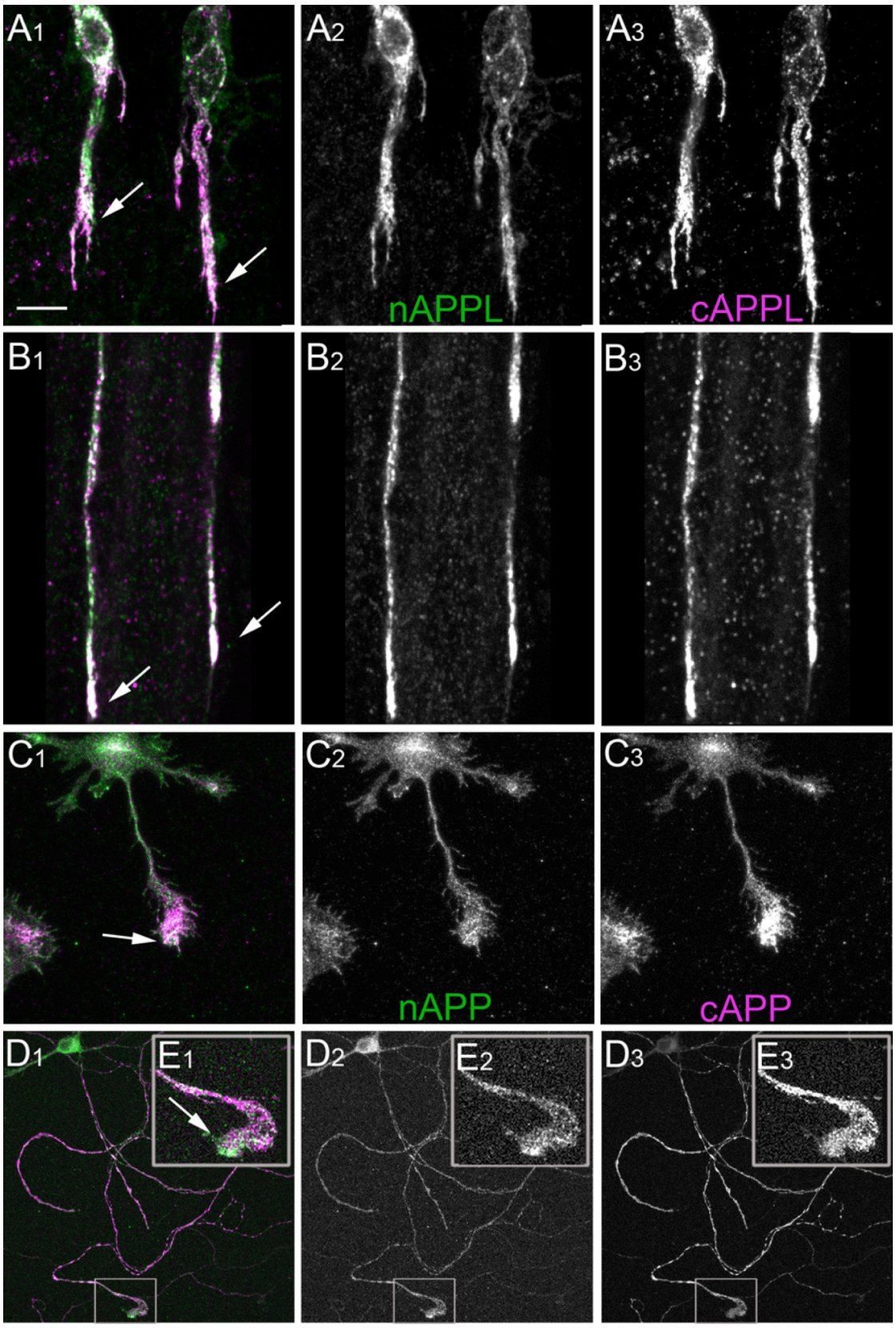

Figure 4.3

Figure 4.3. *Comparison of APPL distributions in Manduca neurons and APP in cultured rat neurons at analogous stages of outgrowth.* **A-E)** Whole-mount *Manduca* embryos and cultured rat primary hippocampal neurons immunostained with N-terminal (green) and C-terminal (magenta) APP(L) antibodies at two periods in neuronal development. Columns 2-3 show matched gray scale images of nAPP(L) and cAPP(L) immunostaining, respectively. **A)** Immunostaining *Manduca* embryos during periods of neuronal migration (58 hpf) reveals that both n- and cAPPL are localized to the leading growth cone regions of axons (arrows), as well within subcellular regions of the motile cell body. Whereas nAPPL is highly expressed in cell bodies, cAPPL is predominantly expressed in axons. **B)** Motile growth cones in *Manduca* embryos at 65 hpf (during axon outgrowth) exhibit high levels of colocalized n- and cAPPL (arrows), compared to their more segregated distribution along axons. **C)** Immunostaining rat neurons at 1 DIV (during the establishment of an identifiable axon) reveals that, similar to the expression pattern of *Manduca* APPL, cAPP is abundant in axons (magenta), whereas nAPP is abundant in the cell bodies (green). Compared to their relatively segregated pattern of expression in the rest of the neuron, both nAPP and cAPP are highly expressed in growth cones (arrow). **D)** Rat neurons at 5 DIV (a period of active axon outgrowth) express high levels of nAPP in their cell bodies (green) and high levels of cAPP in their axons (magenta). **E)** Magnified view of the boxed region in **D**. Similar to the expression pattern of APPL in *Manduca* EP cells during periods of axon elongation, n- and cAPP are highly colocalized in axonal growth cones (arrow). Images are maximum projections from 14 optical sections (**A**); 3 optical sections (**B**); 10 optical sections (**C-E**). Antibodies used were: nAPPL #21506 (**A,B**); nAPP #22c11 (**C-E**); cAPPL (**A,B,C**); (Thr_{668}) cAPP (**D,E**). Scale bars: (in **A,B**) 10 μm; (in **C,E**); 30 μm; (in **D**) 60 μm.

APP modifications may regulate APP-Go signaling in developing neurons

APP undergoes numerous forms of post-translational modification that may alter its function in neurons. In addition to secretase cleavage (described above) and glycosylation (Swanson et al., 2005), APP is subject to phosphorylation at a number of cytoplasmic residues, including Thr_{654}, Ser_{655}, Thr_{668}, and Tyr_{682} (Oishi et al., 1997).

In particular, Tyr_{682}, within the highly conserved Y682ENPTY motif, is necessary for APP to interact with a number of adapter molecules, such as Fe65, Dab1, and X11. For example, phosphorylation of APP at Tyr_{682} reduces its interaction with Dab1 (Howell et al., 1999) and Fe65 (Zhou et al., 2009), whereas binding by X11 at this residue is independent of the phosphorylation state (Tamayev et al., 2009). These data support a model whereby phosphorylation of APP may provide a mechanism for regulating its interaction with other downstream signaling molecules, such as Goα. Similarly, within the highly conserved TPEER region of the Go-binding domain in APP (100% conserved in *Manduca* APPL), APP is subject to phosphorylation at Thr_{668}. The role of Thr_{668} phosphorylation is currently not known, and given its location within the Go-binding domain, I investigated whether phosphorylation at this site might regulate APP-Goα interactions.

For this analysis, I triple-immunostained stage 3, hippocampal neurons with antibodies targeting Goα, nAPP, and different modified forms of cAPP. A schematic illustration of the epitopes recognized by the anti-APP antibodies used in this experiment are shown in Figure 4.4F. Consistent with our previous studies, I found that N- and C-terminal APP epitopes tended to localize to distinct regions within hippocampal neurons. Most nAPP fragments localized to the cell body and neurite terminals, whereas most C-terminal epitopes localized throughout the axon (Fig. $4.4A_1$). Notably, immunostaining with antibodies recognizing nonphosphorylated Thr_{668} APP (Thr_{668}) was particularly

strong in the growth cone regions, where it colocalized with nAPP. This expression pattern suggests that although neurons exhibit high levels of nAPP and (Thr_{668}) cAPP cleavage products, full-length forms of (Thr_{668}) APP are most prevalent within motile growth cones (Fig. 4.4A_{1-2}). Additionally, colocalization between nAPP, (Thr_{668}) APP, and Goα was apparent throughout the peripheral regions of the growth cones and extended into their filopodia (Fig. 4.4A_{3-4}), where interactions between full-length APP and Goα may play a role in regulating responses to local guidance cues (as discussed in Chapter 3).

In contrast, immunostaining with antibodies specific to the phosphorylated form of this same epitope, p(Thr_{668})APP, only weakly labeled the peripheral regions of growth cones (Fig. 4.4B_{1-2}). Rather, anti-p(Thr_{668}) APP staining was robustly expressed throughout the axon and central domain of growth cones, but its signal dropped off within the peripheral domains and was mostly absent from the filopodia (Fig. 4.4B_2, arrows). Therefore, even though nAPP epitopes could be detected in these regions, full-length p(Thr_{668}) APP only minimally colocalized with Goα in the leading tips of growth cones (Fig. 4.4B_{3-4}, arrows), where APP-Goα signaling is postulated to occur. These observations are in opposition to studies conducted in CAD cells, which suggested that C-terminal fragments containing the p(Thr_{668}) APP epitope were most highly expressed in actin-rich regions of growth cones (including lamellipodia and filopodia; Muresan et al., 2009). Based on this observation, the authors concluded that phosphorylation of cAPP fragments at Thr_{668} could promote growth cone turning. However, their study only compared p(Thr_{668}) APP expression with that of nAPP, and did not analyze the distribution pattern of p(Thr_{668}) versus nonphosphorylated (Thr_{668}) APP epitopes at high resolution. Our results highlight the value of pursuing these investigations with endogenously expressed APP in neurons. In future studies, I hope to test the role of

phosphorylation at Thr_{668} in modulating APP-Goα signaling as a mechanism to control neuronal motility.

In contrast to the distinct expression pattern for p(Thr_{668}) and nonphosphorylated (Thr_{668}) APP in developing neurons, p(Tyr_{682}) APP expression was found to be relatively uniform throughout neurons (Fig. 4.4C_2), generally colocalizing with nAPP (Fig. 4.4C_1). These results suggest that p(Tyr_{682}) APP is primarily present as full-length protein. Although p(Tyr_{682}) APP expression overlapped with Goα immunostaining, it was not elevated at regions of neuronal motility, nor did this modified form of APP coimmunoprecipitate with Goα (as discussed below), indicating that this isoform may not participate in APP-Goα signaling in developing neurons (Fig 4.4$C_{3\text{-}4}$).

As a biochemical approach to determine if specific cAPP modifications might regulate interactions between APP and Goα, mouse brain lysates were immunoprecipitated with a panel of APP antibodies and subsequently immunoblotted for Goα (Fig. 4.4D). Additional counterblotting for nAPP showed relative levels of APP immunoprecipitated with each antibody (top blot). The input lane shows that abundant levels of full-length APP and Goα were present in the lysates before immunoprecipitation (Lane 1).

When lysates were immunoprecipitated with nAPP antibodies, Goα could be readily detected in western blots of the coimmunoprecipitated proteins, even though relatively little full-length APP was pulled down in this experiment (Lane 2). These results are consistent with previously published work demonstrating that Goα interacts with full-length APP in developing neurons (Ramaker et. al. 2013). To determine whether Goα preferentially interacts with nonphosphorylated or phosphorylated forms of APP, lysates were immunoprecipitated with each of the antibodies described above, and the immunoprecipitates were probed with anti-nAPP to verify that equivalent levels of full-

length APP were immunoprecipitated. Whereas Goα coimmunoprecipitated strongly with (Thr_{668}) APP, its interaction with p(Thr_{668}) APP was negligible (Lanes 3-4). These results are consistent with immunohistochemical patterns of each epitope (as noted above), in which (Thr_{668}) APP, rather than p(Thr_{668}) forms of full-length APP colocalized with Goα in the peripheral region of growth cones. Likewise, Goα did not coimmunoprecipitate with p(Tyr_{682}) APP in mouse brain lysates (Lane 5), supporting our immunochemical studies that this form of APP does not specifically colocalize with Goα in developing neurons.

Based on this immunohistochemical and biochemical evidence that Goα preferentially interacts with nonphosphorylated (Thr_{668}) APP, rather than p(Thr_{668}) APP, I hypothesize that phosphorylation at this residue may provide an additional mechanism for regulating APP-Goα signaling in neurons. In particular, I predict that APP might directly interact with Goα in the absence of Thr_{668} phosphorylation, whereas phosphorylation at this residue could function to either prevent the association of APP and Goα in motile growth cones (precluding activation of this pathway) or possibly trigger the activation and release of Goα, independent of ligand activation (an area of investigation for future studies). To determine whether (Thr_{668}) APP interacts with the inactive, heterotrimeric form of Go, we immunoprecipitated mouse brain lysates with anti-(Thr_{668}) APP antibodies and immunoblotted for Gβ. Input lanes show that Gβ is abundant in lysates before immunoprecipitation (4.4E Lane 6). Consistent with our previous evidence that APP interacts with trimeric Go (Goαβγ), (Thr_{668}) APP coimmunoprecipitated with Gβ (Lane 9) as well as Goα (Lane 3). As positive controls, we also verified that Gβ could be coimmunoprecipitated with full-length forms of APP in this assay (immunoprecipitated with nAPP antibodies, Lane 7), as well as other antibodies against cAPP (using polyclonal antibodies generated against the entire internalization domain, Lane 8). Immunoprecipitations performed with matched

concentrations of IgG served as a negative control (Lane 10). Future experiments will be needed to test if Gβγ preferentially interacts with (Thr_{668}) APP versus p(Thr_{668}) APP, and to confirm that this interaction occurs as part of the Goαβγ trimeric complex (as opposed to Gβγ interacting with APP independent of Goα). However, these results are consistent with the model that inactive, heterotrimeric forms of Go associate with (Thr_{668}) APP, but not p(Thr_{668}) APP. Whether or not phosphorylation of APP can serve as a convergent mechanism to regulate APP-Go signaling, independent of ligand-dependent activation, will also be the focus of future investigations (discussed in the following chapter).

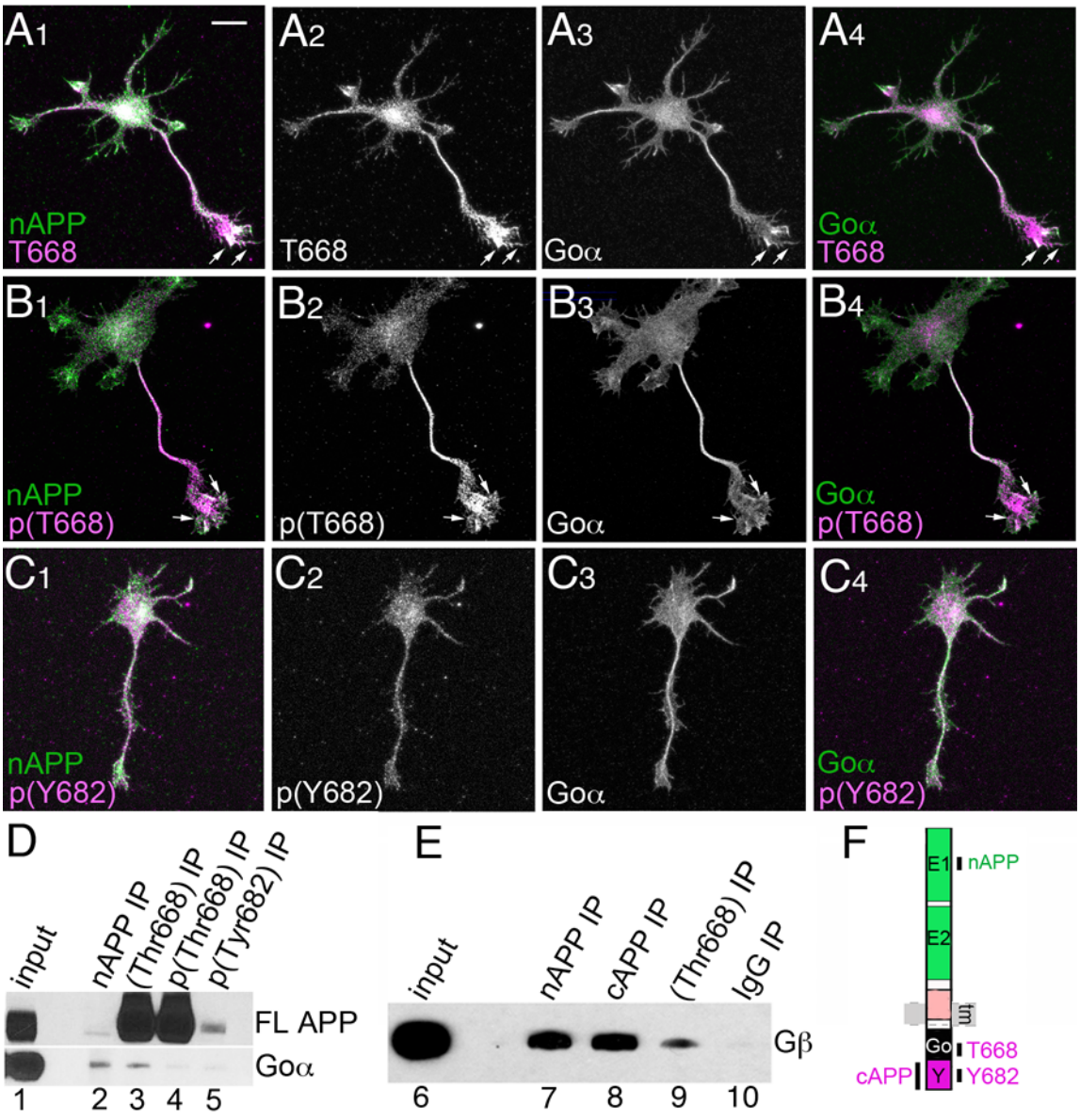
A1
nAPP
T668
A2
T668
A3
Goα
A4
Goα
T668
B1
nAPP
p(T668)
B2
p(T668)
B3
Goα
B4
Goα
p(T668)
C1
nAPP
p(Y682)
C2
p(Y682)
C3
Goα
C4
Goα
p(Y682)
D
input
nAPP IP
(Thr668) IP
p(Thr668) IP
p(Tyr682) IP
FL APP
Goα
1 2 3 4 5
E
input
nAPP IP
cAPP IP
(Thr668) IP
IgG IP
Gβ
6 7 8 9 10
F
E1
nAPP
E2
Go
T668
cAPP
Y
Y682

Figure 4.4

Figure 4.4. *Nonphosphorylated versus phosphorylated forms of APP exhibit distinct localization patterns within developing neurons*. **A-C)** 1 DIV rat primary hippocampal neurons immunostained for Goα (green) and different cAPP-specific epitopes (magenta). Each image is a maximum projection from flattened 10 confocal sections. Scale bar = 30 μm. **A)** (Thr_{668}) APP (magenta) is highly expressed in axons and throughout peripheral regions of the growth cone (arrows), where it colocalizes with nAPP and Goα (arrows). **B)** In contrast, p(Thr_{668}) APP is highly expressed in axons and in the central regions of growth cones, but has little overlap with nAPP. (Thr_{668}) APP is only weakly expressed in peripheral regions of the growth cone, and is not detected in the most distal regions of Goα expression (arrows). **C)** p(Tyr_{682}) APP is uniformly distributed throughout neurons, and does not appear to preferentially overlap with nAPP or Goα in particular subcellular regions. **D)** Mouse brain lysates were immunoprecipitated with APP antibodies specific to different epitopes, and blotted with Goα. Immunostaining with α-nAPP (22C11) on the upper blot shows relative levels of full-length APP immunoprecipitated with each antibody. **Lane 1:** Input lane shows that APP and Goα were abundant in lysates before immunoprecipitation. **Lane 2:** Goα was detected in lysates immunoprecipitated with nAPP antibodies (8967), verifying that it interacts with full-length APP. **Lane 3-4:** Although (Thr_{668}) APP and p(Thr_{668}) APP antibodies immunoprecipitated roughly equivalent levels of full-length APP, Goα coimmunoprecipitated strongly with (Thr_{668}) APP but was negligible in lysates immunoprecipitated with p(Thr_{668}) APP. **Lane 5:** Goα was not detected in lysates immunoprecipitated with p(Tyr_{682}) APP antibodies. The size of APPL is ~135 kDa. The size of Goα is ~41 kDa. **E)** Mouse brain lysates were immunoprecipitated with APP antibodies specific for different epitopes and then immunoblotted with anti-Gβ. **Lane 1:** The input shows abundant levels of Gβ in lysates prior to immunoprecipitation. **Lane 2:** Gβ coimmunoprecipitated with nAPP, demonstrating that it interacts with full-length APP. **Lane 3-4:** Gβ coimmunoprecipitated with both polyclonal antibodies against cAPP (which do not distinguish between different modified forms) and (Thr_{668}) APP-specific antibodies. **Lane 5:** Gβ was not detected in the control IgG immunoprecipitation. The size of Gβ is ~37 kDa. **F)** Schematic diagram of APP showing the E1 and E2 extracellular domains, the Aβ region within the transmembrane (TM) domain, the Go-binding domain "Go", and the internalization domain "Y". APP epitopes targeted by each APP antibody are marked with black lines. Antibodies, (Thr_{668}) APP, p(Thr_{668}) APP, and p(Tyr_{682}) APP target the intracellular domain of APP, whereas nAPP antibodies target the extracellular domain.

Based on the foregoing studies, we propose the model that full-length APP is transported to motile regions of neurons, where it can directly interact with the heterotrimeric G protein Go and function to regulate neuronal responses to inhibitory guidance cues. In its inactive form, full-length APP is poised to function as a GPCR, interacting with Goα in the peripheral regions of growth cones. Local activation of this pathway (by extracellular signaling molecules, see Chapter 3) would provide one mechanism for inducing retraction responses and prevent inappropriate growth; convergent input from other pathways that regulate APP dephosphorylation at Thr_{668} might provide a second, independent way of regulating this pathway. Subsequently, secretase cleavage, phosphorylation, or regulated mechanisms of internalization might function to remove APP from the membrane, thereby terminating this aspect of the response. All of these mechanisms are consistent with the patterns of immunohistochemical colocalization that we observed in these studies. Although these data are preliminary, they represent intriguing areas of future research that may reveal mechanisms by which APP-Goα signaling is regulated in developing neurons.

CHAPTER 5

Conclusions and future directions

The overall goal of this thesis was to investigate the normal functions of APP family proteins in the developing nervous system, and to identify the signaling mechanisms by which APP may control key aspects of neuronal migration and motility. Based on previous evidence from multiple systems that APP and its orthologs are strongly upregulated in neurons undergoing active phases of motility (including migration, outgrowth, synaptogenesis, and response to injury), I used a combination of invertebrate model systems and primary cultures of murine hippocampal neurons to test the hypothesis that APP family proteins function to restrict excessive or inappropriate growth responses. I also investigated the controversial model that APP family proteins function as unconventional G protein-coupled receptors that specifically interact with Goα, whereby stimulation of APP signaling induces the activation of Goα, which in turn regulates neuronal behavior via downstream effector pathways. The results of my studies in *Manduca*, *Drosophila*, murine neuronal cultures, and human brain samples have provided new evidence in support of this model, indicating that the regulation of Goα-dependent signaling responses may represent a fundamental role for APP family proteins in both the developing and mature nervous system.

Amyloid precursor proteins interact with the heterotrimeric G protein Go in the control of neuronal migration

In Chapter 2 of this thesis, I demonstrated that full-length APP and its conserved ortholog in *Manduca*, APPL, are expressed in growing regions of motile neurons, where they colocalize with Goα. Using an established assay for neuronal migration in the

hawkmoth *Manduca*, I demonstrated that APPL and Goα regulate similar aspects of neuronal migration and outgrowth. When APPL signaling was disrupted (by using APPL morpholinos or APPL blocking antibodies), cell migration and axon outgrowth occurred ectopically into normally inhibitory regions. This same phenotype resulted from inhibiting Goα activation, suggesting that APPL and Goα activity may normally regulate inappropriate migration and outgrowth in the nervous system. In line with evidence that APP can directly bind and activate Goα *in vitro* (Nishimoto et al., 1993), I used bimolecular complementation assays (BiFC) to demonstrate that APPL and Goα directly interact in growing axons and synapses in the *Drosophila* brain. Using *Manduca* embryonic lysates, I also showed that activating Goα causes it to dissociate from APPL, consistent with the model that APPL functions as a Goα-associated receptor in the nervous system. These studies support the model that APPL is an upstream receptor that regulates Goα-dependent aspects of neuronal migration in the developing nervous system: activation of this pathway causes axon retraction and restricts migration, whereas inhibiting the pathway causes excessive migration and outgrowth. This work was published in The Journal of Neuroscience (Ramaker et. al. 2013 33 (24) p. 10165-10181).

Based on previous work from the Copenhaver laboratory, which demonstrated that Goα activation leads to Ca^{+2}-dependent filopodial retraction, I hypothesize that signaling through this pathway alters the cytoskeletal dynamics that regulate the motile behavior of developing neurons. Whether stimulating APP in developing neurons leads to Goα activation as a mechanism for regulating these events still needs to be verified. Identification of upstream molecules capable of stimulating APP-dependent pathways will also be essential for defining the mechanisms by which APP signaling is normally regulated in the nervous system (the focus of my on-going investigations).

Ligand-induced stimulation of APP regulates Go-dependent aspects of neuronal development

In Chapter 3, I used a combination of *in vitro* assays in cultured rodent neurons and *in vivo* assays in the hawkmoth *Manduca* to test the role of APP signaling in developing neurons. Using established protocols for activating APP in cell culture, I treated stage 3 primary hippocampal neurons with antibodies targeting the extracellular domain of APP. This treatment resulted in growth cone collapse and retraction that required Go activation. These results are consistent with experiments in *Manduca* demonstrating that inhibiting either APPL or Goα caused ectopic migration and outgrowth, consistent with a role for these molecules in negatively regulating neuronal migration and outgrowth in the nervous system. To stimulate APPL signaling *in vivo,* I treated developing embryos with a candidate APPL ligand, Mscontactin. Treating EP cells with Mscontactin-Fc at the onset of migration resulted in premature stalling by the EP cells and abnormal neuronal positioning within the developing ENS. Whether APPL-Goα signaling transduction normally functions downstream of Mscontactin in this pathway still needs to be proven. A manuscript describing this work is in progress.

Given my preliminary data demonstrating that Mscontactin and APPL regulate similar aspects of neuronal migration in *Manduca* embryos, future efforts will be focused on determining whether Mscontactin functions as an endogenous APPL ligand during neuronal development. In particular, a number of controls still have to be conducted to determine whether APPL and Mscontactin interact *in vitro* and *in vivo*; whether they are expressed at the right time and place to function as receptor-ligand pairs; and whether APPL and Go are required for Mscontactin to mediate its effects on migration. These future directions will be discussed below.

APP family proteins undergo developmentally-regulated modifications that may affect their functions in the nervous system

In Chapter 4, I used immunohistochemical staining methods in whole-mount *Manduca* embryos to demonstrate that full-length APPL undergoes a pattern of developmental expression and trafficking in migratory neurons that is consistent with its role in regulating Goα-dependent aspects of neuronal motility. In contrast to the widespread distribution of both N- and C-terminal APPL cleavage fragments detected throughout the EP cells and their processes, full-length APPL was mostly expressed in their leading processes and motile growth cones. Over the course of development, the intracellular localization of full-length APPL changed: In both premigratory and postmigratory cells, full-length APPL was predominantly confined to large perinuclear compartments. However, during periods of axon outgrowth, these intracellular accumulations became less evident and instead full-length APPL became increasingly localized to growth cones, indicating a developmental change in its intracellular trafficking. In complementary studies, I also examined the expression pattern of mammalian APP in cultured rat hippocampal neurons, which revealed similar patterns of expression and trafficking during axon outgrowth. By combining biochemical and immunohistochemical approaches to investigate how the phosphorylation of specific residues in APP might affect APP-Goα interactions, I have also discovered that the phosphorylation of APP on Thr_{668} negatively correlates with APP-Goα interactions, suggesting that this post-translational modification might play an important role in regulating APP-Goα signaling. Together, these data provide new insight into the mechanisms by which APP-Goα signaling may be regulated to control the behavior of

developing neurons. These studies also have identified a number of additional questions that still need to be addressed to fully validate this model, as summarized below.

FUTURE DIRECTIONS

Determine whether contactins can regulate APPL-dependent aspects of neuronal migration

Chapter 3 demonstrated that treating *Manduca* embryos with Mscontactin-Fc led to errors in EP cell migration. To determine whether APPL is downstream of Mscontactin in mediating these effects, I will treat embryos with Mscontactin-Fc in combination with APPL morpholinos to knock down its expression. As a control, Mscontactin-Fc treatment will be combined with the application of standard control morpholinos. I would expect that the migration defect caused by Mscontactin-Fc treatment would persist in the presence of standard control MOs, but not in the presence of APPL morpholinos. Because attractive cues on the muscle band pathways can guide EP cells independent of APPL signaling, combining Mscontactin-Fc with APPL morpholinos would be expected to overcome the stalling response induced by Mscontactin-Fc and restore normal migration along the pathways; however, migration and outgrowth onto the interbands might still occur in the absence of APPL. In this case, combining Mscontactin-Fc treatment with subthreshold concentrations of APPL morpholinos might restore normal migration and prevent ectopic growth. In contrast, if Mscontactin functions independent of APPL to regulate EP cell migration, neither control nor APPL-specific morpholinos would be expected to rescue the Mscontactin-Fc phenotype, and APPL-specific morpholinos would likely cause additional ectopic outgrowth in addition to the stalling response induced by Mscontactin-Fc.

As a complementary approach to using APPL MOs, I could also block APPL signaling with APPL blocking antibodies. Since my previous studies indicated that these antibodies disrupt normal APP-dependent interactions, it is possible that treatment with anti-APPL may act by blocking endogenous interactions between APPL and Mscontactin

in the developing ENS. In this case, I would expect that combining Mscontactin-Fc treatments with application of nAPPL antibodies would also prevent the Mscontactin-Fc-induced phenotype. IgG controls or antibodies targeting non-neuronal proteins would serve as a negative control.

If the experiments described above reveal that Mscontactin is a functional ligand for APPL in migrating neurons, I will also investigate whether Goα activation is a downstream consequence of APPL stimulation by Mscontactin. For these experiments, I will treat *Manduca* embryos with Mscontactin-Fc constructs in the presence of PTX or Goα morpholinos. If Goα activity is required for the effects of Mscontactin-APPL signaling on neuronal migration, blocking Goα activity should prevent the neuronal stalling and mispositioning phenotypes. If these molecules function in distinct pathways, however, I expect the Mscontactin-induced defects in neuronal migration to persist, while inhibiting Goα activity might also enhance ectopic outgrowth on the bands and in the interband regions (consistent with my previous studies). Given our hypothesis that multiple signaling pathways most likely converge on Goα to regulate neuronal motility, subthreshold levels of Go inhibition may be more informative than a complete blockage, since global Goα inhibition might also perturb other cell functions and mask the effect of manipulating Mscontactin signaling. If these studies indicate that Mscontactin-APPL-Goα signaling does indeed regulate key aspects of EP cell motility, future studies could also investigate whether Ca^{+2} influx is required for this effect, consistent with earlier work by Horgan and Copenhaver (Horgan and Copenhaver, 1998).

The search for other candidate ligands

If APPL is found to *not* be required for Mscontactin-induced defects in EP cell migration, I will investigate whether other candidate ligands regulate APPL-dependent

aspects of neuronal behavior. In the original studies that identified members of the contactin family as ligand/binding partners for APP and its orthologs (Osterfield et al., 2008), the investigators initially identified contactin-4 by incubating surface-biotinylated chick optic tectas with sAPP-AP and then immunoprecipitating for the AP probe. After western blotting for biotin, contactin-4 was identified using tandem mass spectrometry to identify the most prominent interacting proteins. However, as an alternative approach, the same group also cross-linked sAPP-AP to biotinylated tectas, immunoprecipitated for the AP probe, and then western blotted for candidate proteins. Included in this screen were: CHL1, contactin 1, NCAM, neogenein, neurofescin, NgCAM, NrCAM, prominin-like 2, and tenascin, of which only NgCAM coimmunoprecipitated sAPP-AP. NgCAM is the chick ortholog of mammalian L1CAM and *Drosophila* neuroglian. These transmembrane cell adhesion molecules are highly expressed on certain subsets of axons and glial cells (Faissner et al., 1984, Kallunki et al., 1997). Interestingly, in *Drosophila* and *Manduca*, neuroglian is also expressed by a number of non-neuronal cells (Chen et al., 1997, Nardi et al., 2006), including glial cells (Bieber et al., 1989, Knittel et al., 2001), skeletal muscle cells (flybase**:** FBgn0002968), and, most notably, the muscle band pathways of the ENS at later stages of embryogesis (Wright et. al., 1999). Moreover, loss of neuroglian in *Drosophila* can lead to errors in axon pathfinding, consistent with its role as a candidate APPL ligand (Garcia-Alonso et al., 2000).

Determine the role of Mscontactin-APPL signaling in development

If Mscontactin is shown to regulate neuronal migration through APPL-dependent mechanisms, I will further investigate the nature of this interaction. First, I will determine whether APPL and Mscontactin interact in *Manduca* embryonic lysates using coimmunoprecipitation protocols. Two antibodies have been generated against *Drosophila* contactin: rat anti-Dcontactin (targets AA 772-1138, the 5th and 6th IgG

domains plus the hinge to the FN domains), and guinea pig anti-Dcontactin (targets AA 24-195, an N-terminal C-lectin domain adjacent to the IgG domains) (Faivre-Sarrailh et al., 2004). I will test both of these antibodies in *Manduca* using western blotting and immunohistochemistry. As needed, I will also generate additional antibodies against peptide sequences specific to MsContactin, using our published protocols (Coate et al., 2007).

To validate the model that Mscontactin can regulate key aspects of neuronal motility in *Manduca* embryos, I will investigate whether it is expressed at the right time and place to do so. I will collect embryos throughout the migratory sequence (45-65% of development) and immunostain for anti-Dcontactin (or anti-Mscontactin), while counterstaining for anti-APPL. I will also examine the pattern of Mscontactin-specific mRNA expression by in situ hybridization. Based on our model that Mscontactin-APPL signaling regulates EP cell behavior, I expect to detect Mscontactin in the interband regions of the midgut, possibly confined to the anterior regions where the EP cells and their ensheathing glia reside. This expression pattern would be consistent with our observations that APPL knockdown led to ectopic growth that was predominately restricted to the anterior, but not posterior, interband regions. Alternatively, Mscontactin might be selectively expressed by the enteric glial cells that ensheath the EP cells around the time that they normally complete their migration, which again would be consistent with my observation that most ectopic growth occurs in the vicinity of the EP cell bodies, rather than their more distal processes. However, Mscontactin expression could be more widespread than just these regions. For example, Mscontactin might also be expressed by the EP cells and function as a co-receptor by binding APPL in *cis*. Determining the expression pattern of endogenous Mscontactin will therefore provide insight into the nature of its interaction with APPL.

In the event that neither of the anti-Dcontactin antibodies specifically labels Mscontactin in *Manduca* and we are unable to generate our own antibody against Mscontactin, a less ideal approach would be to continue to focus on the interaction between APPL and exogenous Mscontactin-Fc. In this case, I would treat embryos with Mscontactin-Fc and perform coimmunoprecipitations between APPL and the fusion protein. I could also utilize antibodies against the Fc tag to determine where Mscontactin-Fc binds in the embryo. In preliminary experiments, I detected the constructs bound to EP axons and they strongly labeled a set of interband midline cells, as well as more diffuse and variable labeling in other interband regions. Very few embryos were examined in this initial study, however. With improved resolution, I would expect to detect Mscontactin-Fc binding to the EP cell bodies, given that transmembrane APPL is present on both the EP cell bodies and axons (Ramaker et al., 2013). These experiments will provide additional insight into whether and how Mscontactin may function as a candidate APPL ligand in *Manduca.*

Determine the mechanisms of APP-Goα signaling *in vitro*

Although ascertaining the role of APP-Goα signaling in neuronal motility *in vivo* would be ideal, the experiments in *Manduca* are contingent on identifying an APPL ligand or developing an antibody activation protocol capable of producing robust APPL-dependent phenotypes, both of which are still in progress. On the other hand, since we have established a method for inducing APP signaling in cultured hippocampal neurons, these assays provide many advantages for testing the role of this signaling pathway in neurons. Notably, an array of tools are available in mammalian neurons, such as a wider availability of APP antibodies and the availability of antibodies against activated Goα, which provide advantages over studying this pathway in *Manduca*. Although there are

also important caveats to using cultured neurons (including the loss of endogenous signaling interactions that normally occur in the brain), hippocampal neurons *in vitro* have the advantages that they are available in high quantities, and can be isolated from the complex assortment of other cell types and environmental cues that they normally encounter *in vivo*, enabling changes in individual neurons to be more easily quantified. Therefore, even if we discover that contactins function in a pathway independent of APP-Goα signaling, our established assays for antibody-induced APP signaling in cultured neurons will provide an informative means for investigating the role of this pathway in different aspects of neuronal motility.

In Chapter 2, I provided evidence that APPL functions as a Goα-associated receptor. Namely, we showed that APPL and Goα directly bind both *in vitro* and *in vivo*, and that activating Goα reduced its interaction with APPL. Additionally, in Chapter 3, I discovered that Go activation is required for APP-dependent growth cone responses. Although these data support the role of APP as a Goα-associated receptor, they do not explicitly show that APP activation leads to Goα activation. To further verify this point, I will treat cultured neurons with anti-APP antibodies (or Fc constructs of contactin 4; Osterfield et al., 2008) and determine whether either method of stimulating APP signaling causes enhanced Goα-GTP levels. For these experiments, neurons will be treated in culture for 1-5 hr, then fixed and immunostained with anti-Goα-GTP antibodies (See Figure 5.1A-B), which are specific to the activated form of Goα. By normalizing immunofluorescence levels of Goα-GTP to signals produced by anti-Goα (visualized in a separate channel) we can determine whether APP signaling increases Goα activation. These experiments will be especially interesting, given previous evidence in *Manduca* that Goα activation causes local filopodial retraction, inhibiting axon outgrowth in a Ca^{+2}-dependent manner (Horgan and Copenhaver, 1998). We therefore expect that Goα-GTP

might be particularly enhanced within the motile growth cones and axons, and that stimulation of APP signaling would further enhance its expression in these regions.

To further demonstrate that APP signaling causes Goα activation, future studies will investigate their biochemical interactions. In Chapter 2, we demonstrated that APPL-Goα interactions in *Manduca* lysates could be enhanced with PTX and reduced upon Goα/iα activation with Mas 7. I therefore hypothesize that treating cultured neurons with APP antibodies (or contactin 4-Fc constructs) should also induce Goα activation and release from APP. To test this model, I will apply our anti-APP antibodies (versus control IgG) to cultured neurons, then prepare lysates of the cultures, and use our coimmunoprecipitation protocols to quantify the interaction between APP and Goα. In preliminary experiments, I showed that in the absence of any treatment, endogenous APP could be coimmunoprecipitated with Goα from cultured rodent neurons (see Figure 5.1C). I expect that treating cultures with APP-specific antibodies or with contactin 4-Fc will decrease APP-Goα interactions, whereas pretreating with PTX should prevent these effects. Similar to previous experiments, PTX by itself might enhance this interaction, suggesting a low basal level of APP-Goα signaling. Additionally, by immunoblotting with anti-Goα-GTP, I may be able to determine if treating neurons with APP antibodies causes Goα activation, while mastoparan and PTX treatments will serve as positive and negative controls, respectively. Together, these experiments will provide support for the model that APP signaling results in Goα activation and release, consistent with its role as a Goα-coupled receptor that undergoes ligand-induced activation to mediate its effect in neurons.

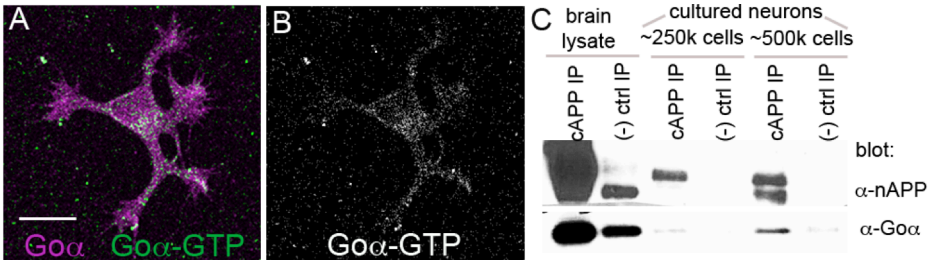

Figure 5.1. A-B) Goα and Goα-GTP are both detected in immunostained hippocampal neurons grown in primary culture. **C)** Mouse brain lysates were immunoprecipitated with cAPP antibodies. Immunoblotting for Goα revealed that endogenous Goα interacts with cAPP, whereas only background levels of Goα were detected in immunoprecipitates pulled down with control IgYproteins. Blotting for nAPP revealed that robust levels of APP were also immunoprecipitated in this sample. By comparison, when lysates from cultured hippocampal neurons were immunoprecipitated with anti-cAPP, Goα was detected only in the samples that had sufficient APP present. In samples with low levels of APP and in samples immunoprecipitated with IgY, only background levels of Goα were detected. This assay can now be used to examine whether stimulating APP reduces APP-Goα interactions.

Determining additional roles for APP-Goα signaling in developing neurons

In Chapter 3, I discovered that APP-Go signaling regulates growth cone responses. However, this assay only analyzed growth cone morphologies after five hours of treatment, whereas more acute changes in their behavior might have occurred prior to this time. Therefore, in future studies, I will use time-lapse imaging to observe the immediate response of growth cones to treatments designed to stimulate APP and Go. This approach will also allow me to track individual neurons over time, providing a more accurate means of assessing the role of this signaling pathway in growth cone dynamics. Analyzing these changes in real-time will also provide insight into how changes in growth cone morphology influence the overall behavior of the neuron. For example, by assessing the number of filopodia and their rates of extension and retraction, I can determine how changes in growth cone dynamics contribute to such behaviors as growth cone turning, axon growth, and pathfinding in neurons.

In addition to delineating the role of APP-Go signaling in growth cone dynamics, I will also be able to determine whether this signaling pathway regulates axon outgrowth. In Chapter 3, to analyze the effect of APP antibody treatment on growth cone morphology, we randomly imaged and quantified 55 axonal growth cones from each group, treated at 1 DIV. However, at this time, many of the cultured hippocampal neurons were still transitioning from a multipolar state (stage 2) to a more differentiated state (stage 3), when they acquire a single well-defined axon (Dotti et al., 1988, Kaech and Banker, 2006). As a result, there was a substantial amount of variability in the initial morphologies of neurons used in these studies. Additionally, our criteria for analysis included only stage 3 neurons (possessing single axons that were substantially longer than any of the other neurites) and neurons that were not in contact with other neurons (to avoid potential complications arising from neuron-neuron interactions). These criteria complicated an attempt to measure the effect of treatment on axon length *per se*. By

implementing time-lapse imaging protocols, we will be able to acutely treat neurons with APP antibodies and Go-specific reagents to determine the role of this signaling pathway on axonal outgrowth in individual neurons at specific stages of their development.

In addition to investigating the role of APP-Go signaling during axon outgrowth, we are also interested in determining the role of this pathway at other periods of development. For example, although I have uncovered a role for APP-Go signaling in regulating growth cone collapse/retraction during early stages of development, it may be only play a functional role after axon polarity has been established. By investigating the role of APP-Go signaling at different developmental stages, we may uncover distinct roles for APP-Go in the control of neuronal migration, axonal outgrowth, growth cone responses, and synapse formation. Likewise, this approach might reveal important context-specific differences in the growth responses that are induced by APP signaling under different conditions, which could explain why APP has been found to promote motility in some assays but inhibit growth in others (Young-Pearse et al., 2008, Hoe et al., 2009a, Rama et al., 2012, Billnitzer et al., 2013).

Verify that APP mediates growth cone responses specifically via Go, but not other G proteins

Based on my data demonstrating that PTX inhibits APP-dependent growth cone collapse and retraction, and that APPL directly binds Goα but not Giα, we concluded that growth cone dynamics are regulated by APP-Go signaling. However, unlike insect systems, PTX inhibits both Goα and Giα in mammalian neurons, and therefore we have not yet proven that the growth cone responses are specific to Goα in this assay. To verify that Goα activation is required for growth cone collapse/retraction, we could overexpress a non-activatable mutant of Goα, GoαG204A. If Go activation mediates the

growth cone responses induced by APP signaling, then GoαG204A will function like a dominant negative and reduce the collapse/retraction response (Yamatsuji et al., 1996b). This assay would be informative regardless of whether the α or βγ subunits of Go mediate the effect, because this dominant negative mutant would both reduce levels of activated Goα and chelate endogenous Gβγ. In contrast, dominant-negative Giα (GiαG204A) should have no effect unless APP-dependent growth responses are mediated by Gi signaling. Similarly, since PTX rescued APP-induced growth cone collapse and retraction, overexpressing PTX-insensitive forms of Goα or Giα would reveal which of these G proteins was involved (Leaney and Tinker, 2000).

Finally, although studies in *Manduca* revealed a role for the α-subunit of Go in regulating neuronal motility, I cannot yet exclude the possibility that APP-induced growth cone collapse and retraction responses in cultured hippocampal neurons are mediated by the βγ dimer, as both the α and βγ subunits have been ascribed roles in APP-Go signaling in other assays. For example, in studies using NK1 cells transfected with FAD-associated forms of APP, APP-Go dependent apoptosis was mediated by βγ subunits (Giambarella et al., 1997), whereas suppression of CRE was evoked by α subunits (Ikezu et al., 1996).

To determine which Go subunits are involved in APP-induced growth cone responses in cultured hippocampal neurons, I could overexpress GTPase-deficient forms of Goα (constitutively active Goα-Q205L or $Go\alpha_2$-A205L). If growth cone collapse is mediated by Goα, I would expect that overexpression of constitutively active Goα would induce growth cone collapse, similar to the effect of treating neurons with mastoparan. However, if the effect is mediated by βγ subunits, then expressing the constitutively active Goα subunits might have no effect on our outgrowth assays. As a complementary test, I could overexpress the c-terminus of the β-adrenergic receptor

kinase-1, which has been shown to bind βγ and block its activity (Giambarella et al., 1997). Therefore, I would predict that this construct would only prevent growth cone collapse/retraction if APP-dependent responses are mediated by βγ.

How is APP-Goα signaling regulated?

We have provided evidence that APP regulates neuronal motility by functioning as a Goα-associated receptor. However, the mechanism by which APP activates Go and permits its release from membrane-associated receptor complexes has not been investigated. Conventional GPCRs typically activate their associated G proteins by undergoing a ligand-induced conformational shift in their transmembrane-spanning domains. This modification displaces GDP, allows the association of GTP, and drives the release of the activated subunits from the receptor (Hille, 2001). Although previous studies have identified other examples of single-pass membrane GPCRs (Maghazachi, 2005), the mechanism by which they can activate G proteins has not been determined. Therefore, I am interested in further elucidating 1) which ligand-induced changes in APP might be responsible for activating Go, and 2) how APP-Go signaling is subsequently regulated.

Both APP and APPL are subject to numerous forms of post-translational modifications, such as glycosylation, secretase cleavage (Swanson et al., 2005), and phosphorylation at a number of residues (Oishi et al., 1997). In Chapter 4, I showed intriguing expression patterns of phosphorylated versus nonphosphorylated forms of full-length APP within motile regions of developing neurons. In particular, I observed trends in which (Thr_{668}) APP was highly expressed in the peripheral regions of growth cones where Goα expression was also high, whereas p(Thr_{668}) APP was less abundant in the peripheral regions and strongly expressed in central regions of growth cones. Given

preliminary data that Goα coimmunoprecipitated with (Thr$_{668}$) APP, but not p(Thr$_{668}$) APP in mouse brain lysates, it will be interesting to determine whether phosphorylation of APP at Thr$_{668}$ plays a role in APP-Goα signaling.

To address this issue, I could induce APP or Goα activation in cultured neurons and use western blotting and immunofluorescence assays to measure changes in (Thr$_{668}$) APP phosphorylation. Specifically, by using a panel of APP antibodies against different phospho- and nonphospho-specific epitopes (including Thr$_{668}$ and Tyr$_{682}$), I may find that APP activation is associated with increases in (p)Thr$_{668}$ levels, along with enhanced Goα activation and release. As a complementary approach, quantifying levels of (Thr$_{668}$) versus p(Thr$_{668}$) APP in the central and peripheral domains of growth cones may providing insight into whether this modification regulates APP localization in developing neurons as a mechanism to facilitate its interaction with Go. A potential caveat to this analysis is that phosphorylation of APP might also alter its secretase cleavage or degradation; in this case, simply comparing levels of phosphorylated versus nonphosphorylated APP before and after treatment would not provide straightforward answers about the involvement of APP phosphorylation in regulating Goα signaling.

Another caveat to the above experiments is that solely analyzing the colocalization between Goα and APP epitopes in cultured neurons will not be informative in establishing the relationship between APP modifications and APP-Goα activation. For example, in the case of conventional GPCRs, studies have suggested that receptors only interact with G proteins in their inactive heterotrimeric state, whereas modifications that activate the receptor would lead to G protein dissociation. By this scenario, modifications that enhance APP-Goα colocalization would represent inactive interactions. Alternatively, from a physiological standpoint, any modification that brings the two molecules together may facilitate their interaction and subsequent activation. For this

reason, using coimmunoprecipitations between APP-Goα interactions might be more informative than APP-Goα colocalization. Thus far, our data argue that Goα bound to APP represents an inactive protein complex, since PTX treatment both enhanced APP-Goα interactions and prevented APP-Go-induced induced growth cone collapse (albeit in separate assays). Thus, although the proposed experiments would provide insight into whether APP modifications are associated with APP activation or APP-induced growth cone collapse, their results must be interpreted with caution.

As a more functional approach for relating APP phosphorylation with APP signaling, we could treat cultured neurons with reagents targeting kinases or phosphatases known to regulate APP phosphorylation. This approach would reveal whether altering their activity (1) induces growth cone collapse in an APP-dependent manner; (2) decreases APP-Goα interactions; and (3) enhances Goα-GTP levels. For example, if Thr_{668} dephosphorylation is necessary for APP to interact with Go at the cell surface, then introducing the serine/threonine phosphatase PP2A might promote APP-Go signaling, thereby enhancing growth cone collapse and Goα-GTP levels. Likewise, Thr_{668} APP phosphorylation might prevent APP from colocalizing with Goα at the cell surface. In this model, overexpressing c-Jun kinase (JNK; known to interact with Thr_{668}; Standen et al., 2001), might prevent antibody-induced APP activation, thereby reducing growth cone collapse and Goα-GTP levels. However, since most kinases and phosphatases target multiple phosphorylation sites, subsequent analysis would be needed to demonstrate that the effect is specific to APP and specific to the Thr_{668} residue. Future experiments could be performed in the presence of APP containing mutations at this residue to provide insight into whether altered phosphorylation at this site plays a critical role in regulating APP-Go interactions an neuronal motility.

What is the role of secretase cleavage in APP-Goα signaling?

Similar to mammalian APP, APPL undergoes secretase cleavage that both decreases levels of full-length protein and produces APP fragments. Based on our model that APP functions as a Goα-associated receptor when it is present as a transmembrane protein, I would expect that secretase cleavage would reduce APP-Goα signaling. However, the opposite may be true: APP may associate with Goα as a full-length receptor, while secretase cleavage would facilitate the activation and release of the Goα subunit. We could test this model by using secretase inhibitors or secretase-deficient forms of APP in a variety of assays.

To determine if APP-Go signaling in primary neurons is disrupted by cleavage of the protein, we could apply secretase inhibitors to primary cultured neurons and analyze their effects on APP-induced growth cone collapse/retraction, Goα-GTP levels, and Goα-APP dissociations. Inhibiting cleavage should result in higher levels of full-length protein at the membrane. According to our preferred model, elevated levels of transmembrane APP should facilitate APP-Go signaling, thereby augmenting APP-dependent growth cone collapse, Goα-GTP levels, and Goα-APP dissociation. On the other hand, if secretase cleavage is necessary for Goα activation, inhibiting secretase cleavage should attenuate APP-induced growth cone collapse, Goα-GTP activation, and APP-Goα dissociation. In our *Manduca* embryo cultures, if full-length APPL is necessary to prevent ectopic outgrowth, secretase inhibitors would be expected to stall migration and outgrowth by enhancing APPL signaling. On the other hand, if secretase cleavage is necessary for APP signaling, secretase inhibitors would be expected to prevent APPL signaling, resulting in ectopic migration and outgrowth, thereby phenocopying the results of disrupting APPL with morpholinos or blocking antibodies. These experiments would therefore provide insight into the role of secretase cleavage in APP(L)-Go signaling.

One caveat to these experiments is that APP activation may itself regulate cleavage as a feedback mechanism to terminate APP-Go signaling after retraction has occurred. To determine whether APP-Go signaling induces secretase cleavage, we could use APP antibodies to activate APP-Go signaling and perform western blots to analyze changes in full-length APP versus cleavage fragments. However, if APP-Go signaling alters other aspects of APP bioavailability, such as its degradation or its localization at the membrane, simply analyzing levels of fragments versus holoproteins might not be informative. An alternative approach would be to express epitope-tagged forms of APP, whose cleavage, trafficking, and degradation could be analyzed after the induction of APP signaling. Although most of these future directions are beyond the scope of the current project, they would provide useful strategies for further delineating the role of APP-Go signaling in neuronal development.

Reconciling the opposing roles for APP in neurite outgrowth

In some studies, APP has been shown to promote neurite outgrowth, while, many others have demonstrated that APP inhibits neurite outgrowth. These discrepancies may simply reflect the caveats of comparing different experimental approaches, but they might also reflect important biological differences, indicating that neurons respond to APP signaling in a context-specific manner. To determine the role of APPL in neuronal migration and outgrowth in the developing ENS, I treated *Manduca* embryos with either APPL morpholinos (to knockdown APPL expression) or with APPL antibodies (to block APPL signaling). Both of these manipulations resulted in ectopic migration and outgrowth, suggesting that APPL signaling normally inhibits axonal outgrowth (Chapter 2). Consistent with this effect, applying sAPPL-AP constructs to embryos caused similar patterns of ectopic outgrowth (P. Copenhaver, unpublished data). These results indicate that sAPPL-AP functions by interfering with endogenous

APPL-dependent interactions, disrupting normal APPL responses that prevent inappropriate outgrowth. Also in support of the model that APP signaling functions to restrict neurite motility, we have discovered that inducing APP signaling in cultured neurons triggers growth cone collapse (Chapter 3), although a role for APP in regulating neurite outgrowth *per se* in this assay still needs to be determined (as noted above).

Consistent with the model that APP signaling restricts neurite outgrowth in a variety of contexts, a number of *in vitro* studies have demonstrated that knocking out APP enhances different aspects of neuronal motility. For example, when hippocampal neurons from APP KO mice were grown in culture, their axons were longer than those from wild type animals after 1 day (Billnitzer et al., 2013), while other investigators have shown that neurons from APP KO mice grow longer neurites than wild type neurons after 3 days in culture (Young-Pearse et al., 2008). Additionally, knocking down APP with shRNA caused a similar effect in cultured neurons, whereby the length of the longest neurite after 3 DIV was enhanced in neurons without APP compared to controls, an effect that was cell-autonomous (Young-Pearse et al., 2008).

However, as noted above, a complicating factor in these assays is that APP undergoes rapid secretase cleavage, producing a number of cleavage products that can also regulate distinct aspects of neurite outgrowth. Numerous studies have demonstrated that treating neuronal cultures with sAPPα, the APP ectodomain fragment produced by α secretase cleavage, enhances neurite length (Araki et al., 1991, Milward et al., 1992, Ohsawa et al., 1995, Wallace et al., 1997). In contrast, a more recent study demonstrated that this effect only occurred in the presence of endogenous APP, which by our model would suggest that sAPPα might have a dominant negative effect, interfering with the normal inhibition of outgrowth by endogenous APP. However, additional research will be needed to elucidate the complex balance between the effects

of full-length APP and its cleavage products in regulating neuronal behaviors in an endogenous setting.

In contrast to our model that APP signaling restricts neuronal motility, other studies have shown that APP can also promote neurite outgrowth and axon elongation under some conditions. In primary hippocampal neurons from E18-19 mice, infecting 1 DIV neurons with APP shRNA decreased neurite length, whereas overexpressing APP significantly increased subsequent neurite growth (Hoe et al., 2009b). Likewise, cortical neurons from 4-wk old mouse brains showed a similar trend, in that dendritic length was reduced in APP KO mice and enhanced in neurons from APP transgenic mice (Hoe et al., 2009b). Additionally, when spinal cord explants from E13 mice were cultured in the presence of the growth-promoting factor netrin, commissural axon length was significantly reduced in APP KO explants, compared to spinal cords from wild type mice (Rama et al., 2012). These studies suggest that APP-dependent interactions can also promote neurite outgrowth. However, it has yet to be demonstrated whether APP overexpression or deletion recapitulates physiologically relevant signaling responses in developing neurons.

Although the opposing roles for APP in promoting versus preventing neurite outgrowth in different assays appear contradictory, an alternative possibility is that APP regulates outgrowth by controlling the balance of cell adhesion versus repulsion (in response to a variety of guidance cues), which is likely to be more sensitive to experimental manipulations under different experimental conditions. This hypothesis is supported by a study demonstrating that substrate adhesion was enhanced in neurons cultured for 1 hour on APP-expressing monolayers (restricting growth), whereas after 24 hours, neurite outgrowth was enhanced (Qiu et al., 1995). A similar phenomenon was detected in other studies that examined the effects of APP on neurite length over time (Perez et al., 1997). Notably, although neurite lengths from APP KO neurons were

initially shorter than those from wild type neurons at 1 DIV, neurite length in APP KO neurons subsequently grew longer than controls (by 3 DIV). These results argue that neurons respond differently to APP at different developmental stages (at least *in vitro*), such that APP may initially promote adhesive responses that permit growth, whereas at later stages of development APP may inhibit outgrowth. However, these models have yet to be validated *in vivo*, and are complicated by the fact that deleting and overexpressing APP may not reflect physiological responses associated with the dynamic inhibition and activation of APP signaling that presumably occurs within the developing nervous system.

As an alternative approach for determining the role of APP signaling on neurite outgrowth, we can now use our established protocols for inducing APP signaling with antibody crosslinking or with contactin-Fc constructs. These protocols can be used to assess the role of signaling responses regulated by endogenous APP, potentially identifying more physiologically relevant properties of this pathway than genetic deletion studies. Additionally, by utilizing neurons at different stages of neuronal development, the role of APP in promoting or restricting neurite outgrowth can be determined for distinct phases of cell adhesion, axon establishment, neurite outgrowth, and axon elongation. As a complementary strategy, systematically testing the role of APP signaling in multiple neuronal subtypes may provide insight into whether APP mediates different outgrowth responses in different regions of the brain. Finally, although examining the response to APP in cultured neurons can be informative, establishing an APP activation protocol *in vivo* would be ideal to elucidate the role of APP in neuronal development in conjunction with other endogenous cues. For these reason, we are interested in identifying a potential APPL ligand in *Manduca* (Chapter 3) and investigating the role of this signaling pathway in the developing nervous system.

A role for APP-Go signaling in disease

Inherited forms of Alzheimer's disease are caused by mutations within either APP or presenilin genes, which result in enhanced Aβ levels and increased ratios of Aβ42:40 in the brain. Aβ plaques are also a hallmark feature of AD pathology in sporadic cases of AD, although the mechanisms by which APP misregulation leads to Aβ accumulations in this form of the disease are not understood. However, the correlation between AD and Aβ in both inherited and sporadic cases of AD has led to the amyloid hypothesis, which postulates a role for toxic Aβ as a primary cause of AD (Hardy and Selkoe, 2002, Tanzi and Bertram, 2005). Indeed, applying Aβ oligomers to primary cultured neurons results in toxic responses (Izuo et al., 2012), and animals with mutations that enhance Aβ levels display disruptions in synaptic transmission (Johnson-Wood et al., 1997, Hsia et al., 1999, Larson et al., 1999) that are associated with impairments in learning and memory (Hsiao et al., 1996, Saura et al., 2005). However, therapies targeting Aβ have not resulted in clinical improvements (Golde et al., 2010), and in both human (Price et al., 2009) and mouse models of Alzheimer's disease (Games et al., 1995), Aβ plaque density does not correlate well with cognitive decline (Hardy and Selkoe, 2002). On the other hand, synaptic loss may more closely reflect disease severity (Terry et al., 1991). Given that APP has been postulated to regulate multiple aspects of synaptic maintenance, including neuronal outgrowth, synaptic formation, and long-term potentiation (Cullen et al., 1997, Galvan et al., 2006), these observations suggest that in addition to producing Aβ fragments, aberrant cleavage of APP may contribute to the progression of AD by disrupting the normal function of APP in neurons.

Consistent with this hypothesis, numerous studies have demonstrated that hyperactivation of Go by APP can induce cell death (Yamatsuji et al., 1996a, Yamatsuji

et al., 1996b, Galvan et al., 2006, Shaked et al., 2009, Sola Vigo et al., 2009). When soluble (monomeric and oligomeric) Aβ was applied to rat neuroblastoma cells in culture, it caused enhanced cell death, possibly by promoting APP dimerization and inducing Go activation (since both full-length APP and Go stimulation were necessary for the effect) (Shaked et al., 2009). Ca^{+2} influx was shown to be downstream of APP and Go in this pathway (Shaked et al., 2009). Since disruptions in Ca^{2+} homeostasis have been linked to AD (Khachaturian, 1994, Copenhaver et al., 2011), these studies suggest that misregulated APP-Goα signaling might result in pathological responses by inducing Ca^{2+} overload. In support of this model, an analysis of post-mortem AD brains revealed that elevated G protein activity and decreased APP-Goα interactions (suggesting enhanced APP activation and Goα release) correlated with disease progression (Reis et al., 2007, Shaked et al., 2009). These studies suggest that aberrant APP-Go signaling may contribute to the progression of neuropathological responses associated with AD, but understanding how this signaling pathway functions in a pathological context will require a better understanding of how it normally functions in neurons.

In summary, our data have revealed a role for APP signaling in regulating Go-dependent growth cone responses (Chapter 3), and for APPL and Goα in mediating similar aspects of neuronal migration and axon outgrowth (Chapter 2). Previous work from the Copenhaver laboratory demonstrated that Goα activation restricts the migration and outgrowth of EP cells by regulating Ca^{2+} influx. Therefore, we hypothesize that APPL functions as a GPCR that mediates key aspects of neuronal motility and maintenance by inducing Go-dependent Ca^{2+} channel activation. Given that many neuronal functions (such as synaptic transmission, cytoskeletal dynamics, and long-term potentiation) require tightly regulated Ca^{2+} homeostasis in the brain (LaFerla, 2002), Ca^{2+} signaling may provide a mechanism by which APP-Go signaling controls both

physiological and pathological functions in the brain. In particular, we hypothesize that APP-Goα-Ca^{2+} signaling plays an important role in regulating the extent of neuronal growth, which in turn contributes to the establishment and maintenance of appropriate synaptic connections. Hyperstimulation of this pathway would therefore cause growth cone collapse and axon retraction during development, and later cause abnormal synaptic growth and plasticity, whereas persistent hyperstimulation would lead to Ca^{2+} dysregulation and cell death. Further elucidation of the normal role of APP-Go signaling in neurons, as well as the identity of molecules that can regulate this signaling cascade, may therefore provide insight into how this evolutionarily conserved pathway contributes to human disease.

REFERENCES

Allinquant B, Moya KL, Bouillot C, Prochiantz A (1994) Amyloid precursor protein in cortical neurons: coexistence of two pools differentially distributed in axons and dendrites and association with cytoskeleton. The Journal of neuroscience : the official journal of the Society for Neuroscience 14:6842-6854.

Andersen OM, Reiche J, Schmidt V, Gotthardt M, Spoelgen R, Behlke J, von Arnim CA, Breiderhoff T, Jansen P, Wu X, Bales KR, Cappai R, Masters CL, Gliemann J, Mufson EJ, Hyman BT, Paul SM, Nykjaer A, Willnow TE (2005) Neuronal sorting protein-related receptor sorLA/LR11 regulates processing of the amyloid precursor protein. Proceedings of the National Academy of Sciences of the United States of America 102:13461-13466.

Araki W, Kitaguchi N, Tokushima Y, Ishii K, Aratake H, Shimohama S, Nakamura S, Kimura J (1991) Trophic effect of beta-amyloid precursor protein on cerebral cortical neurons in culture. Biochemical and biophysical research communications 181:265-271.

Ashley J, Packard M, Ataman B, Budnik V (2005) Fasciclin II signals new synapse formation through amyloid precursor protein and the scaffolding protein dX11/Mint. The Journal of neuroscience : the official journal of the Society for Neuroscience 25:5943-5955.

Banker G GK (1998) Culturing nerve cells.

Bates CA, Meyer RL (1996) Heterotrimeric G protein activation rapidly inhibits outgrowth of optic axons from adult and embryonic mouse, and goldfish retinal explants. Brain research 714:65-75.

Beher D, Hesse L, Masters CL, Multhaup G (1996) Regulation of amyloid protein precursor (APP) binding to collagen and mapping of the binding sites on APP and collagen type I. The Journal of biological chemistry 271:1613-1620.

Benton R, Sachse S, Michnick SW, Vosshall LB (2006) Atypical membrane topology and heteromeric function of Drosophila odorant receptors in vivo. PLoS biology 4:e20.

Bergmans BA, Shariati SA, Habets RL, Verstreken P, Schoonjans L, Muller U, Dotti CG, De Strooper B (2010) Neurons generated from APP/APLP1/APLP2 triple knockout embryonic stem cells behave normally in vitro and in vivo: lack of evidence for a cell autonomous role of the amyloid precursor protein in neuronal differentiation. Stem Cells 28:399-406.

Berry M, Rogers AW (1965) The migration of neuroblasts in the developing cerebral cortex. Journal of anatomy 99:691-709.

Bieber AJ, Snow PM, Hortsch M, Patel NH, Jacobs JR, Traquina ZR, Schilling J, Goodman CS (1989) Drosophila neuroglian: a member of the immunoglobulin superfamily with extensive homology to the vertebrate neural adhesion molecule L1. Cell 59:447-460.

Billnitzer AJ, Barskaya I, Yin C, Perez RG (2013) APP independent and dependent effects on neurite outgrowth are modulated by the receptor associated protein (RAP). J Neurochem 124:123-132.

Blennow K, de Leon MJ, Zetterberg H (2006) Alzheimer's disease. Lancet 368:387-403.

Bolkan BJ, Triphan T, Kretzschmar D (2012) beta-secretase cleavage of the fly amyloid precursor protein is required for glial survival. The Journal of neuroscience : the official journal of the Society for Neuroscience 32:16181-16192.

Bourne HR, Sanders DA, McCormick F (1991) The GTPase superfamily: conserved structure and molecular mechanism. Nature 349:117-127.

Brand AH, Perrimon N (1993) Targeted gene expression as a means of altering cell fates and generating dominant phenotypes. Development 118:401-415.

Breen KC, Bruce M, Anderton BH (1991) Beta amyloid precursor protein mediates neuronal cell-cell and cell-surface adhesion. J Neurosci Res 28:90-100.

Brodeur J, Theriault C, Lessard-Beaudoin M, Marcil A, Dahan S, Lavoie C (2012) LDLR-related protein 10 (LRP10) regulates amyloid precursor protein (APP) trafficking and processing: evidence for a role in Alzheimer's disease. Mol Neurodegener 7:31.

Bromberg KD, Iyengar R, He JC (2008) Regulation of neurite outgrowth by G(i/o) signaling pathways. Frontiers in bioscience : a journal and virtual library 13:4544-4557.

Brouillet E, Trembleau A, Galanaud D, Volovitch M, Bouillot C, Valenza C, Prochiantz A, Allinquant B (1999) The amyloid precursor protein interacts with Go heterotrimeric protein within a cell compartment specialized in signal transduction. The Journal of neuroscience : the official journal of the Society for Neuroscience 19:1717-1727.
Buck KB, Zheng JQ (2002) Growth cone turning induced by direct local modification of microtubule dynamics. The Journal of neuroscience : the official journal of the Society for Neuroscience 22:9358-9367.
Cao X, Sudhof TC (2001) A transcriptionally [correction of transcriptively] active complex of APP with Fe65 and histone acetyltransferase Tip60. Science 293:115-120.
Carmine-Simmen K, Proctor T, Tschape J, Poeck B, Triphan T, Strauss R, Kretzschmar D (2009) Neurotoxic effects induced by the Drosophila amyloid-beta peptide suggest a conserved toxic function. Neurobiology of disease 33:274-281.
Cerretti DP, Vanden Bos T, Nelson N, Kozlosky CJ, Reddy P, Maraskovsky E, Park LS, Lyman SD, Copeland NG, Gilbert DJ, et al. (1995) Isolation of LERK-5: a ligand of the eph-related receptor tyrosine kinases. Molecular immunology 32:1197-1205.
Chang KJ, Pugh W, Blanchard SG, McDermed J, Tam JP (1988) Antibody specific to the alpha subunit of the guanine nucleotide-binding regulatory protein Go: developmental appearance and immunocytochemical localization in brain. Proceedings of the National Academy of Sciences of the United States of America 85:4929-4933.
Chen CL, Lampe DJ, Robertson HM, Nardi JB (1997) Neuroglian is expressed on cells destined to form the prothoracic glands of Manduca embryos as they segregate from surrounding cells and rearrange during morphogenesis. Developmental biology 181:1-13.
Chen LT, Gilman AG, Kozasa T (1999) A candidate target for G protein action in brain. The Journal of biological chemistry 274:26931-26938.
Chen WJ, Goldstein JL, Brown MS (1990) NPXY, a sequence often found in cytoplasmic tails, is required for coated pit-mediated internalization of the low density lipoprotein receptor. The Journal of biological chemistry 265:3116-3123.
Clarris HJ, Key B, Beyreuther K, Masters CL, Small DH (1995) Expression of the amyloid protein precursor of Alzheimer's disease in the developing rat olfactory system. Brain research Developmental brain research 88:87-95.
Coate TM, Swanson TL, Copenhaver PF (2009) Reverse signaling by glycosylphosphatidylinositol-linked Manduca ephrin requires a SRC family kinase to restrict neuronal migration in vivo. The Journal of neuroscience : the official journal of the Society for Neuroscience 29:3404-3418.
Coate TM, Swanson TL, Proctor TM, Nighorn AJ, Copenhaver PF (2007) Eph receptor expression defines midline boundaries for ephrin-positive migratory neurons in the enteric nervous system of Manduca sexta. J Comp Neurol 502:175-191.
Coate TM, Wirz JA, Copenhaver PF (2008) Reverse signaling via a glycosyl-phosphatidylinositol-linked ephrin prevents midline crossing by migratory neurons during embryonic development in Manduca. The Journal of neuroscience : the official journal of the Society for Neuroscience 28:3846-3860.
Copenhaver PF (1993) Origins, migration and differentiation of glial cells in the insect enteric nervous system from a discrete set of glial precursors. Development 117:59-74.
Copenhaver PF (2007) How to innervate a simple gut: familiar themes and unique aspects in the formation of the insect enteric nervous system. Developmental dynamics : an official publication of the American Association of Anatomists 236:1841-1864.
Copenhaver PF, Anekonda TS, Musashe D, Robinson KM, Ramaker JM, Swanson TL, Wadsworth TL, Kretzschmar D, Woltjer RL, Quinn JF (2011) A translational continuum of model systems for evaluating treatment strategies in Alzheimer's disease: isradipine as a candidate drug. Dis Model Mech.
Copenhaver PF, Horgan AM, Combes S (1996) An identified set of visceral muscle bands is essential for the guidance of migratory neurons in the enteric nervous system of Manduca sexta. Developmental biology 179:412-426.
Copenhaver PF, Horgan AM, Nichols DC, Rasmussen MA (1995) Developmental expression of heterotrimeric G proteins in the nervous system of Manduca sexta. Journal of neurobiology 26:461-484.

Copenhaver PF, Taghert PH (1989a) Development of the enteric nervous system in the moth. I. Diversity of cell types and the embryonic expression of FMRFamide-related neuropeptides. Developmental biology 131:70-84.
Copenhaver PF, Taghert PH (1989b) Development of the enteric nervous system in the moth. II. Stereotyped cell migration precedes the differentiation of embryonic neurons. Developmental biology 131:85-101.
Copenhaver PF, Taghert PH (1990) Neurogenesis in the insect enteric nervous system: generation of premigratory neurons from an epithelial placode. Development 109:17-28.
Cullen WK, Suh YH, Anwyl R, Rowan MJ (1997) Block of LTP in rat hippocampus in vivo by beta-amyloid precursor protein fragments. Neuroreport 8:3213-3217.
Daigle I, Li C (1993) apl-1, a Caenorhabditis elegans gene encoding a protein related to the human beta-amyloid protein precursor. Proceedings of the National Academy of Sciences of the United States of America 90:12045-12049.
Dawson GR, Seabrook GR, Zheng H, Smith DW, Graham S, O'Dowd G, Bowery BJ, Boyce S, Trumbauer ME, Chen HY, Van der Ploeg LH, Sirinathsinghji DJ (1999) Age-related cognitive deficits, impaired long-term potentiation and reduction in synaptic marker density in mice lacking the beta-amyloid precursor protein. Neuroscience 90:1-13.
Devisme L, Bouchet C, Gonzales M, Alanio E, Bazin A, Bessieres B, Bigi N, Blanchet P, Bonneau D, Bonnieres M, Bucourt M, Carles D, Clarisse B, Delahaye S, Fallet-Bianco C, Figarella-Branger D, Gaillard D, Gasser B, Delezoide AL, Guimiot F, Joubert M, Laurent N, Laquerriere A, Liprandi A, Loget P, Marcorelles P, Martinovic J, Menez F, Patrier S, Pelluard F, Perez MJ, Rouleau C, Triau S, Attie-Bitach T, Vuillaumier-Barrot S, Seta N, Encha-Razavi F (2012) Cobblestone lissencephaly: neuropathological subtypes and correlations with genes of dystroglycanopathies. Brain : a journal of neurology 135:469-482.
Deyts C, Vetrivel KS, Das S, Shepherd YM, Dupre DJ, Thinakaran G, Parent AT (2012) Novel GalphaS-Protein Signaling Associated with Membrane-Tethered Amyloid Precursor Protein Intracellular Domain. The Journal of neuroscience : the official journal of the Society for Neuroscience 32:1714-1729.
Diez-Roux G, Banfi S, Sultan M, Geffers L, Anand S, Rozado D, Magen A, Canidio E, Pagani M, Peluso I, Lin-Marq N, Koch M, Bilio M, Cantiello I, Verde R, De Masi C, Bianchi SA, Cicchini J, Perroud E, Mehmeti S, Dagand E, Schrinner S, Nurnberger A, Schmidt K, Metz K, Zwingmann C, Brieske N, Springer C, Hernandez AM, Herzog S, Grabbe F, Sieverding C, Fischer B, Schrader K, Brockmeyer M, Dettmer S, Helbig C, Alunni V, Battaini MA, Mura C, Henrichsen CN, Garcia-Lopez R, Echevarria D, Puelles E, Garcia-Calero E, Kruse S, Uhr M, Kauck C, Feng G, Milyaev N, Ong CK, Kumar L, Lam M, Semple CA, Gyenesei A, Mundlos S, Radelof U, Lehrach H, Sarmientos P, Reymond A, Davidson DR, Dolle P, Antonarakis SE, Yaspo ML, Martinez S, Baldock RA, Eichele G, Ballabio A (2011) A high-resolution anatomical atlas of the transcriptome in the mouse embryo. PLoS biology 9:e1000582.
Dotti CG, Sullivan CA, Banker GA (1988) The establishment of polarity by hippocampal neurons in culture. The Journal of neuroscience : the official journal of the Society for Neuroscience 8:1454-1468.
Dumanis SB, Chamberlain KA, Jin Sohn Y, Jin Lee Y, Guenette SY, Suzuki T, Mathews PM, Pak D, Rebeck GW, Suh YH, Park HS, Hoe HS (2012) FE65 as a link between VLDLR and APP to regulate their trafficking and processing. Mol Neurodegener 7:9.
Edmonds BT, Moomaw CR, Hsu JT, Slaughter C, Ellis L (1990) The p38 and p34 polypeptides of growth cone particle membranes are the alpha- and beta-subunits of G proteins. Brain research Developmental brain research 56:131-136.
Faissner A, Kruse J, Nieke J, Schachner M (1984) Expression of neural cell adhesion molecule L1 during development, in neurological mutants and in the peripheral nervous system. Brain research 317:69-82.
Faivre-Sarrailh C, Banerjee S, Li J, Hortsch M, Laval M, Bhat MA (2004) Drosophila contactin, a homolog of vertebrate contactin, is required for septate junction organization and paracellular barrier function. Development 131:4931-4942.

Falk J, Bonnon C, Girault JA, Faivre-Sarrailh C (2002) F3/contactin, a neuronal cell adhesion molecule implicated in axogenesis and myelination. Biology of the cell / under the auspices of the European Cell Biology Organization 94:327-334.
Ferreira A, Caceres A, Kosik KS (1993) Intraneuronal compartments of the amyloid precursor protein. The Journal of neuroscience : the official journal of the Society for Neuroscience 13:3112-3123.
Forloni G, Demicheli F, Giorgi S, Bendotti C, Angeretti N (1992) Expression of amyloid precursor protein mRNAs in endothelial, neuronal and glial cells: modulation by interleukin-1. Brain Res Mol Brain Res 16:128-134.
Fremion F, Astier M, Zaffran S, Guillen A, Homburger V, Semeriva M (1999) The heterotrimeric protein Go is required for the formation of heart epithelium in Drosophila. J Cell Biol 145:1063-1076.
Fuentealba RA, Barria MI, Lee J, Cam J, Araya C, Escudero CA, Inestrosa NC, Bronfman FC, Bu G, Marzolo MP (2007) ApoER2 expression increases Abeta production while decreasing Amyloid Precursor Protein (APP) endocytosis: Possible role in the partitioning of APP into lipid rafts and in the regulation of gamma-secretase activity. Mol Neurodegener 2:14.
Gales C, Van Durm JJ, Schaak S, Pontier S, Percherancier Y, Audet M, Paris H, Bouvier M (2006) Probing the activation-promoted structural rearrangements in preassembled receptor-G protein complexes. Nature structural & molecular biology 13:778-786.
Galvan V, Gorostiza OF, Banwait S, Ataie M, Logvinova AV, Sitaraman S, Carlson E, Sagi SA, Chevallier N, Jin K, Greenberg DA, Bredesen DE (2006) Reversal of Alzheimer's-like pathology and behavior in human APP transgenic mice by mutation of Asp664. Proceedings of the National Academy of Sciences of the United States of America 103:7130-7135.
Games D, Adams D, Alessandrini R, Barbour R, Berthelette P, Blackwell C, Carr T, Clemens J, Donaldson T, Gillespie F, et al. (1995) Alzheimer-type neuropathology in transgenic mice overexpressing V717F beta-amyloid precursor protein. Nature 373:523-527.
Garcia-Alonso L, Romani S, Jimenez F (2000) The EGF and FGF receptors mediate neuroglian function to control growth cone decisions during sensory axon guidance in Drosophila. Neuron 28:741-752.
Giambarella U, Yamatsuji T, Okamoto T, Matsui T, Ikezu T, Murayama Y, Levine MA, Katz A, Gautam N, Nishimoto I (1997) G protein betagamma complex-mediated apoptosis by familial Alzheimer's disease mutant of APP. The EMBO journal 16:4897-4907.
Golde TE, Petrucelli L, Lewis J (2010) Targeting Abeta and tau in Alzheimer's disease, an early interim report. Experimental neurology 223:252-266.
Gralle M, Botelho MG, Wouters FS (2009) Neuroprotective secreted amyloid precursor protein acts by disrupting amyloid precursor protein dimers. The Journal of biological chemistry 284:15016-15025.
Gralle M, Ferreira ST (2007) Structure and functions of the human amyloid precursor protein: the whole is more than the sum of its parts. Prog Neurobiol 82:11-32.
Guenette S, Chang Y, Hiesberger T, Richardson JA, Eckman CB, Eckman EA, Hammer RE, Herz J (2006) Essential roles for the FE65 amyloid precursor protein-interacting proteins in brain development. The EMBO journal 25:420-431.
Hardy J, Selkoe DJ (2002) The amyloid hypothesis of Alzheimer's disease: progress and problems on the road to therapeutics. Science 297:353-356.
Hartenstein V (1988) Development of *Drosophila* larval sensory organs: spatiotemporal pattern of sensory neurones, peripheral axonal pathways and sensilla differentiation. Development 102:869-886.
He JC, Neves SR, Jordan JD, Iyengar R (2006) Role of the Go/i signaling network in the regulation of neurite outgrowth. Can J Physiol Pharmacol 84:687-694.
Heber S, Herms J, Gajic V, Hainfellner J, Aguzzi A, Rulicke T, von Kretzschmar H, von Koch C, Sisodia S, Tremml P, Lipp HP, Wolfer DP, Muller U (2000) Mice with combined gene knock-outs reveal essential and partially redundant functions of amyloid precursor protein family members. The Journal of neuroscience : the official journal of the Society for Neuroscience 20:7951-7963.

Herms J, Anliker B, Heber S, Ring S, Fuhrmann M, Kretzschmar H, Sisodia S, Muller U (2004) Cortical dysplasia resembling human type 2 lissencephaly in mice lacking all three APP family members. The EMBO journal 23:4106-4115.
Higashijima T, Burnier J, Ross EM (1990) Regulation of Gi and Go by mastoparan, related amphiphilic peptides, and hydrophobic amines. Mechanism and structural determinants of activity. The Journal of biological chemistry 265:14176-14186.
Higashijima T, Uzu S, Nakajima T, Ross EM (1988) Mastoparan, a peptide toxin from wasp venom, mimics receptors by activating GTP-binding regulatory proteins (G proteins). The Journal of biological chemistry 263:6491-6494.
Hille B (2001) Modulation, Slow Synaptic Action, and Second Messengers: Sinauer Associates, Inc.
Hiruma K, Riddiford LM (2004) Differential control of MHR3 promoter activity by isoforms of the ecdysone receptor and inhibitory effects of E75A and MHR3. Developmental biology 272:510-521.
Ho A, Sudhof TC (2004) Binding of F-spondin to amyloid-beta precursor protein: a candidate amyloid-beta precursor protein ligand that modulates amyloid-beta precursor protein cleavage. Proceedings of the National Academy of Sciences of the United States of America 101:2548-2553.
Hoe HS, Fu Z, Makarova A, Lee JY, Lu C, Feng L, Pajoohesh-Ganji A, Matsuoka Y, Hyman BT, Ehlers MD, Vicini S, Pak DT, Rebeck GW (2009a) The effects of amyloid precursor protein on postsynaptic composition and activity. The Journal of biological chemistry 284:8495-8506.
Hoe HS, Lee KJ, Carney RS, Lee J, Markova A, Lee JY, Howell BW, Hyman BT, Pak DT, Bu G, Rebeck GW (2009b) Interaction of reelin with amyloid precursor protein promotes neurite outgrowth. The Journal of neuroscience : the official journal of the Society for Neuroscience 29:7459-7473.
Hoe HS, Rebeck GW (2008) Functional interactions of APP with the apoE receptor family. J Neurochem 106:2263-2271.
Hoe HS, Tran TS, Matsuoka Y, Howell BW, Rebeck GW (2006) DAB1 and Reelin effects on amyloid precursor protein and ApoE receptor 2 trafficking and processing. The Journal of biological chemistry 281:35176-35185.
Horgan AM, Copenhaver PF (1998) G protein-mediated inhibition of neuronal migration requires calcium influx. The Journal of neuroscience : the official journal of the Society for Neuroscience 18:4189-4200.
Horgan AM, Lagrange MT, Copenhaver PF (1994) Developmental expression of G proteins in a migratory population of embryonic neurons. Development 120:729-742.
Horgan AM, Lagrange MT, Copenhaver PF (1995) A developmental role for the heterotrimeric G protein Go alpha in a migratory population of embryonic neurons. Developmental biology 172:640-653.
Hornsten A, Lieberthal J, Fadia S, Malins R, Ha L, Xu X, Daigle I, Markowitz M, O'Connor G, Plasterk R, Li C (2007) APL-1, a Caenorhabditis elegans protein related to the human beta-amyloid precursor protein, is essential for viability. Proceedings of the National Academy of Sciences of the United States of America 104:1971-1976.
Hortsch M (1994) Preparation and analysis of membranes and membrane proteins from Drosophila. Methods in cell biology 44:289-301.
Hosoya H, Shimazaki K, Kobayashi S, Takahashi H, Shirasawa T, Takenawa T, Watanabe K (1995) Developmental expression of the neural adhesion molecule F3 in the rat brain. Neuroscience letters 186:83-86.
Howell BW, Lanier LM, Frank R, Gertler FB, Cooper JA (1999) The disabled 1 phosphotyrosine-binding domain binds to the internalization signals of transmembrane glycoproteins and to phospholipids. Molecular and cellular biology 19:5179-5188.
Hsia AY, Masliah E, McConlogue L, Yu GQ, Tatsuno G, Hu K, Kholodenko D, Malenka RC, Nicoll RA, Mucke L (1999) Plaque-independent disruption of neural circuits in Alzheimer's disease mouse models. Proceedings of the National Academy of Sciences of the United States of America 96:3228-3233.

Hsiao K, Chapman P, Nilsen S, Eckman C, Harigaya Y, Younkin S, Yang F, Cole G (1996) Correlative memory deficits, Abeta elevation, and amyloid plaques in transgenic mice. Science 274:99-102.
Hu QD, Ma QH, Gennarini G, Xiao ZC (2006) Cross-talk between F3/contactin and Notch at axoglial interface: a role in oligodendrocyte development. Developmental neuroscience 28:25-33.
Igarashi M, Strittmatter SM, Vartanian T, Fishman MC (1993) Mediation by G proteins of signals that cause collapse of growth cones. Science 259:77-79.
Ikezu T, Okamoto T, Komatsuzaki K, Matsui T, Martyn JA, Nishimoto I (1996) Negative transactivation of cAMP response element by familial Alzheimer's mutants of APP. The EMBO journal 15:2468-2475.
Iwata A, Chen XH, McIntosh TK, Browne KD, Smith DH (2002) Long-term accumulation of amyloid-beta in axons following brain trauma without persistent upregulation of amyloid precursor protein genes. Journal of neuropathology and experimental neurology 61:1056-1068.
Izuo N, Kume T, Sato M, Murakami K, Irie K, Izumi Y, Akaike A (2012) Toxicity in rat primary neurons through the cellular oxidative stress induced by the turn formation at positions 22 and 23 of Abeta42. ACS chemical neuroscience 3:674-681.
Jackson GR (2008) Guide to understanding Drosophila models of neurodegenerative diseases. PLoS biology 6:e53.
Johnson-Wood K, Lee M, Motter R, Hu K, Gordon G, Barbour R, Khan K, Gordon M, Tan H, Games D, Lieberburg I, Schenk D, Seubert P, McConlogue L (1997) Amyloid precursor protein processing and A beta42 deposition in a transgenic mouse model of Alzheimer disease. Proceedings of the National Academy of Sciences of the United States of America 94:1550-1555.
Kaech S, Banker G (2006) Culturing hippocampal neurons. Nature protocols 1:2406-2415.
Kaech S, Huang CF, Banker G (2012) Long-term time-lapse imaging of developing hippocampal neurons in culture. Cold Spring Harbor protocols 2012:335-339.
Kallunki P, Edelman GM, Jones FS (1997) Tissue-specific expression of the L1 cell adhesion molecule is modulated by the neural restrictive silencer element. J Cell Biol 138:1343-1354.
Kang J, Lemaire HG, Unterbeck A, Salbaum JM, Masters CL, Grzeschik KH, Multhaup G, Beyreuther K, Muller-Hill B (1987) The precursor of Alzheimer's disease amyloid A4 protein resembles a cell-surface receptor. Nature 325:733-736.
Karran E, Mercken M, De Strooper B (2011) The amyloid cascade hypothesis for Alzheimer's disease: an appraisal for the development of therapeutics. Nature reviews Drug discovery 10:698-712.
Kerppola TK (2008) Bimolecular fluorescence complementation (BiFC) analysis as a probe of protein interactions in living cells. Annu Rev Biophys 37:465-487.
Khachaturian ZS (1987) Hypothesis on the regulation of cytosol calcium concentration and the aging brain. Neurobiology of aging 8:345-346.
Khachaturian ZS (1994) Calcium hypothesis of Alzheimer's disease and brain aging. Annals of the New York Academy of Sciences 747:1-11.
Knittel LM, Copenhaver PF, Kent KS (2001) Remodeling of motor terminals during metamorphosis of the moth Manduca sexta: expression patterns of two distinct isoforms of Manduca fasciclin II. J Comp Neurol 434:69-85.
LaFerla FM (2002) Calcium dyshomeostasis and intracellular signalling in Alzheimer's disease. Nature reviews Neuroscience 3:862-872.
Larson J, Lynch G, Games D, Seubert P (1999) Alterations in synaptic transmission and long-term potentiation in hippocampal slices from young and aged PDAPP mice. Brain research 840:23-35.
Leaney JL, Tinker A (2000) The role of members of the pertussis toxin-sensitive family of G proteins in coupling receptors to the activation of the G protein-gated inwardly rectifying potassium channel. Proceedings of the National Academy of Sciences of the United States of America 97:5651-5656.

Lefort R, Pozueta J, Shelanski M (2012) Cross-linking of cell surface amyloid precursor protein leads to increased beta-amyloid peptide production in hippocampal neurons: implications for Alzheimer's disease. The Journal of neuroscience : the official journal of the Society for Neuroscience 32:10674-10685.
Leyssen M, Ayaz D, Hebert SS, Reeve S, De Strooper B, Hassan BA (2005) Amyloid precursor protein promotes post-developmental neurite arborization in the Drosophila brain. The EMBO journal 24:2944-2955.
Li Y, Liu T, Peng Y, Yuan C, Guo A (2004) Specific functions of Drosophila amyloid precursor-like protein in the development of nervous system and nonneural tissues. Journal of neurobiology 61:343-358.
Loo DT, Copani A, Pike CJ, Whittemore ER, Walencewicz AJ, Cotman CW (1993) Apoptosis is induced by beta-amyloid in cultured central nervous system neurons. Proceedings of the National Academy of Sciences of the United States of America 90:7951-7955.
Lopez-Sanchez N, Muller U, Frade JM (2005) Lengthening of G2/mitosis in cortical precursors from mice lacking beta-amyloid precursor protein. Neuroscience 130:51-60.
Luo L, Tully T, White K (1992) Human amyloid precursor protein ameliorates behavioral deficit of flies deleted for Appl gene. Neuron 9:595-605.
Luo LQ, Martin-Morris LE, White K (1990) Identification, secretion, and neural expression of APPL, a Drosophila protein similar to human amyloid protein precursor. The Journal of neuroscience : the official journal of the Society for Neuroscience 10:3849-3861.
Ma QH, Futagawa T, Yang WL, Jiang XD, Zeng L, Takeda Y, Xu RX, Bagnard D, Schachner M, Furley AJ, Karagogeos D, Watanabe K, Dawe GS, Xiao ZC (2008) A TAG1-APP signalling pathway through Fe65 negatively modulates neurogenesis. Nat Cell Biol 10:283-294.
Maghazachi AA (2005) Insights into seven and single transmembrane-spanning domain receptors and their signaling pathways in human natural killer cells. Pharmacological reviews 57:339-357.
Mangialasche F, Solomon A, Winblad B, Mecocci P, Kivipelto M (2010) Alzheimer's disease: clinical trials and drug development. Lancet Neurol 9:702-716.
Mangmool S, Kurose H (2011) G(i/o) protein-dependent and -independent actions of Pertussis Toxin (PTX). Toxins 3:884-899.
Martin-Morris LE, White K (1990) The Drosophila transcript encoded by the beta-amyloid protein precursor-like gene is restricted to the nervous system. Development 110:185-195.
McLoughlin DM, Miller CC (2008) The FE65 proteins and Alzheimer's disease. J Neurosci Res 86:744-754.
Mervine SM, Yost EA, Sabo JL, Hynes TR, Berlot CH (2006) Analysis of G protein betagamma dimer formation in live cells using multicolor bimolecular fluorescence complementation demonstrates preferences of beta1 for particular gamma subunits. Molecular pharmacology 70:194-205.
Milward EA, Papadopoulos R, Fuller SJ, Moir RD, Small D, Beyreuther K, Masters CL (1992) The amyloid protein precursor of Alzheimer's disease is a mediator of the effects of nerve growth factor on neurite outgrowth. Neuron 9:129-137.
Mitchison T, Kirschner M (1988) Cytoskeletal dynamics and nerve growth. Neuron 1:761-772.
Mora N, Almudi I, Alsina B, Corominas M, Serras F (2013) beta amyloid protein precursor-like (Appl) is a Ras1/MAPK-regulated gene required for axonal targeting in Drosophila photoreceptor neurons. Journal of cell science 126:53-59.
Muresan V, Varvel NH, Lamb BT, Muresan Z (2009) The cleavage products of amyloid-beta precursor protein are sorted to distinct carrier vesicles that are independently transported within neurites. The Journal of neuroscience : the official journal of the Society for Neuroscience 29:3565-3578.
Muresan Z, Muresan V (2005) Coordinated transport of phosphorylated amyloid-beta precursor protein and c-Jun NH2-terminal kinase-interacting protein-1. J Cell Biol 171:615-625.
Nadarajah B, Brunstrom JE, Grutzendler J, Wong RO, Pearlman AL (2001) Two modes of radial migration in early development of the cerebral cortex. Nature neuroscience 4:143-150.
Nadarajah B, Parnavelas JG (2002) Modes of neuronal migration in the developing cerebral cortex. Nature reviews Neuroscience 3:423-432.

Nakaya T, Suzuki T (2006) Role of APP phosphorylation in FE65-dependent gene transactivation mediated by AICD. Genes to cells : devoted to molecular & cellular mechanisms 11:633-645.
Nakayama T, Goshima Y, Misu Y, Kato T (1999) Role of cdk5 and tau phosphorylation in heterotrimeric G protein-mediated retinal growth cone collapse. Journal of neurobiology 41:326-339.
Nalbantoglu J, Tirado-Santiago G, Lahsaini A, Poirier J, Goncalves O, Verge G, Momoli F, Welner SA, Massicotte G, Julien JP, Shapiro ML (1997) Impaired learning and LTP in mice expressing the carboxy terminus of the Alzheimer amyloid precursor protein. Nature 387:500-505.
Nardi JB, Pilas B, Bee CM, Zhuang S, Garsha K, Kanost MR (2006) Neuroglian-positive plasmatocytes of Manduca sexta and the initiation of hemocyte attachment to foreign surfaces. Developmental and comparative immunology 30:447-462.
Narindrasorasak S, Lowery DE, Altman RA, Gonzalez-DeWhitt PA, Greenberg BD, Kisilevsky R (1992) Characterization of high affinity binding between laminin and Alzheimer's disease amyloid precursor proteins. Laboratory investigation; a journal of technical methods and pathology 67:643-652.
Nishimoto I (1993) The IGF-II receptor system: a G protein-linked mechanism. Molecular reproduction and development 35:398-406; discussion 406-397.
Nishimoto I, Hata Y, Ogata E, Kojima I (1987) Insulin-like growth factor II stimulates calcium influx in competent BALB/c 3T3 cells primed with epidermal growth factor. Characteristics of calcium influx and involvement of GTP-binding protein. The Journal of biological chemistry 262:12120-12126.
Nishimoto I, Okamoto T, Matsuura Y, Takahashi S, Okamoto T, Murayama Y, Ogata E (1993) Alzheimer amyloid protein precursor complexes with brain GTP-binding protein G(o). Nature 362:75-79.
Noctor SC, Martinez-Cerdeno V, Ivic L, Kriegstein AR (2004) Cortical neurons arise in symmetric and asymmetric division zones and migrate through specific phases. Nature neuroscience 7:136-144.
O'Brien RJ, Wong PC (2011) Amyloid precursor protein processing and Alzheimer's disease. Annual review of neuroscience 34:185-204.
Ohsawa I, Hirose Y, Ishiguro M, Imai Y, Ishiura S, Kohsaka S (1995) Expression, purification, and neurotrophic activity of amyloid precursor protein-secreted forms produced by yeast. Biochemical and biophysical research communications 213:52-58.
Oishi M, Nairn AC, Czernik AJ, Lim GS, Isohara T, Gandy SE, Greengard P, Suzuki T (1997) The cytoplasmic domain of Alzheimer's amyloid precursor protein is phosphorylated at Thr654, Ser655, and Thr668 in adult rat brain and cultured cells. Mol Med 3:111-123.
Okamoto T, Katada T, Murayama Y, Ui M, Ogata E, Nishimoto I (1990) A simple structure encodes G protein-activating function of the IGF-II/mannose 6-phosphate receptor. Cell 62:709-717.
Okamoto T, Takeda S, Giambarella U, Murayama Y, Matsui T, Katada T, Matsuura Y, Nishimoto I (1996) Intrinsic signaling function of APP as a novel target of three V642 mutations linked to familial Alzheimer's disease. The EMBO journal 15:3769-3777.
Okamoto T, Takeda S, Murayama Y, Ogata E, Nishimoto I (1995) Ligand-dependent G protein coupling function of amyloid transmembrane precursor. The Journal of biological chemistry 270:4205-4208.
Osterfield M, Egelund R, Young LM, Flanagan JG (2008) Interaction of amyloid precursor protein with contactins and NgCAM in the retinotectal system. Development 135:1189-1199.
Patel TB (2004) Single transmembrane spanning heterotrimeric g protein-coupled receptors and their signaling cascades. Pharmacological reviews 56:371-385.
Perez RG, Zheng H, Van der Ploeg LH, Koo EH (1997) The beta-amyloid precursor protein of Alzheimer's disease enhances neuron viability and modulates neuronal polarity. The Journal of neuroscience : the official journal of the Society for Neuroscience 17:9407-9414.

Phinney AL, Calhoun ME, Wolfer DP, Lipp HP, Zheng H, Jucker M (1999) No hippocampal neuron or synaptic bouton loss in learning-impaired aged beta-amyloid precursor protein-null mice. Neuroscience 90:1207-1216.
Poeck B, Strauss R, Kretzschmar D (2012) Analysis of amyloid precursor protein function in Drosophila melanogaster. Experimental brain research Experimentelle Hirnforschung Experimentation cerebrale 217:413-421.
Pramatarova A, Chen K, Howell BW (2008) A genetic interaction between the APP and Dab1 genes influences brain development. Molecular and cellular neurosciences 37:178-186.
Price JL, McKeel DW, Jr., Buckles VD, Roe CM, Xiong C, Grundman M, Hansen LA, Petersen RC, Parisi JE, Dickson DW, Smith CD, Davis DG, Schmitt FA, Markesbery WR, Kaye J, Kurlan R, Hulette C, Kurland BF, Higdon R, Kukull W, Morris JC (2009) Neuropathology of nondemented aging: presumptive evidence for preclinical Alzheimer disease. Neurobiology of aging 30:1026-1036.
Priller C, Bauer T, Mitteregger G, Krebs B, Kretzschmar HA, Herms J (2006) Synapse formation and function is modulated by the amyloid precursor protein. The Journal of neuroscience : the official journal of the Society for Neuroscience 26:7212-7221.
Qiu WQ, Ferreira A, Miller C, Koo EH, Selkoe DJ (1995) Cell-surface beta-amyloid precursor protein stimulates neurite outgrowth of hippocampal neurons in an isoform-dependent manner. The Journal of neuroscience : the official journal of the Society for Neuroscience 15:2157-2167.
Rakic P (1974) Neurons in rhesus monkey visual cortex: systematic relation between time of origin and eventual disposition. Science 183:425-427.
Rama N, Goldschneider D, Corset V, Lambert J, Pays L, Mehlen P (2012) Amyloid precursor protein regulates netrin-1-mediated commissural axon outgrowth. The Journal of biological chemistry 287:30014-30023.
Ramaker JM, Swanson TL, Copenhaver PF (2013) Amyloid precursor proteins interact with the heterotrimeric g protein go in the control of neuronal migration. The Journal of neuroscience : the official journal of the Society for Neuroscience 33:10165-10181.
Reinhard C, Hebert SS, De Strooper B (2005) The amyloid-beta precursor protein: integrating structure with biological function. The EMBO journal 24:3996-4006.
Reis K, Zharkovsky A, Bogdanovic N, Karelson E, Land T (2007) Critical role of methionine-722 in the stimulation of human brain G-proteins and neurotoxicity induced by London familial Alzheimer's disease (FAD) mutated V717G-APP(714-723). Neuroscience 144:571-578.
Remy I, Montmarquette A, Michnick SW (2004) PKB/Akt modulates TGF-beta signalling through a direct interaction with Smad3. Nat Cell Biol 6:358-365.
Rice HC, Townsend M, Bai J, Suth S, Cavanaugh W, Selkoe DJ, Young-Pearse TL (2012) Pancortins interact with amyloid precursor protein and modulate cortical cell migration. Development 139:3986-3996.
Rice HC, Young-Pearse TL, Selkoe DJ (2013) Systematic Evaluation of Candidate Ligands Regulating Ectodomain Shedding of Amyloid Precursor Protein. Biochemistry.
Robida AM, Kerppola TK (2009) Bimolecular fluorescence complementation analysis of inducible protein interactions: effects of factors affecting protein folding on fluorescent protein fragment association. Journal of molecular biology 394:391-409.
Rohn TT, Ivins KJ, Bahr BA, Cotman CW, Cribbs DH (2000) A monoclonal antibody to amyloid precursor protein induces neuronal apoptosis. J Neurochem 74:2331-2342.
Rosen DR, Martin-Morris L, Luo LQ, White K (1989) A Drosophila gene encoding a protein resembling the human beta-amyloid protein precursor. Proceedings of the National Academy of Sciences of the United States of America 86:2478-2482.
Rossjohn J, Cappai R, Feil SC, Henry A, McKinstry WJ, Galatis D, Hesse L, Multhaup G, Beyreuther K, Masters CL, Parker MW (1999) Crystal structure of the N-terminal, growth factor-like domain of Alzheimer amyloid precursor protein. Nature structural biology 6:327-331.
Sabo SL, Ikin AF, Buxbaum JD, Greengard P (2003) The amyloid precursor protein and its regulatory protein, FE65, in growth cones and synapses in vitro and in vivo. The Journal of neuroscience : the official journal of the Society for Neuroscience 23:5407-5415.

Sabo SL, Lanier LM, Ikin AF, Khorkova O, Sahasrabudhe S, Greengard P, Buxbaum JD (1999) Regulation of beta-amyloid secretion by FE65, an amyloid protein precursor-binding protein. The Journal of biological chemistry 274:7952-7957.
Salbaum JM, Ruddle FH (1994) Embryonic expression pattern of amyloid protein precursor suggests a role in differentiation of specific subsets of neurons. The Journal of experimental zoology 269:116-127.
Saura CA, Chen G, Malkani S, Choi SY, Takahashi RH, Zhang D, Gouras GK, Kirkwood A, Morris RG, Shen J (2005) Conditional inactivation of presenilin 1 prevents amyloid accumulation and temporarily rescues contextual and spatial working memory impairments in amyloid precursor protein transgenic mice. The Journal of neuroscience : the official journal of the Society for Neuroscience 25:6755-6764.
Senechal Y, Kelly PH, Dev KK (2008) Amyloid precursor protein knockout mice show age-dependent deficits in passive avoidance learning. Behavioural brain research 186:126-132.
Shaked GM, Chauv S, Ubhi K, Hansen LA, Masliah E (2009) Interactions between the amyloid precursor protein C-terminal domain and G proteins mediate calcium dysregulation and amyloid beta toxicity in Alzheimer's disease. The FEBS journal 276:2736-2751.
Shariati SA, Lau P, Hassan BA, Muller U, Dotti CG, De Strooper B, Gartner A (2013) APLP2 regulates neuronal stem cell differentiation during cortical development. Journal of cell science 126:1268-1277.
Small DH, Clarris HL, Williamson TG, Reed G, Key B, Mok SS, Beyreuther K, Masters CL, Nurcombe V (1999) Neurite-outgrowth regulating functions of the amyloid protein precursor of Alzheimer's disease. Journal of Alzheimer's disease : JAD 1:275-285.
Soba P, Eggert S, Wagner K, Zentgraf H, Siehl K, Kreger S, Lower A, Langer A, Merdes G, Paro R, Masters CL, Muller U, Kins S, Beyreuther K (2005) Homo- and heterodimerization of APP family members promotes intercellular adhesion. The EMBO journal 24:3624-3634.
Sola Vigo F, Kedikian G, Heredia L, Heredia F, Anel AD, Rosa AL, Lorenzo A (2009) Amyloid-beta precursor protein mediates neuronal toxicity of amyloid beta through Go protein activation. Neurobiology of aging 30:1379-1392.
Sotelo C (2002) The chemotactic hypothesis of Cajal: a century behind. Progress in brain research 136:11-20.
Sprecher SG, Cardona A, Hartenstein V (2011) The Drosophila larval visual system: high-resolution analysis of a simple visual neuropil. Developmental biology 358:33-43.
Standen CL, Brownlees J, Grierson AJ, Kesavapany S, Lau KF, McLoughlin DM, Miller CC (2001) Phosphorylation of thr(668) in the cytoplasmic domain of the Alzheimer's disease amyloid precursor protein by stress-activated protein kinase 1b (Jun N-terminal kinase-3). J Neurochem 76:316-320.
Stein E, Lane AA, Cerretti DP, Schoecklmann HO, Schroff AD, Van Etten RL, Daniel TO (1998) Eph receptors discriminate specific ligand oligomers to determine alternative signaling complexes, attachment, and assembly responses. Genes & development 12:667-678.
Steller H FK, Rubin GM (1987) Disconnected: a locus required for neuronal pathway formation in the visual system of *Drosophila*. Cell 50:1139-1153.
Sternweis PC, Gilman AG (1982) Aluminum: a requirement for activation of the regulatory component of adenylate cyclase by fluoride. Proceedings of the National Academy of Sciences of the United States of America 79:4888-4891.
Strathmann M, Simon MI (1990) G protein diversity: a distinct class of alpha subunits is present in vertebrates and invertebrates. Proceedings of the National Academy of Sciences of the United States of America 87:9113-9117.
Strickler JG, Rooney MT, d'Amore ES, Copenhaver CM, Roche PC (1993) Detection of Epstein-Barr virus by in situ hybridization with a commercially available biotinylated oligonucleotide probe. Modern pathology : an official journal of the United States and Canadian Academy of Pathology, Inc 6:208-211.
Strittmatter SM (1992) GAP-43 as a modulator of G protein transduction in the growth cone. Perspectives on developmental neurobiology 1:13-19.
Stryer L, Bourne HR (1986) G proteins: a family of signal transducers. Annual review of cell biology 2:391-419.

Sudo H, Jiang H, Yasukawa T, Hashimoto Y, Niikura T, Kawasumi M, Matsuda S, Takeuchi Y, Aiso S, Matsuoka M, Murayama Y, Nishimoto I (2000) Antibody-regulated neurotoxic function of cell-surface beta-amyloid precursor protein. Molecular and cellular neurosciences 16:708-723.
Sugaya K, Chouinard M, Greene R, Robbins M, Personett D, Kent C, Gallagher M, McKinney M (1996) Molecular indices of neuronal and glial plasticity in the hippocampal formation in a rodent model of age-induced spatial learning impairment. The Journal of neuroscience : the official journal of the Society for Neuroscience 16:3427-3443.
Swanson TL, Knittel LM, Coate TM, Farley SM, Snyder MA, Copenhaver PF (2005) The insect homologue of the amyloid precursor protein interacts with the heterotrimeric G protein Go alpha in an identified population of migratory neurons. Developmental biology 288:160-178.
Tabata H, Nakajima K (2003) Multipolar migration: the third mode of radial neuronal migration in the developing cerebral cortex. The Journal of neuroscience : the official journal of the Society for Neuroscience 23:9996-10001.
Tamayev R, Zhou D, D'Adamio L (2009) The interactome of the amyloid beta precursor protein family members is shaped by phosphorylation of their intracellular domains. Mol Neurodegener 4:28.
Tanzi RE, Bertram L (2005) Twenty years of the Alzheimer's disease amyloid hypothesis: a genetic perspective. Cell 120:545-555.
Terry RD, Masliah E, Salmon DP, Butters N, DeTeresa R, Hill R, Hansen LA, Katzman R (1991) Physical basis of cognitive alterations in Alzheimer's disease: synapse loss is the major correlate of cognitive impairment. Annals of neurology 30:572-580.
Tessier-Lavigne M, Goodman CS (1996) The molecular biology of axon guidance. Science 274:1123-1133.
Thambi NC, Quan F, Wolfgang WJ, Spiegel A, Forte M (1989) Immunological and molecular characterization of Go alpha-like proteins in the Drosophila central nervous system. The Journal of biological chemistry 264:18552-18560.
Timossi C, Ortiz-Elizondo C, Pineda DB, Dias JA, Conn PM, Ulloa-Aguirre A (2004) Functional significance of the BBXXB motif reversed present in the cytoplasmic domains of the human follicle-stimulating hormone receptor. Molecular and cellular endocrinology 223:17-26.
Tix S, Minden JS, Technau GM (1989) Pre-existing neuronal pathways in the developing optic lobes of Drosophila. Development 105:739-746.
Torroja L, Chu H, Kotovsky I, White K (1999a) Neuronal overexpression of APPL, the Drosophila homologue of the amyloid precursor protein (APP), disrupts axonal transport. Current biology : CB 9:489-492.
Torroja L, Packard M, Gorczyca M, White K, Budnik V (1999b) The Drosophila beta-amyloid precursor protein homolog promotes synapse differentiation at the neuromuscular junction. The Journal of neuroscience : the official journal of the Society for Neuroscience 19:7793-7803.
Turner PR, O'Connor K, Tate WP, Abraham WC (2003) Roles of amyloid precursor protein and its fragments in regulating neural activity, plasticity and memory. Prog Neurobiol 70:1-32.
Van Den Heuvel C, Blumbergs P, Finnie J, Manavis J, Lewis S, Jones N, Reilly P, Pereira R (2000) Upregulation of amyloid precursor protein and its mRNA in an experimental model of paediatric head injury. Journal of clinical neuroscience : official journal of the Neurosurgical Society of Australasia 7:140-145.
Visel A, Thaller C, Eichele G (2004) GenePaint.org: an atlas of gene expression patterns in the mouse embryo. Nucleic acids research 32:D552-556.
Wallace WC, Akar CA, Lyons WE (1997) Amyloid precursor protein potentiates the neurotrophic activity of NGF. Brain Res Mol Brain Res 52:201-212.
Wang P, Yang G, Mosier DR, Chang P, Zaidi T, Gong YD, Zhao NM, Dominguez B, Lee KF, Gan WB, Zheng H (2005) Defective neuromuscular synapses in mice lacking amyloid precursor protein (APP) and APP-Like protein 2. The Journal of neuroscience : the official journal of the Society for Neuroscience 25:1219-1225.

Wang Z, Wang B, Yang L, Guo Q, Aithmitti N, Songyang Z, Zheng H (2009) Presynaptic and postsynaptic interaction of the amyloid precursor protein promotes peripheral and central synaptogenesis. The Journal of neuroscience : the official journal of the Society for Neuroscience 29:10788-10801.
Wentzell JS, Bolkan BJ, Carmine-Simmen K, Swanson TL, Musashe DT, Kretzschmar D (2012) Amyloid precursor proteins are protective in Drosophila models of progressive neurodegeneration. Neurobiology of disease 46:78-87.
West RE, Jr., Moss J, Vaughan M, Liu T, Liu TY (1985) Pertussis toxin-catalyzed ADP-ribosylation of transducin. Cysteine 347 is the ADP-ribose acceptor site. The Journal of biological chemistry 260:14428-14430.
Wimo A, Winblad B, Jonsson L (2010) The worldwide societal costs of dementia: Estimates for 2009. Alzheimers Dement 6:98-103.
Wolfgang WJ, Quan F, Thambi N, Forte M (1991) Restricted spatial and temporal expression of G-protein alpha subunits during Drosophila embryogenesis. Development 113:527-538.
Wright JW, Copenhaver PF (2000) Different isoforms of fasciclin II play distinct roles in the guidance of neuronal migration during insect embryogenesis. Developmental biology 225:59-78.
Wright JW, Schwinof KM, Snyder MA, Copenhaver PF (1998) A delayed role for nitric oxide-sensitive guanylate cyclases in a migratory population of embryonic neurons. Developmental biology 204:15-33.
Wright JW, Snyder MA, Schwinof KM, Combes S, Copenhaver PF (1999) A role for fasciclin II in the guidance of neuronal migration. Development 126:3217-3228.
Wu D, Jiang H, Simon MI (1995) Different alpha 1-adrenergic receptor sequences required for activating different G alpha subunits of Gq class of G proteins. The Journal of biological chemistry 270:9828-9832.
Yamatsuji T, Matsui T, Okamoto T, Komatsuzaki K, Takeda S, Fukumoto H, Iwatsubo T, Suzuki N, Asami-Odaka A, Ireland S, Kinane TB, Giambarella U, Nishimoto I (1996a) G protein-mediated neuronal DNA fragmentation induced by familial Alzheimer's disease-associated mutants of APP. Science 272:1349-1352.
Yamatsuji T, Okamoto T, Takeda S, Murayama Y, Tanaka N, Nishimoto I (1996b) Expression of V642 APP mutant causes cellular apoptosis as Alzheimer trait-linked phenotype. The EMBO journal 15:498-509.
Yamazaki T, Koo EH, Selkoe DJ (1997) Cell surface amyloid beta-protein precursor colocalizes with beta 1 integrins at substrate contact sites in neural cells. The Journal of neuroscience : the official journal of the Society for Neuroscience 17:1004-1010.
Young-Pearse TL, Bai J, Chang R, Zheng JB, LoTurco JJ, Selkoe DJ (2007) A critical function for beta-amyloid precursor protein in neuronal migration revealed by in utero RNA interference. The Journal of neuroscience : the official journal of the Society for Neuroscience 27:14459-14469.
Young-Pearse TL, Chen AC, Chang R, Marquez C, Selkoe DJ (2008) Secreted APP regulates the function of full-length APP in neurite outgrowth through interaction with integrin beta1. Neural development 3:15.
Yuan XB, Jin M, Xu X, Song YQ, Wu CP, Poo MM, Duan S (2003) Signalling and crosstalk of Rho GTPases in mediating axon guidance. Nat Cell Biol 5:38-45.
Zheng H, Koo EH (2011) Biology and pathophysiology of the amyloid precursor protein. Mol Neurodegener 6:27.
Zhou D, Zambrano N, Russo T, D'Adamio L (2009) Phosphorylation of a tyrosine in the amyloid-beta protein precursor intracellular domain inhibits Fe65 binding and signaling. Journal of Alzheimer's disease : JAD 16:301-307.